F 1503/3

BULETINUL INSTITUTULUI POLITEHNIC DIN IAŞI

Tomul XXXIX (XLIII)
Fasc. 1–4

Secţia III

ELECTROTEHNICĂ. ENERGETICĂ. ELECTRONICĂ

1993

BULETINUL INSTITUTULUI POLITEHNIC DIN IAŞI

Tomul XXXIX (XLIII)
Fasc. 1–4

Secţia III

ELECTROTEHNICĂ. ENERGETICĂ. ELECTRONICĂ

ORSZÁGOS MŰSZAKI INFORMÁCIÓS KÖZPONT ÉS KÖNYVTÁR 1883

1993

EDITORIAL STAFF

Prof. dr. eng. **VITALIE BELOUSOV** (President)
Prof. dr. eng. **PAULICĂ RĂILEANU** (Secretary)
Prof. dr. eng. **EFTIMIE NIŢESCU**
Prof. dr. doc. **ALFRED BRAIER** (Editor)
Prof. dr. eng. **HUGO ROSMAN** (Editor)
Prof. dr. eng. **MIHAIL VOICU** (Head of the Exchange Service)
Prof. dr. **AUREL BEJANCU**
Prof. dr. eng. **VICTOR BULACOVSCHI**
Prof. dr. eng. **DIMITRIE ALEXA**
Prof. dr. eng. **SPIRIDON CREŢU**
Prof. dr. eng. **ADRIAN RADU**
Prof. dr. eng. **ION GIURMĂ**
Prof. dr. eng. **MIRCEA MATEESCU**

TEXredaction:
Computing Centre of the Technical University of Iaşi

BULETINUL INSTITUTULUI POLITEHNIC DIN IAŞI
BULLETIN OF THE POLYTECHNIC INSTITUTE OF JASSY
Tome XXXIX (XLIII), Fasc. 1–4 1993

Section III

ELECTROTECHNICS. ENERGETICS. ELECTRONICS

CONTENTS

Pp.

CAMELIA PETRESCU, Calculation of the Electric Field of a Line Charge in the Presence of a Dielectric Tube (English, Romanian summary) 7

HUGO ROSMAN, Sur la définition de la puissance réactive dans les circuits électriques, en régime permanent périodique nonharmonique (French, Romanian summary) 17

ADRIAN LEUCIUC and LIVIU GORAŞ, Synthesis of a Class of Nonlinear Filters (English, Romanian summary) 27

PAUL COTAE and N.D. ALEXANDRU, A Class of Generalized Constant Envelope Shaping Functions (English, Romanian summary) 33

PAUL COTAE and N.D. ALEXANDRU, Some General Remarks on Smoothed Shaping Functions (English, Romanian summary) 39

IRINEL CASIAN, Characteristic Output and Semi-infinite Distributed Systems (English, Romanian summary) 45

MARIANA BUZDUGA et VALENTIN BUZDUGA, Sur l'inversion des polynômes d'approximation des caractéristiques des éléments nonlinéaires (French, Romanian summary) 51

RADU URSULEAN and I. SUCHAR, On Generating Random Variables with Gaussian Distribution (English, Romanian summary) 59

DORU-FLORIN CHIPER, A Highly Parallel Architecture which Efficiently Operate with Boolean Functions (English, Romanian summary) 65

N. DAMEAN, Considerations Concerning the Thermic Regime in the Measurement Process of Resistances (English, Romanian summary) 76

ADRIAN CREŢU, RADU COCIU, ELENA CREŢU et LIVIA COCIU, Méthode de zéro et appareil pour la mesure des paramètres des bobines linéaires (French, Romanian summary) 83

C. SĂRMĂŞANU, M. CREŢU et LIVIU BRENIUC, Sur une méthode de mesure en flux du volume des grumes (French, Romanian summary) 91

	Pp.
AL. SIMION, Sur les conventions unitaires pour l'énonciation des équations des circuits électriques (French, Romanian summary)	97
MIRCEA-SORIN OPRIŞOR and SIMONA-ANA CABA, On the Experimental Tests Results Regarding the Undersynchronous Condensers Braking of the Asynchronous Three-Phase Motor (English, Romanian summary)	105
GH. CÂRŢINĂ et VIRGIL ALEXANDRESCU, L'augmentation de la vitesse de calcul dans les problèmes d'optimisation du réglage tension–puissance réactive (French, Romanian summary)	117
M. GAVRILAŞ, Remarks about the Study of Self-Compensated Overhead Lines with Bundled Conductors (English, Romanian summary)	121
JAN IGNAT, Sur l'application de la méthode d'identification et localisation d'une mise à terre à l'aide du contrôle des déphasages dans les réseaux électriques de moyenne tension ayant le point neutre mis à terre (French, Romanian summary)	129
BOOK REVIEWS	137

BULETINUL INSTITULUI POLITEHNIC DIN IAŞI
BULLETIN OF THE POLYTECHNIC INSTITUTE OF JASSY
Tomul XXXIX (XLIII), Fasc. 1–4 1993

Secţia III

ELECTROTEHNICĂ. ENERGETICĂ. ELECTRONICĂ

SUMAR

Pag.

CAMELIA PETRESCU, Calculul câmpului electric al unei sarcini liniare în prezenţa unui tub dielectric (engl., rez. rom.) 7

HUGO ROSMAN, Asupra definiţiei puterii reactive în circuite electrice în regim permanent periodic nearmonic (franc., rez. rom.) 17

ADRIAN LEUCIUC şi LIVIU GORAŞ, Sinteza unei clase de filtre neliniare (engl., rez. rom.) 27

PAUL COTAE şi N.D. ALEXANDRU, O clasă generalizată de funcţii de anvelopă constantă (engl., rez. rom.) 33

PAUL COTAE şi N.D. ALEXANDRU, Câteva observaţii generale asupra funcţiilor „netede" (engl., rez. rom.) 39

IRINEL CASIAN, Sisteme distribuite semi-infinite şi „terminaţia caracteristică" (engl., rez. rom.) 45

MARIANA BUZDUGA şi VALENTIN BUZDUGA, Asupra inversării polinoamelor de aproximare a caracteristicilor elementelor neliniare (franc., rez. rom.) 51

RADU URSULEAN şi I. SUCHAR, Asupra generării variabilelor aleatoare cu distribuţie gaussiană (engl., rez. rom.) 59

DORU-FLORIN CHIPER, O arhitectură cu grad ridicat de paralelism ce operează eficient cu funcţii booleene (engl., rez. rom.) 65

N. DAMEAN, Consideraţii privind regimul termic în procesul de măsurare a rezistenţelor (engl., rez. rom.) 76

ADRIAN CREŢU, RADU COCIU, ELENA CREŢU şi LIVIA COCIU, Metodă de zero şi aparat pentru măsurarea parametrilor bobinelor liniare (franc., rez. rom.) 83

C. SĂRMĂŞANU, M. CREŢU şi LIVIU BRENIUC, Asupra unei metode de măsurare în flux a volumului la buşteni (franc., rez. rom.) 91

	Pag.
AL. SIMION, Propuneri de convenţii unitare pentru scrierea ecuaţiilor circuitelor electrice (franc., rez. rom.)	97
MIRCEA-SORIN OPRIŞOR şi SIMONA-ANA CABA, Rezultatele încercărilor frânării subsincrone cu condensatoare a motorului asincron trifazat (engl., rez. rom.)	105
GH. CÂRŢINĂ şi VIRGIL ALEXANDRESCU, Creşterea vitezei de calcul în problemele de optimizare a reglajului tensiune–putere reactivă (franc., rez. rom.)	117
M. GAVRILAŞ, Contribuţii la studiul liniilor electrice autocompensate cu faze scindate (engl., rez. rom.)	121
JAN IGNAT, Cu privire la aplicarea metodei bazate pe controlul defazajelor în reţele cu neutrul izolat (franc., rez. rom.)	129
RECENZII	137

BULETINUL INSTITUTULUI POLITEHNIC DIN IAŞI
Tomul XXXIX (XLIII), Fasc. 1–4, 1993
Secţia III
ELECTROTEHNICĂ. ENERGETICĂ. ELECTRONICĂ

D.C. 612.319.7

CALCULATION OF THE ELECTRIC FIELD OF A LINE CHARGE IN THE PRESENCE OF A DIELECTRIC TUBE

BY
CAMELIA PETRESCU

1. Introduction

The method of images, applied for conductors neighboring conducting surfaces (plane, cylinder, sphere) proves useful sometimes in the case of field computation when boundaries between two (or more) dielectrics appear. Classical electrostatics books give the solution for the electric potential created by a line charge in infinite space when a plane or cylindrical surface between two dielectrics appears [1] ... [3].

This paper presents the solution given by the images' method relative to a dielectric tube surrounded by dielectric media. The solution is compared to those obtained using the separation of variable method.

2. Problem Definition

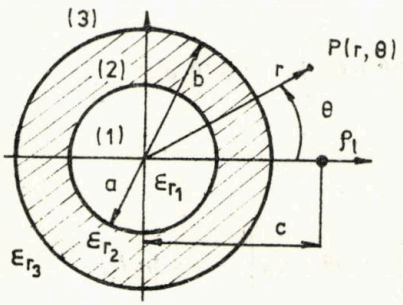

Fig. 1

A dielectric tube having the dielectric constant ε_{r_2}, the inner radius a, and the outer radius b, has the length much greater than its radius (Fig. 1).

The dielectric constant is piece-wise constant:

$$\varepsilon_r = \begin{cases} \varepsilon_{r_1}, & 0 < r < a, \\ \varepsilon_{r_2}, & a < r < b, \\ \varepsilon_{r_3}, & r > b. \end{cases}$$

A line charge (ρ_l) is placed in axial direction in the point $r = c$, $\theta = 0$. The electric potential satisfies the L a p l a c e equation at all points, except the point

$r = c$, $\theta = 0$. The symmetry of the problem requires that:

$$V(r, \theta) = V(r, -\theta).$$

3. Solution by Means of the Separation of Variable Method

Outside the dielectric tube the potential is given both by the line charge [2]:

$$V_3'(r, \theta) = \frac{\rho_l}{2\pi\varepsilon_{r_3}\varepsilon_0}\left[\sum_{n=1}^{\infty}\frac{1}{n}\left(\frac{r}{c}\right)^n \cos n\theta - \ln c\right] + C_1 \tag{1}$$

and by the polarized tube [2]:

$$V_3''(r, \theta) = \frac{\rho_l}{2\pi\varepsilon_0\varepsilon_{r_3}}\sum_{n=1}^{\infty}\frac{A_n}{r^n}\cos n\theta, \tag{2}$$

so that:

$$V_3(r, \theta) = \frac{\rho_l}{2\pi\varepsilon_0\varepsilon_{r_3}}\left\{\sum_{n=1}^{\infty}\left[\frac{1}{n}\left(\frac{r}{c}\right)^n + \frac{A_n}{r^n}\right]\cos n\theta - \ln c\right\} + C_1. \tag{3}$$

In the other two regions the potential is given by:

$$V_1(r, \theta) = \frac{\rho_l}{2\pi\varepsilon_0\varepsilon_{r_3}}\left(\sum_{n=1}^{\infty} E_n r^n \cos n\theta + C_2\right), \quad r \in (0, a], \tag{4}$$

and

$$V_2(r, \theta) = \frac{\rho_l}{2\pi\varepsilon_0\varepsilon_{r_3}}\left[\left(\sum_{n=1}^{\infty} B_n r^n + \frac{D_n}{r^n}\right)\cos n\theta + C_3\right], \quad r \in [a, b], \tag{5}$$

respectively.

The constants A_n, B_n, D_n and E_n may be obtained from the four boundary conditions at the surfaces $r = a$ and $r = b$:

(6)

$$E_{1\theta} = E_{2\theta}|_{r=a}, \quad E_{2\theta} = E_{3\theta}|_{r=b}; \quad \varepsilon_{r_1} E_{1r} = \varepsilon_{r_2} E_{2r}|_{r=a}, \quad \varepsilon_{r_2} E_{2r} = \varepsilon_{r_3} E_{3r}|_{r=b},$$

where the index θ denotes the tangential component and the index r – the radial one. System (6) has the solution:

$$(7)\qquad \begin{cases} A_n = \dfrac{K_1 b^{2n} + K_2 a^{2n}}{nc^n[1+K_1K_2(a/b)^{2n}]}, & B_n = \dfrac{2\varepsilon_{r_3}/(\varepsilon_{r_2}+\varepsilon_{r_3})}{nc^n[1+K_1K_2(a/b)^{2n}]}, \\ D_n = \dfrac{2\varepsilon_{r_3}a^{2n}K_2/(\varepsilon_{r_2}+\varepsilon_{r_3})}{nc^n[1+K_1K_2(a/b)^{2n}]}, & E_n = \dfrac{4\varepsilon_{r_3}\varepsilon_{r_2}/(\varepsilon_{r_1}+\varepsilon_{r_2})(\varepsilon_{r_2}+\varepsilon_{r_3})}{nc^n[1+K_1K_2(a/b)^{2n}]}, \end{cases}$$

where:

$$(8)\qquad K_1 = \frac{\varepsilon_{r_3}-\varepsilon_{r_2}}{\varepsilon_{r_3}+\varepsilon_{r_2}}, \quad K_2 = \frac{\varepsilon_{r_2}-\varepsilon_{r_1}}{\varepsilon_{r_1}+\varepsilon_{r_2}}.$$

The case $a = 0$, substituted in (7), gives immediately the wellknown solution for the potential established by a line charge in the presence of a dielectric cylinder [1].

The components of the electric field are:

$$\boldsymbol{E_r}(r,\theta) = \begin{cases} \dfrac{-2\varepsilon_{r_2}\rho_l}{\pi\varepsilon_0}\displaystyle\sum_{n=1}^{\infty}\frac{r^{n-1}\cos n\theta}{c^n v(n)}, & r\in[0,a], \\ \dfrac{-\rho_l}{\pi\varepsilon_0}\displaystyle\sum_{n=1}^{\infty}\frac{[(\varepsilon_{r_1}+\varepsilon_{r_2})r^{n-1}-a^{2n}/r^{n+1}(\varepsilon_{r_2}-\varepsilon_{r_1})]\cos n\theta}{c^n v(n)}, & r\in[a,b], \\ \dfrac{-\rho_l}{2\pi\varepsilon_0\varepsilon_{r_3}}\displaystyle\sum_{n=1}^{\infty}\left\{\frac{r^{n-1}}{c^n}-\frac{(b^2/c)^n}{r^{n+1}}\left[\frac{(\varepsilon_{r_2}+\varepsilon_{r_1})(\varepsilon_{r_3}-\varepsilon_{r_2})}{v(n)}+\right.\right. & \\ \left.\left.+\dfrac{(a/b)^{2n}(\varepsilon_{r_2}-\varepsilon_{r_1})(\varepsilon_{r_3}+\varepsilon_{r_2})}{v(n)}\right]\right\}, & r\in[b,c], \end{cases}$$

(9)

$$\boldsymbol{E_\theta}(r,\theta) = \begin{cases} \dfrac{2\varepsilon_{r_2}\rho_l}{\pi\varepsilon_0}\displaystyle\sum_{n=1}^{\infty}\frac{r^{n-1}}{c^n}\cdot\frac{\sin n\theta}{v(n)}, & r\in[0,a], \\ \dfrac{\rho_l}{\pi\varepsilon_0}\displaystyle\sum_{n=1}^{\infty}\left[(\varepsilon_{r_1}+\varepsilon_{r_2})r^{n-1}+\frac{a^{2n}}{r^{n+1}}(\varepsilon_{r_2}-\varepsilon_{r_1})\right]\frac{\sin n\theta}{c^n v(n)}, & r\in[a,b], \\ \dfrac{\rho_l}{2\pi\varepsilon_{r_0}\varepsilon_{r_3}}\displaystyle\sum_{n=1}^{\infty}\left[\frac{r^{n-1}}{c^n}+\frac{(b^2/c)^n}{r^{n+1}}\cdot\frac{K_1+(a/b)^nK_2}{1+K_1K_2(a/b)^{2n}}\right]\sin n\theta, & r\in[b,c), \end{cases}$$

where:

$$v(n) = (\varepsilon_{r_2}+\varepsilon_{r_1})(\varepsilon_{r_2}+\varepsilon_{r_3}) - (\varepsilon_{r_2}-\varepsilon_{r_3})(\varepsilon_{r_2}-\varepsilon_{r_1})\left(\frac{a}{b}\right)^{2n}.$$

If the change of variables $c = r_0$ and $\theta = \theta - \theta_0$ is made, then the expressions (3)...(5), give, for $\rho_l = 1$, G r e e n's function $G((r,\theta)|(r_0,\theta_0))$ in infinite space for a dielectric tube.

4. Solution by Means of the Image Method

The image method can't be applied directly for the geometry presented in Fig. 1. In order to use this method a conformal transform is applied. The complex function:

$$w = \ln\frac{z}{c} = \ln\frac{r}{c} + \mathrm{j}\theta, \tag{10}$$

where $z = re^{\mathrm{j}\theta}$, transforms the circles $r = k$ in the z-plane into straight lines $x = \ln(r/c)$ in the w-plane, and the straight lines $\theta = \alpha$ into the straight lines $y = \theta$ in the w-plane. Region $r < a$ is transformed into $x < \ln(a/c)$, region $r \in [a,b]$ into $x \in [\ln(a/c), \ln(b/c)]$ and the region $r > b$ into $x > \ln(b/c)$, situated in the w-plane. The origin $r = 0$ corresponds to the point $x \to -\infty$ in the w-plane. The straight line $\theta = \pm\pi$ in the z-plane makes a cut in order to render the function uniform. The geometry obtained in the w-plane is presented in Fig. 2.

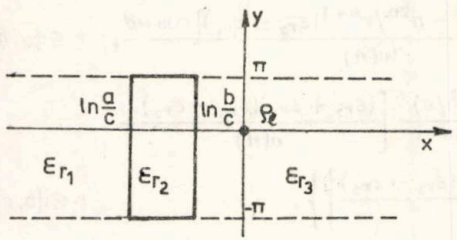

Fig. 2

The line charge is placed in the origin of the w-plane. The field configuration presented in Figs. 1 and 2 are identical if the same boundary conditions are met, namely: a) the electric potential and the normal component of the flux density are continuous for $x = \ln(a/c)$ and $x = \ln(b/c)$; b) the electric field has only radial component for $\theta = \pm\pi$.

The first condition gives a series of line charges disposed as follows:

1° For $r < a$ the line charges are placed in the points $x = 2p\ln(b/a)$, $y = 0$ and have the values $\rho_{l_p} = (-K_1K_2)^p(1-K_1)(1-K_2)\rho_l$, $(p = 0,1,2,...)$, (Fig. 3).

2° For $r \in (a,b)$ a set of line charges is placed in the points $(2p\ln(b/a), 0)$ with $\rho_{1l_p} = (-K_1K_2)^p(1-K_1)\rho_l$, $(p = 0,1,2,...)$, for the positive x-axis and another set of images is placed along the negative x-axis at the points $(-2\ln(c/b) - 2(p+1)\ln(b/a), 0)$ having the line charges $\rho_{2l_p} = K_2(-K_1K_2)^p(1-K_1)\rho_l$, (Fig. 4).

3° For $r > b$ the images are placed at the following points: a) $(0,0)$ – a line charge ρ_l; b) $(-2\ln(c/b), 0)$ – a line charge $K_1\rho_l$; c) $(-2\ln(c/b) - 2(p+1)\ln(b/a), 0)$ – a distribution of line charges with the values $\rho_{l_p} = K_2(-K_1K_2)^p(1-K_1^2)\rho_l$, $(p = 0,1,2,...)$, (Fig. 5).

The constants K_1 and K_2 are given by the expressions (8) being identical with those derived in the separation of variable method.

$$E(w) =$$

(11)

$$= \begin{cases} \dfrac{(1-K_1)(1-K_2)\rho_l}{2\pi\varepsilon_0\varepsilon_{r_1}} \displaystyle\sum_{p=0}^{\infty}\sum_{q=-\infty}^{\infty} \frac{-(K_1K_2)^p}{w^* - [2p\ln(b/a) + \mathrm{j}2q\pi]^*}, & x < \ln\dfrac{a}{c}, \\ \dfrac{(1-K_1)\rho_l}{2\pi\varepsilon_0\varepsilon_{r_2}} \displaystyle\sum_{p=0}^{\infty}\sum_{q=-\infty}^{\infty} \frac{(-K_1K_2)^p}{w^* - [2p\ln(b/a) + \mathrm{j}2q\pi]^*} + \\ + \dfrac{K_2(1-K_1)\rho_l}{2\pi\varepsilon_0\varepsilon_{r_2}} \displaystyle\sum_{p=0}^{\infty}\sum_{q=-\infty}^{\infty} \frac{(-K_1K_2)^p}{w^* - [-2\ln(c/b) - 2(p+1)\ln(b/a) + \mathrm{j}2q\pi]^*}, \\ \qquad\qquad x \in \left(\ln\dfrac{a}{c}, \ln\dfrac{b}{c}\right) \\ \dfrac{\rho_l}{2\pi\varepsilon_0\varepsilon_{r_3}} \left(\displaystyle\sum_{q=-\infty}^{\infty} \left\{ \frac{1}{w^* + \mathrm{j}2q\pi} + \frac{K_1}{w^* - [2\ln(b/c) + \mathrm{j}2q\pi]^*} + \right.\right. \\ \left.\left. + K_2(1-K_1^2) \displaystyle\sum_{p=0}^{\infty} \frac{(-K_1K_2)^p}{w^* - [2\ln(b/c) - 2(p+1)\ln(b/a) + \mathrm{j}2q\pi]^*} \right\} \right), \\ \qquad\qquad x > \ln\dfrac{b}{c}, \end{cases}$$

where $w = u + \mathrm{j}v$ and the symbol w^* stands for the conjugate of w.

In the z-plane the electric field intensity is:

$$E(z) = E(w)\left(\frac{\mathrm{d}w}{\mathrm{d}z}\right)^*,$$

with $\mathrm{d}w/\mathrm{d}z = 1/z$.

The components of the electric field intensity are given by expressions:

(12)

$$\begin{cases} E_r(r,\theta) = \dfrac{1}{2\pi\varepsilon_{r_i} r\varepsilon_0} \displaystyle\sum_p \sum_q \frac{\rho_{lp}[\ln(r/c) - x_{p,q}]}{[\ln(r/c) - x_{p,q}]^2 + (\theta - y_{p,q})^2} = \Re e[E(z)], \\ E_\theta(r,\theta) = \dfrac{1}{2\pi\varepsilon_{r_i} r\varepsilon_0} \displaystyle\sum_p \sum_q \frac{\rho_{lp}(\theta - y_{p,q})}{[\ln(r/c) - x_{p,q}]^2 + (\theta - y_{p,q})^2} = \Im m[E(z)], \end{cases}$$

where $(x_{p,q}, y_{p,q})$ is the position of a generic image line charge $\rho_{l_{p,q}}$. The index $i = 1$, or 2, or 3 depends on the medium where the field is computed.

5. Numerical Results

In order to compare the solution obtained with the two methods a PASCAL program was written.

The compiler used gives 11 significant digits.

The modulus of the electric field intensity was computed for several values of r and θ in the three above designed regions. The numerical values considered were: $a = 2.25$ cm, $b = 2.75$ cm, $\varepsilon_{r_1} = \varepsilon_{r_3} = 1$, $\varepsilon_{r_2} = 4$ and $c = 3$ cm or $c = 5$ cm.

Table 1

The Ratio between the Electric Field Modulus Computed with the Images Method and with the Separation of Variables Method

Nr.	θ / $\rho = r/c$	0	$\frac{\pi}{4}$	$\frac{\pi}{2}$	$\frac{3\pi}{4}$	π	Region	c cm
1.	0.0075	77.0	77.3	77.0	76.7	76.5	(1)	3
2.	0.23	3.02	2.9	2.59	2.24	2.08	(1)	5
3.	0.3825	1.99	1.89	1.60	1.24	1.06	(1)	3
4.	0.4545	1.71	1.06	1.01	0.98	0.78	(2)	5
5.	0.5045	1.41	1.05	0.99	0.89	0.38	(2)	5
6.	0.5545	1.29	1.54	0.81	0.40	0.16	(3)	5
7.	0.7575	1.19	1.01	0.98	0.89	0.28	(2)	3
8.	0.7795	1.13	1.09	0.68	0.32	0.05	(3)	5
9.	0.8408	1.06	0.99	0.95	0.83	0.03	(2)	3
10.	0.9242	1.03	0.81	0.60	0.30	0.11	(3)	3
11.	0.9658	1.02	0.80	0.58	0.33	0.13	(3)	3

Table 1 presents the results obtained for $E_{\text{im}}/E_{\text{var. sep.}}$ representing the ratio between the values obtained with the two methods. These results show that there are regions where the two solutions give almost identical results and there are other regions where the results are quite different. The largest errors are obtained for small values of $\rho = r/c$ and for θ close to π. These facts may be explained by the presence of the factor $1/r$ in the expressions of E_r and E_θ obtained with the images method (a factor which does not exist in the solution given by the separation of variables method in region (1)) and also by the fact that $\theta = \pi$ is a cut in the z-plane.

The rate of convergence is significantly higher for the separation of variables method for a given precision. The value of ρ for which the ratio $E_{\text{im}}/E_{\text{var. sep.}}$ is closest to unity, decreases with increasing θ between the values $\rho \approx 1$, for $\theta = 0$ and $\theta \approx 0.38$ for $\theta = \pi$. The band width in the radial direction for which the error is under 10% when using the second method decreases with increasing θ.

All these observation show that the separation of variables method is more efficient than the images method both concerning the rate of convergence and the precision.

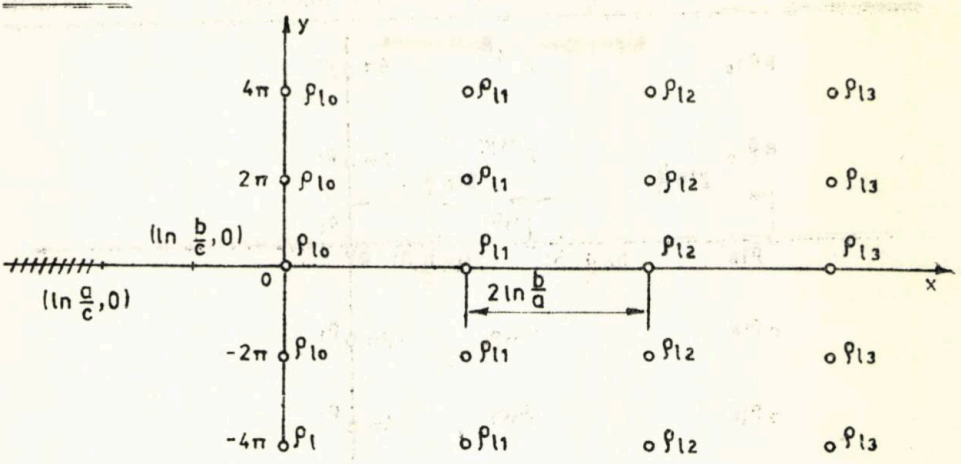

Region 1: $r < a$

Fig. 3

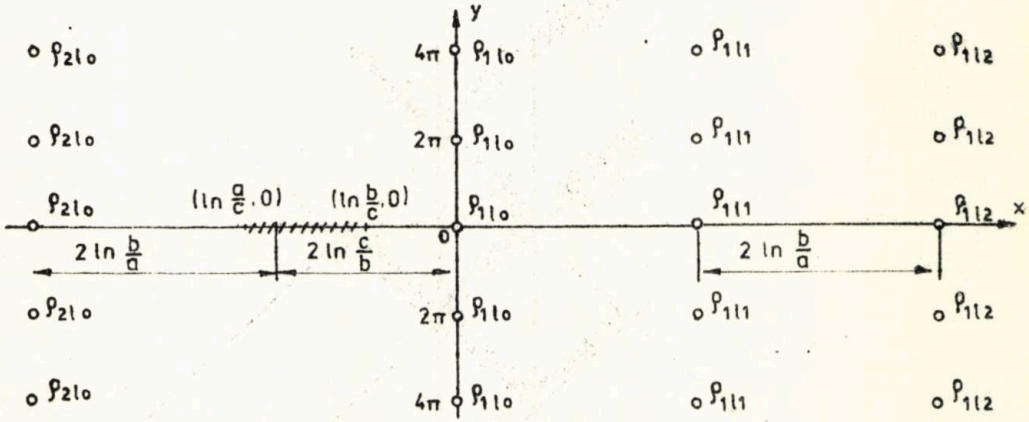

Region 2: $r \in [a, b]$

Fig. 4

Fig. 6 gives an outline of the principle used in obtaining the images in the x-direction.

The second boundary condition requires that $E_\theta = 0$ for $\theta = \pm\pi$. This implies $E_y = 0$ in the w plane for $y = \pm\pi$ thus imposing a repetition of the image obtained along the $0x$-axis in direction y, for $y = 2q\pi$, $q \in Z$.

Figs. 3...5 represent the images meeting the two boundary conditions.

The electric field intensity in the w-plane, computed with the relation $E = -\left(\frac{dW}{dw}\right)^*$, is given by expressions:

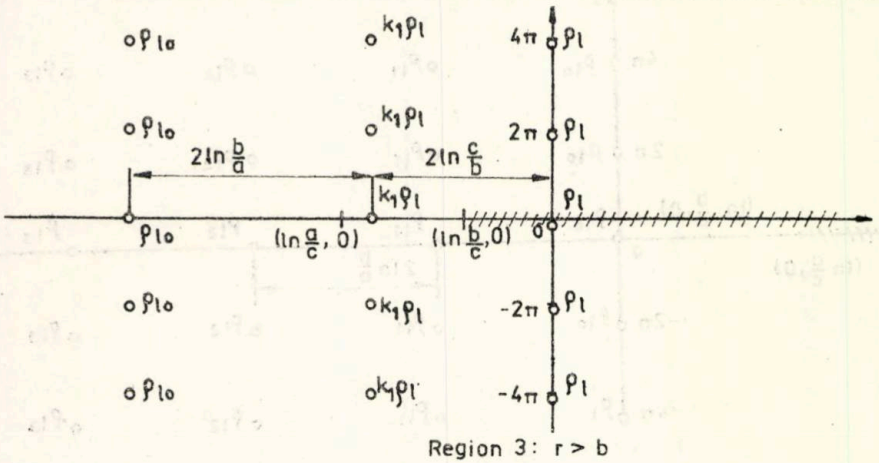
ρ1o
k1ρ1
4π ρ1
2π ρ1
2ln b/a
2ln c/b
(ln a/c, 0)
(ln b/c, 0)
-2π ρ1
-4π ρ1
Region 3: r > b

Fig. 5

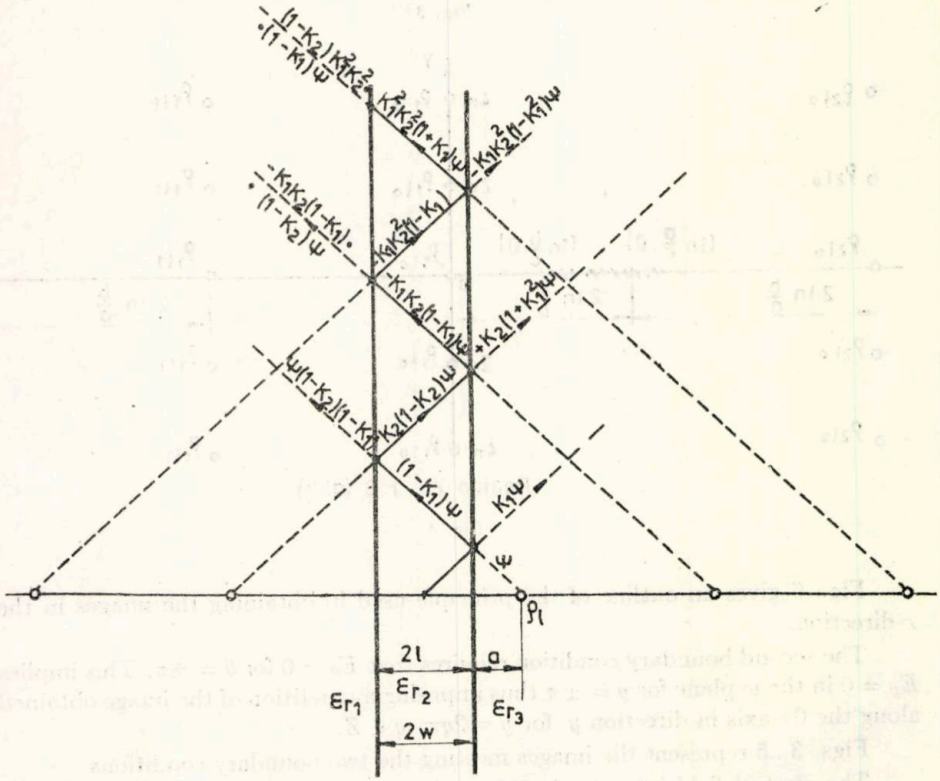
2l
a
2w
εr1
εr2
εr3
ρ1

Fig. 6

6. Conclusions

Two solutions for the electric field created by a line charge in the presence of a dielectric tube are derived: one obtained with help of the separation of variables method and the other with the images method relative to a dielectric slab, this new configuration being obtained from the original one after a conformal transformation is applied.

Numerical results show that the two solutions do not behave similarly at all points of the analyzed field region. The conformal transformation introduces the factor $1/r$ in the expressions of the electric field components in all the three domains of the problem, ($r \in [0,a]$, $r \in [a,b]$, $r \in [b,c]$), a factor which is deliberately excluded in the region $r \in [0,a]$ from the solution obtained with the separation of variables method. This particular factor worsens the accuracy of the solution obtained with the electric images method.

Another drawback for the method presented in §4 is the cut made in the z-plane by the conformal transformation used, for $\theta = \pm\pi$, a cut which introduces great disturbances in the numerical values of the field for θ close to π.

All these facts, and also the greater rate of convergence, make the separation of variables technique the better choice for the computation of the electric field.

However the solution obtained in §4 for the electric field created by a line charge in the presence of a dielectric slab, surrounded by other dielectric media, may be applied successfully for this configuration.

Received, December 17, 1992

Polytechnic Institute, Jassy,
Department of Electrotechnics

REFERENCES

1. S m i t h e W.R, *Static and Dynamic Electricity.* Mc. Graw Hill, 1956.
2. D u r a n d R., *Electrostatique et magnétostatique.* Masson, Paris, 1957.
3. A n g o t A., *Compléments de mathématiques.* Editions de la Revue d'Optique, Paris, 1961.
4. S i l v e s t e r P.P., F e r r a r i R.L., *Finite Elements for Electrical Engineering.* Cambridge University Press, 1983.

CALCULUL CÂMPULUI ELECTRIC AL UNEI SARCINI LINIARE ÎN PREZENŢA UNUI TUB DIELECTRIC

(Rezumat)

Se prezintă soluţia pentru intensitatea câmpului electric produsă de o sarcină liniară în prezenţa unui tub dielectric, Soluţia este obţinută pe două căi: mai întâi cu ajutorul metodei separării variabilelor şi apoi cu ajutorul metodei imaginilor electrice utilizată în configuraţia obţinută după ce se aplică o transformare conformă configuraţiei originale.

În final se efectuează o analiză numerică comparativă a celor două metode privind precizia şi viteza de convergenţă.

BULETINUL INSTITUTULUI POLITEHNIC DIN IAŞI
Tomul XXXIX (XLIII), Fasc. 1–4, 1993
Secţia III
ELECTROTEHNICĂ. ENERGETICĂ. ELECTRONICĂ

C.D. 621.3.016.5

SUR LA DÉFINITION DE LA PUISSANCE RÉACTIVE DANS LES CIRCUITS ÉLECTRIQUES, EN RÉGIME PERMANENT PÉRIODIQUE NONHARMONIQUE

PAR
HUGO ROSMAN

1. Bien qu'ont passé plus de six décennies depuis que C. I. B u d e a n u a proposé, dans un mémoire devenu célèbre [1], les relations bien connues de calcul des puissances réactive et déformante, dans les circuits électriques (linéaires ou nonlinéaires) en régime permanent périodique nonharmonique, les controverses concernant la definition correcte de ces puissances n'ont cessé ni jusqu'à présent.

La proposition avancée par C.I. B u d e a n u, en 1927, se rapporte, à un uniporte linéaire passif dont la tension et le courant à sa porte d'accès sont donnes par:

$$u=U_0+\sqrt{2}\sum_{k=1}^{n}U_k\sin(k\omega t+\gamma_{u_k}),\quad i=I_0+\sqrt{2}\sum_{k=1}^{n}I_k\sin(k\omega t+\gamma_{i_k}). \tag{1}$$

Dans ce cas la puissance apparente est:

$$S=UI=\sqrt{P^2+Q^2+D^2}, \tag{2}$$

où

$$U=\sqrt{\sum_{k=0}^{n}U_k^2},\quad I=\sqrt{\sum_{k=0}^{n}I_k^2} \tag{3}$$

sont les valeurs efficaces de la tension et du courant,

$$P=\sum_{k=0}^{n}U_kI_k\cos\varphi_k,\quad (\varphi_k=\gamma_{u_k}-\gamma_{i_k}), \tag{4}$$

est la puissance active,

$$Q=\sum_{k=1}^{n}U_kI_k\sin\varphi_k \tag{5}$$

et

$$D=\sqrt{\sum_{p=1}^{\infty}\sum_{\substack{q=1\\p<q}}^{\infty}[U_p^2I_q^2+U_q^2I_p^2-2U_pU_qI_pI_q\cos(\varphi_p-\varphi_q)]} \tag{6}$$

en répresentant les puissances réactive, respectivement déformante.

Le point névralgique de la controverse regarde le mode de définition de la puissance réactive en régime permanent périodique nonharmonique. Le long des années ont été fournis des arguments *pro* et *contra* la relation (5) proposée par C.I. B u d e a n u, qui n'ont pas réussi à trancher d'une façon définitive la controverse qui se manifeste dans la littérature de spécialité. En ce sens on peut citer le mémoire de A. Ţ u g u l e a et C. G o l o v a n o v [2], favorable au point de vue de

B u d e a n u ou la note de L. C z a r n e c k i [3] qui, au contraire, le conteste, en représentant, peut être, les plus récentes parutions dans le domaine du problème se trouvant en litige.

Le but de cette Note est d'apporter de nouveaux arguments capables à soutenir les propositions de C.I. B u d e a n u concernant la modalité de calculer les puissances dans les circuits électriques en régime permanent périodique nonharmonique. Ces arguments découlent du fait que dans le cadre des méthodes symboliques élaborées jusqu'à présent en vue du calcul des puissances en tels régimes, on retrouve, d'une façon systématique, la puissance réactive sous la forme (5). Evidemment on ne peut pas considérer que ces nouveaux arguments résolvent, d'une façon tranchante, la controverse qui existe, en infirmant la point de vue de ceux qui contestent celui de C.I. B u d e a n u. Mais on peut les apprécier comme une contribution à la consolidation des propos qui sont en faveur de ce point de vue.

2. Une première méthode symbolique de calcul des puissances dans les circuits électriques linéaires en régime permanent périodique nonharmonique a fait l'objet d'une Note précédente [4], en se basant sur une idée de B.A. R o z e n f e l d [5]. A savoir on dispose de la possibilité d'attacher à chaque fonction périodique nonharmonique de temps ayant la forme:

$$f(t) = \sum_{k=0}^{\infty} (a_k \cos k\omega t + b_k \sin k\omega t) \tag{7}$$

une grandeur hypercomplexe

$$\hat{F} = \sum_{k=1}^{\infty} (1_k a_k + j_k b_k). \tag{8}$$

En introduisant dans l'espace vectoriel des grandeurs $\hat{F}$ le produit vectoriel, associatif et distributif (par rapport à l'addition), l'espace vectoriel muni avec une telle multiplication est un espace H i l b e r t. L'algèbre construite de cette façon est commutative en représentant une somme directe du corps des nombres réels (générés par 1_0) et de l'ensemble nombrable des corps de nombre complexes (générés par la paire d'éléménts 1_k, j_k, $(k = 1, 2, ...)$). L'élément unité de cet algèbre est:

$$\sum_{k=0}^{\infty} 1_k = 1 \tag{9}$$

et

$$1_k^2 = 1_k,\ j_k^2 = -1_k,\ 1_k j_k = j_k 1_k = j_k,\ 1_k j_l = j_l 1_k = 1_k 1_l = j_k j_l = 0,\ (k \neq l). \tag{10}$$

Si la tension et le courant à la porte d'acces d'un uniporte linéaire sont périodiques mais nonharmoniques et donnés par (1), on peut les écrire et sous la forme équivalente:

$$(11) \qquad u = \sum_{k=0}^{\infty}(U'_k \cos k\omega t + U''_k \sin k\omega t), \quad i = \sum_{k=0}^{\infty}(I'_k \cos k\omega t + I''_k \sin k\omega t),$$

avec

$$(12) \qquad \begin{cases} U'_0 = U_0, & U''_0 = 0, & U'_k = \sqrt{2}U_k \sin \gamma_{u_k}, & U''_k = \sqrt{2}U_k \cos \gamma_{u_k}, \\ I'_0 = I_0, & I''_0 = 0, & I'_k = \sqrt{2}I_k \sin \gamma_{i_k}, & I''_k = \sqrt{2}I_k \cos \gamma_{i_k}. \end{cases}$$

Il est possible à attacher aux relations (11) les grandeurs hypercomplexes:

$$(13) \qquad \hat{U} = \sum_{k=0}^{\infty}(1_k U'_k + j_k U''_k), \quad \hat{I} = \sum_{k=0}^{\infty}(1_k I'_k + j_k I''_k)$$

ainsi que leurs conjuguées:

$$(14) \qquad \hat{U}^* = \sum_{k=0}^{\infty}(1_k U'_k - j_k U''_k), \quad \hat{I}^* = \sum_{k=0}^{\infty}(1_k I'_k - j_k I''_k)$$

de sorte que

$$(15) \qquad \hat{U}\hat{U}^* = U^2 = \sum_{k=0}^{\infty}(U'^2_k + U''^2_k), \quad \hat{I}\hat{I}^* = I^2 = \sum_{k=0}^{\infty}(I'^2_k + I''^2_k)$$

représentent les carrés des valeurs efficaces de la tension et du courant.

Par analogie avec le régime permanent harmonique d'un uniporte linéaire on peut définir, en régime permanent périodique nonharmonique, une *puissance apparente hypercomplexe*, donnée par la relation:

$$(16) \qquad \begin{aligned} \hat{S}' \triangleq \hat{U}\hat{I}^* &= \left[\sum_{k=0}^{n}(1_k U'_k + j_k U''_k)\right]\left[\sum_{k=0}^{n}(1_k I'_k - j_k I''_k)\right] = \\ &= \sum_{k=0}^{n} 1_k (U'_k I'_k + U''_k I''_k) + \sum_{k=0}^{n} j_k (U''_k I'_k - U'_k I''_k), \end{aligned}$$

où l'on a tenu compte des relations (10) et (12). Or, dans le régime permanent harmonique où l'uniporte considéré serait alimenté par l'harmonique d'ordre k de la tension:

$$u_k = U'_k \cos k\omega t + U''_k \sin k\omega t, \quad i_k = I'_k \cos k\omega t + I''_k \sin k\omega t, \tag{17}$$

avec

$$\underline{U}_k = U'_k + \mathrm{j}U''_k, \quad \underline{I}_k = I'_k + \mathrm{j}I''_k, \tag{18}$$

de sorte que

$$\underline{S}_k = \underline{U}_k \underline{I}^*_k = P_k + \mathrm{j}Q_k = U'_k I'_k + U''_k I''_k + \mathrm{j}(U''_k I'_k - U'_k I''_k). \tag{19}$$

Si l'on compare les relations (16) et (19) on peut observer aisément que

$$\hat{S}' = \sum_{k=0}^{n} 1_k P_k + \sum_{k=1}^{n} \mathrm{j}_k Q_k, \tag{20}$$

qui suggère la possibilité de calculer les puissances active et réactive en régime permanent périodique nonharmonique à l'aide des relations (4), respectivement (5), proposées par C.I. B u d e a n u. On peut considérer, par conséquent, que le procédé symbolique présenté ci-dessus peut être envisagé comme une justification supplémentaire de la modalité de calcul de la puissance réactive (et en même temps de la puissance déformante) préconisé par C.I. B u d e a n u.

Il est nécessaire à observer, en second lieu, que

$$|\hat{S}'| \neq S = UI, \tag{21}$$

vu que $|\hat{U}\hat{I}^*| \neq |\hat{U}||\hat{I}^*|$.

3. Une autre méthode symbolique qui permet à aborder le problème concernant l'évaluation correcte de la puissance réactive en régime permanent périodique nonharmonique se réfère seulement au cas particulier mais fréquemment rencontré dans la pratique, où les signaux u, i, périodiques, nonharmoniques, appartiennent à la classe de ceux modulés en amplitude. Il est question de la métode symbolique élaborée par A. B r a i e r [6], basée sur la posibilité d'attacher à n'importe quel signal modulé en amplitude, de la forme:

$$a(t) = A_m[1 + \mu \sin(\omega_1 t + \gamma_{a_1})] \sin(\omega_2 t + \gamma_{a_2}), \tag{22}$$

une grandeur hypercomplexe

$$\hat{A} = A_m(\cos\gamma_{a_1} + \mathrm{j}\sin\gamma_{a_1})\mathrm{v} + \mu A_m(\cos\gamma_{a_1}\cos\gamma_{a_2} + \mathrm{i}\sin\gamma_{a_1}\cos\gamma_{a_2} + \mathrm{j}\cos\gamma_{a_1}\sin\gamma_{a_2} + \mathrm{ij}\sin\gamma_{a_1}\sin\gamma_{a_2})\mathrm{w}, \tag{23}$$

avec

$$\mathrm{i}^2 = -1,\ \mathrm{j}^2 = -1,\ (\mathrm{ij})^2 = (\mathrm{ji})^2 = 1,\ \mathrm{v}^2 = \mathrm{v},\ \mathrm{w}^2 = \mathrm{w},\ \mathrm{vw} = \mathrm{wv} = 0, \tag{24}$$

de sorte que la dérivée par rapport au temps du signal (22), considérée en tant que *original*, ait comme *image* hypercomplexe la multiplication de la grandeur hypercomplexe attachée au signal par l'opérateur:

$$\hat{d} = \mathrm{j}\omega_2\mathrm{v} + (\mathrm{i}\omega_1 + \mathrm{j}\omega_2)\mathrm{w}. \tag{25}$$

Par cette voie on peut étudier le régime permanent des circuits linéaires, excités par des signaux modulés en amplitude (ayant la même fréquence modulatrice, la même fréquence porteuse et éventuellement différents degrés de modulation), à l'aide d'un système d'équations algébriques hypercomplexes, qui représentent les *images* des *équations différentielles (originaux)* satisfaites par les valeures instantanées des signaux. Ainsi cette méthode symbolique représente une généralisation naturelle de celle basée sur l'utilisation des grandeurs complexes utilisée à l'analyse du régime permanent harmonique des circuits linéaires.

La possibilité de déterminer, à l'aide de cette méthode symbolique, les puissances dans un circuit électrique linéaire excité par un signal periodique *modulé* en amplitude a été mise en évidence dans une Note antérieure [7]. Le procédé a été illustré en considérant la situation plus simple où l'excitation est un signal modulé en amplitude ayant la porteuse suprimée mais l'on peut généraliser facilement au cas général où l'excitation est de la forme (22).

Par conséquent on considère un uniporte linéaire excité par une tension modulée en amplitude ayant la porteuse suprimée:

$$u = U_m \sin(\omega_1 t + \gamma_{u_1})\sin(\omega_2 t + \gamma_{u_2}). \tag{26}$$

Le courant, en tant que signal réponse, a, en régime permanent, l'expression [6]:

$$i = I'_m \sin(\omega_1 t + \gamma_{u_1} - \varphi_1)\sin(\omega_2 t + \gamma_{u_2} - \varphi_2) + I''_m \cos(\omega_1 t + \gamma_{u_1} - \varphi_1)\cos(\omega_2 t + \gamma_{u_2} - \varphi_2) \tag{27}$$

Si les signaux ont un caractère périodique, à savoir si:

$$\frac{p}{\omega_1} = \frac{q}{\omega_2} = \frac{1}{\omega}, \quad \left(\omega = \frac{2\pi}{T}\right), \tag{28}$$

alors les puissances active, réactive et déformante, déterminées à l'aide des relations (4)...(6), ont les expressions [7]:

$$P = \frac{1}{4}U_m(I'_m \cos\varphi_1 \cos\varphi_2 + I''_m \sin\varphi_1 \sin\varphi_2), \tag{29}$$

$$Q = \frac{1}{4}U_m(I'_m \sin\varphi_1 \cos\varphi_2 - I''_m \sin\varphi_2 \cos\varphi_1), \tag{30}$$

$$D = \frac{1}{4}U_m\sqrt{I'^2_m \sin^2\varphi_2 + I''^2_m \cos^2\varphi_2}. \tag{31}$$

On peut attacher à la tension (26) et au courant (27) les valeurs efficaces hypercomplexes [6]:

$$\begin{aligned}\hat{U} = {} & \frac{1}{2}U_m \cos\gamma_{u_1} \cos\gamma_{u_2} + \mathrm{i}\frac{1}{2}U_m \sin\gamma_{u_1} \cos\gamma_{u_2} + \mathrm{j}\frac{1}{2}U_m \cos\gamma_{u_1} \sin\gamma_{u_2} + \\ & + \mathrm{ij}\frac{1}{2}U_m \sin\gamma_{u_1} \sin\gamma_{u_2},\end{aligned} \tag{32}$$

respectivement

$$\begin{aligned}\hat{I} = {} & \frac{I'_m}{2}\cos(\gamma_{u_1} - \varphi_1)\cos(\gamma_{u_2} - \varphi_2) + \frac{I''_m}{2}\sin(\gamma_{u_1} - \varphi_1)\sin(\gamma_{u_2} - \varphi_2) + \\ & + \mathrm{i}\left[\frac{I'_m}{2}\sin(\gamma_{u_1} - \varphi_1)\cos(\gamma_{u_2} - \varphi_2) - \frac{I''_m}{2}\cos(\gamma_{u_1} - \varphi_1)\sin(\gamma_{u_2} - \varphi_2)\right] + \\ & + \mathrm{j}\left[\frac{I'_m}{2}\cos(\gamma_{u_1} - \varphi_1)\sin(\gamma_{u_2} - \varphi_2) - \frac{I''_m}{2}\sin(\gamma_{u_1} - \varphi_1)\cos(\gamma_{u_2} - \varphi_2)\right] + \\ & + \mathrm{ij}\left[\frac{I'_m}{2}\sin(\gamma_{u_1} - \varphi_1)\sin(\gamma_{u_2} - \varphi_2) + \frac{I''_m}{2}\cos(\gamma_{u_1} - \varphi_1)\cos(\gamma_{u_2} - \varphi_2)\right],\end{aligned} \tag{33}$$

où

$$U = \frac{U_m}{2}, \; I' = \frac{I'_m}{2}, \; I'' = \frac{I''_m}{2}, \; I = \sqrt{I'^2 + I''^2} \tag{34}$$

sont les valeurs efficaces. Toutefois on peut définir par

$$
\begin{aligned}
\hat{I}^* = {} & \frac{I'_m}{2}\cos(\gamma_{u_1}-\varphi_1)\cos(\gamma_{u_2}-\varphi_2)+\frac{I''_m}{2}\sin(\gamma_{u_1}-\varphi_1)\sin(\gamma_{u_2}-\varphi_2)- \\
& -\mathrm{i}\left[\frac{I'_m}{2}\sin(\gamma_{u_1}-\varphi_1)\cos(\gamma_{u_2}-\varphi_2)-\frac{I''_m}{2}\cos(\gamma_{u_1}-\varphi_1)\sin(\gamma_{u_2}-\varphi_2)\right]- \\
& -\mathrm{j}\left[\frac{I'_m}{2}\cos(\gamma_{u_1}-\varphi_1)\sin(\gamma_{u_2}-\varphi_2)-\frac{I''_m}{2}\sin(\gamma_{u_1}-\varphi_1)\cos(\gamma_{u_2}-\varphi_2)\right]+ \\
& +\mathrm{ij}\left[\frac{I'_m}{2}\sin(\gamma_{u_1}-\varphi_1)\sin(\gamma_{u_2}-\varphi_2)+\frac{I''_m}{2}\cos(\gamma_{u_1}-\varphi_1)\cos(\gamma_{u_2}-\varphi_2)\right]
\end{aligned} \tag{35}
$$

l'une des conjuguées hypercomplexes de $\hat{I}$ de sorte qu'il est possible à concevoir la *puissance apparente hypercomplexe*:

$$\hat{S} \triangleq \hat{U}\hat{I}^*, \tag{36}$$

qui, évidemment, diffère de celle définie à l'aide de la relation (16). Il est nécessaire à observer que dans ce cas:

$$|\hat{S}| = S = UI. \tag{37}$$

Compte tenu de (32) et (35) l'expression (36) conduit à

$$
\begin{aligned}
\hat{S} = {} & \frac{1}{4}U_m(I'_m\cos\varphi_1\cos\varphi_2+I''_m\sin\varphi_1\sin\varphi_2)+\mathrm{i}\frac{1}{4}U_m(I'_m\sin\varphi_1\cos\varphi_2- \\
& -I''_m\sin\varphi_2\cos\varphi_1)+\mathrm{j}\frac{1}{4}U_mI'_m\sin\varphi_2-\mathrm{ij}\frac{1}{4}U_mI''_m\cos\varphi_2.
\end{aligned} \tag{38}
$$

Si l'on compare les relations (29)...(31) avec (38) on observe que:

$$\hat{S} = P+\mathrm{i}Q+\mathrm{j}(D'+\mathrm{i}D''), \tag{39}$$

avec

$$D = \sqrt{D'^2+D''^2} \tag{40}$$

– la puissance déformante. Donc, on peut retrouver la puissance réactive, calculée à l'aide de la relation (5), proposée par C.I. B u d e a n u, en tant que composante de la puissance apparente hypercomplexe, ce qu'on peut considérer

comme un argument supplémentaire en faveur de l'acceptation de celle-ci pour le calcul de la puissance réactive dans le régime permanent périodique nonharmonique. En outre, l'hypothèse émise par C.I. B u d e a n u en 1956 [8], concernant la possibilité d'utiliser, en régime permanent périodique nonharmonique, une puissance apparente quaternionique*) de la forme:

$$\hat{S} = P + jQ + kD, \tag{41}$$

s'avère totalement justifiée dans le cadre du procédé symbolique ci-dessus utilisé pour le calcul des puissances.

4. Compte tenu des résultats acquis dans les §§**2** et **3** on peut aboutir à la conclusion que si l'on utilise, pour le calcul des puissances dans les circuits électriques en régime permanent périodiques nonharmonique les méthodes symboliques ci-dessus, c'est seulement la puissance réactive évaluée à l'aide de la relation (5) proposée par C.I. B u d e a n u qu'on peut la mettre en évidence dans la structure analytique des relations de calcul. Au contraire, on ne peut pas identifier d'autres expressions pour la puissance réactive dans ces relations.

Il est raisonnable à considérer que ces observations, ajoutées aux arguments fournis par la littérature de spécialité concernant le mode de calcul de la puissance réactive dans le régime permanent périodique nonharmonique des circuits électriques, vont contribuer à l'élucidation de la controverse quant au calcul correcte de cette puissance, en constituant un appui en faveur de la proposition de C.I. B u d e a n u de calculer la puissance réactive à l'aide de la relation (5).

Reçue le 1 décembre 1992

Institut Polytechnique, Jassy,
Chaire d'Electrotechnique

BIBLIOGRAPHIE

1. B u d e a n u C.I., *Puissances réactives et fictives.* IRE, Bucarest, 1927.
2. Ţ u g u l e a A., G o l o v a n o v C., *Efectele energetice ale regimului deformant.* ENERG, **III**, 130-162 (1987).
3. C z a r n e c k i L., *What is Wrong with the Budeanu Concept of Reactive and Distorsion Power and Why It Should be Abandoned.* IEEE Trans. on Instrum a Meas., **IM-36**, *3*, 834-837 (1987).
4. R o s m a n H., *Reprezentarea simbolică a puterilor în regim permanent periodic, nearmonic.* Bul. Inst. Polit., Iaşi, **VI(X)**, *3-4*, 261-270 (1960).
5. R o z e n f e l d B.A., *Symboliceskyi metod i vektornye diagrammy dlia nesinusoidal'nyh tokov.* Tr. sem. vekt. i tenz. an., **7**, 381-387 (1949).
6. B r a i e r A., *Utilizarea algebrelor pe corpul real în mecanica vibraţiilor.* Thèse de doctorat, Inst. Polyt., Jassy, 1968.
7. R o s m a n H., B r a i e r A., *Powers in Steady State Regime of a Linear, Passive Oneport Excited by a Periodique, Modulated in Amplitude Signal.* Mem. secţ. şt., Acad. Rom., s.IV (sous presse).
8. B u d e a n u C.I., *Aplicaţii în practica de suprapunere a fenomenelor reactive şi deformante.* Bul. Inst. Polit., Bucureşti, **18**, *3-4*, 245-261 (1956).

*) plutôt hypercomplexe.

ASUPRA DEFINIŢIEI PUTERII REACTIVE ÎN CIRCUITE ELECTRICE ÎN REGIM PERMANENT PERIODIC NEARMONIC

(Rezumat)

În cadrul controversei existente cu privire la evaluarea corectă a puterii reactive în circuite electrice, în regim permanent periodic nearmonic, se aduc noi argumente în favoarea definiţiei acestei puteri propusă de C.I. B u d e a n u în 1927. Aceste argumente se bazează pe faptul că relaţia de calcul a puterii reactive, care intervine în diferite metode simbolice de determinare a puterilor în circuite electrice, în regim permanent nearmonic, este în total acord cu cea propusă de C.I. B u d e a n u.

BULETINUL INSTITUTULUI POLITEHNIC DIN IAŞI
Tomul XXXIX (XLIII), Fasc. 1–4, 1993
Secţia III
ELECTROTEHNICĂ. ENERGETICĂ. ELECTRONICĂ

D.C. 621.318.7

SYNTHESIS OF A CLASS OF NONLINEAR FILTERS

BY
ADRIAN LEUCIUC and LIVIU GORAŞ

1. Introduction

In this paper some preliminary considerations concerning a class of nonlinear filters are presented. The main idea is making the behaviour of the filter dependent on the r.m.s. of the input signal. Many other possibilities, including r.m.s. of filtered versions of the input signal can be imagined. Computer simulations envisaged only first and second order filters having one r.m.s.-dependent parameter.

2. R.M.S. Controlled Filters

As it is well known, a continuous time filter can be described by a transfer function consisting of a ratio of two polynomials:

$$H(s) = \frac{P(s)}{Q(s)} = \frac{a_m s^m + a_{m-1} s^{m-1} + \cdots + a_1 s + a_0}{b_n s^n + b_{n-1} s^{n-1} + \cdots + b_1 s + b_0}. \tag{1}$$

The denominator must be H u r w i t z for stability reasons. In principle, any coefficient of the denominator and numerator polynomials can be made r.m.s. dependent. It is possible to imagine a filtering process of the form:

$$H(s) = \frac{P(s)}{Q(s)} = \frac{a_m(e_{\mathrm{rms}}) s^m + a_{m-1}(e_{\mathrm{rms}}) s^{m-1} + \cdots + a_1(e_{\mathrm{rms}}) s + a_0(e_{\mathrm{rms}})}{b_n(e_{\mathrm{rms}}) s^n + b_{n-1}(e_{\mathrm{rms}}) s^{n-1} + \cdots + b_1(e_{\mathrm{rms}}) s + b_0(e_{\mathrm{rms}})}, \tag{2}$$

where $e_{\mathrm{rms}}(t)$ is the r.m.s. value of the input signal, supposed slowly varying. Obviously such a filter is nonlinear. For slow variations of the r.m.s., the input signal can be considered quasistationary. The synthesis problem can be stated as follows:

Synthesize a structure having a prescribed transfer function $H(s, e_{\text{rms}})|_{s=j\omega}$. Intuitively this means a bidimensional surface dependent on frequency and input r.m.s.

The synthesis can be performed in two steps: a) synthesis of a family of linear filters indexed by the r.m.s. value of the input; b) synthesis of the nonlinear functions $a_i(e_{\text{rms}}), b_j(e_{\text{rms}})$, $(i = 1, ..., m; j = 1, ..., n)$.

The block scheme is presented in Fig. 1 for the case $b_n = 1$.

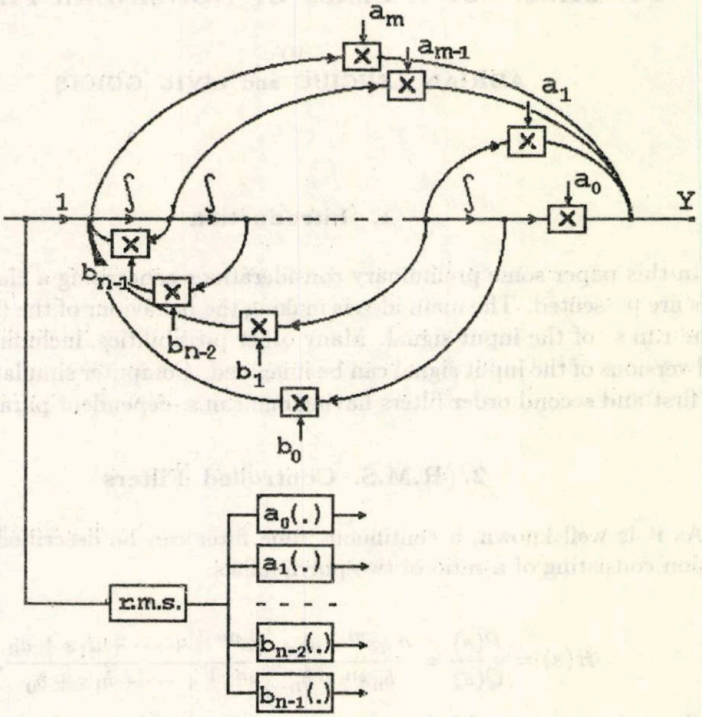

Fig. 1

An alternative realization scheme consists in using pseudo-passive filters based on x-controlled scallor [1], where x can be a voltage or a current.

The above technique can be used for filters derived from passive configurations having simulated elements. The main difference between the two variants is the following: for the first type the coefficients of the transfer function are directly controlled by the r.m.s. through the nonlinearity, since for the second one the r.m.s. controls the values of the elements of the filter; these values are not very simply related to the coefficients of the transfer function.

3. Realization of R.M.S.-controlled Impedances

Obviously, the second variant is much simpler to realize by the synthesis of r.m.s. controlled impedances. In such a structure one can control one, two or more elements of the filter. The solution we propose is based on the General Immittance Converter (GIC) simulation of impedances [2] and on the use of x-controlled scallor [1]. Thus any kind of nonlinear impedances (controlled by the r.m.s. value or any other functional attached to the input signal) can be obtained synthesizing only resistive nonlinear functions. The basic scheme for the realization of such a nonlinear impedance is depicted in Fig. 2.

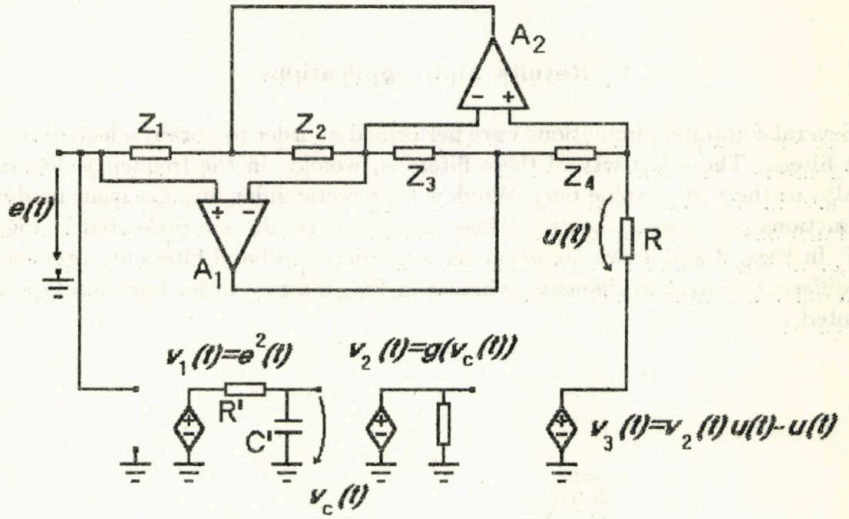

Fig. 2

The GIC structure and the r.m.s. control path are presented in the upper and in the lower side of the figure respectively. Generally, any impedance of the GIC can be r.m.s. controlled. Our choice arose from considerations of grounded impedances.

The voltage-controlled voltage source (VCVS) $v_1(t)$ and the low-pass filter R', C', offer at the output ($v_c(t)$) the r.m.s. value of $e(t)$. Of course the time constant $R'C'$ must be great (with respect to the frequency characteristics of the input signal $e(t)$) in order to achieve, as much as possible, a perfect integrator. The squared transfer characteristic of $v_1(t)$ can be practically obtained with diodes or JFET-s.

The x-controlled scallor (based on a multiplier) is realized by the VCVS $v_3(t)$. Thus, together with the resistor R, it forms a nonlinear resistive element characterized by the following dependence $v(i)$:

$$v(t) - Rv_2(t)i(t) = 0,$$

where

$$v_2(t) = g(v_c(t)) = g(e_{\text{rms}}).$$

The nonlinear impedance simulated by the structure from Fig. 2 has the expression:

$$Z_{\text{eq}} = \frac{Z_1 Z_3}{Z_2 Z_4} Rg(e_{\text{rms}}).$$

4. Results and Applications

Several computer simulations were performed in order to obtain selective nonlinear filters. The selectivity of these filters is twofold: in the frequency domain and also in the r.m.s. value one. Window-type rectangular and gaussian nonlinear functions $g(\cdots)$ were chosen . Three simulation results are presented in Figs. 3,...,5. In Figs. 3 and 4 two nonlinear second order pass-band filters are proposed with different controlled elements, whereas in Fig. 5 a first order low-pass type is presented.

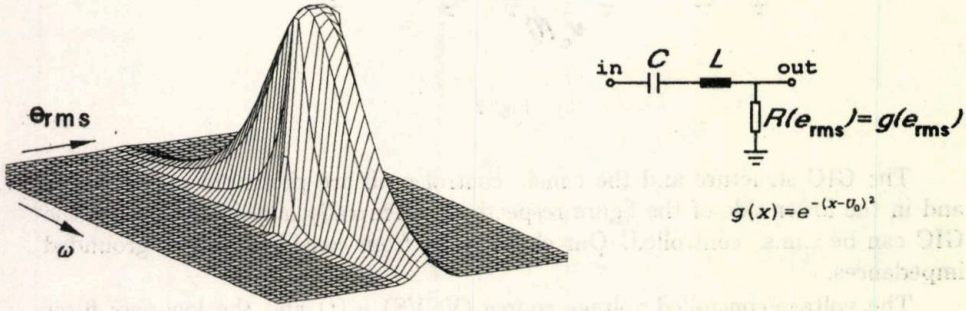

Fig. 3

As a remark, when realizing r.m.s.-controlled impedances which are part of a resonant circuit, multiresonance phenomena can appear.

This class of nonlinear filters is expected to have applications in many fields such as: communications, adaptive filtering and control, noise filtering. The use of such a filter in noise reduction in the field of recording and reproducing the audio signals on and from magnetic tapes is under investigation.

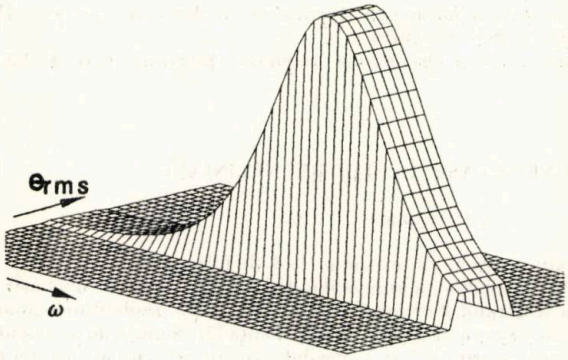

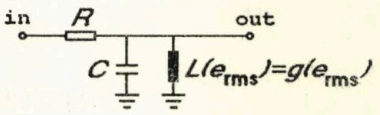

$$g(x) = \sigma(x-U_1) - \sigma(x-U_2)$$

σ - the step function

and $U_2 < U_1$.

Fig. 4

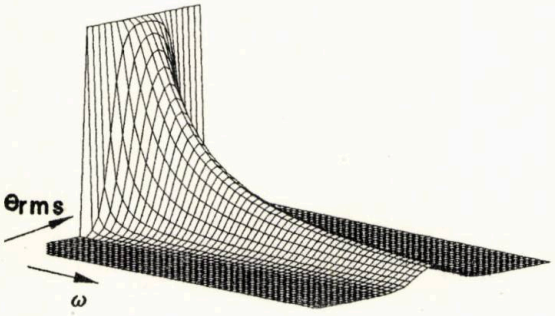

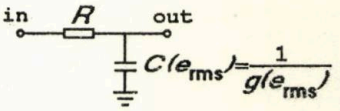

$$g(x) = e^{-(x-U_0)^2}\,[\sigma(x-U_1) - \sigma(x-U_2)]$$

$$U_1 < U_0 < U_2$$

Fig. 5

5. Conclusions

A r.m.s.-controlled class of nonlinear filters and a simple method of synthesizing such a structure based on GIC simulated inductances realization were presented. The simplicity of this method results from the necessity of synthesizing only nonlinear resistive functions. Some general applications of these filters were suggested, but many other could be found, not only for the r.m.s.-controlled filters but for the much general ones commanded by any other functional attached to the input, output or exterior signals.

Received, March 23, 1993

Polytechnic Institute, Jassy,
Department of Electronics

REFERENCES

1. G o r a ş L., *The X-Controlled Scallor and Its Applications to Network Synthesis.* IEEE Trans. Circuits and Syst., **CAS-26**, *4*, 288-290 (1979).

2. A n t o n i o u A., *Gyrator Using Operational Amplifier.* Electron. Lett., **3**, 350-352 (1967).

SINTEZA UNEI CLASE DE FILTRE NELINIARE

(Rezumat)

Se prezintă câteva consideraţii preliminarii privind o clasă de filtre neliniare ale căror caracteristici sunt comandate de valoarea efectivă a semnalului de la intrare. Sinteza unei astfel de structuri se bazează pe utilizarea scalorului x-comandat [1] precum şi pe posibilitatea simulării de diferite impedanţe cu ajutorul convertorului general de impedanţă [2]. Simulările pe calculator au fost efectuate pentru filtre simple de ordinul 1 şi 2. Posibilităţile de aplicare ale acestei clase de filtre în diferite domenii sunt investigate în prezent, urmând ca rezultatele să fie prezentate într-o lucrare ulterioară.

BULETINUL INSTITUTULUI POLITEHNIC DIN IAŞI
Tomul XXXIX (XLIII), Fasc. 1–4, 1993
Secţia III
ELECTROTEHNICĂ. ENERGETICĂ. ELECTRONICĂ

D.C. 621.396.619

A CLASS OF GENERALIZED CONSTANT ENVELOPE SHAPING FUNCTIONS

BY
PAUL COTAE and N.D. ALEXANDRU

1. Introduction

Digital transmission on severely band-limited communication channels implies more efficient modulation techniques in order to maximize the bandwidth efficiency. If in addition the channel is non-linear, or the transmission is performed with portable terminals fed by batteries, then the modulated signal must have a constant envelope.

Constant envelope signals are desirable in communications due to their immunity to fading and non-linear distorsion. The pulse shape, phase transition, and envelope fluctuation are important parameters which affect the spectral properties of modulated, filtered and amplified signals.

Several authors [1]...[7] haved proposed different pulse shapes to improve spectral properties of the modulated signals with constant envelope.

Constant envelope techniques can be generated by modulating the angle of a carrier as it illustrated in Fig. 1 or by a linear quadrature modulation scheme as in Fig. 2.

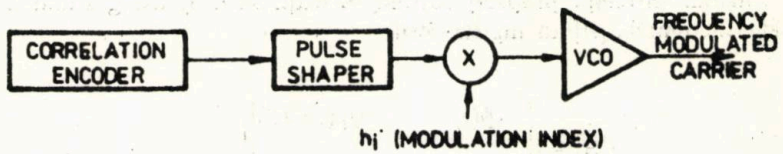

Fig. 1

In Fig. 2 the modulated signal is given by:

$$y(t) = x_i(t)\cos 2\pi f_c t + x_Q(t-T)\sin 2\pi f_c t, \tag{1}$$

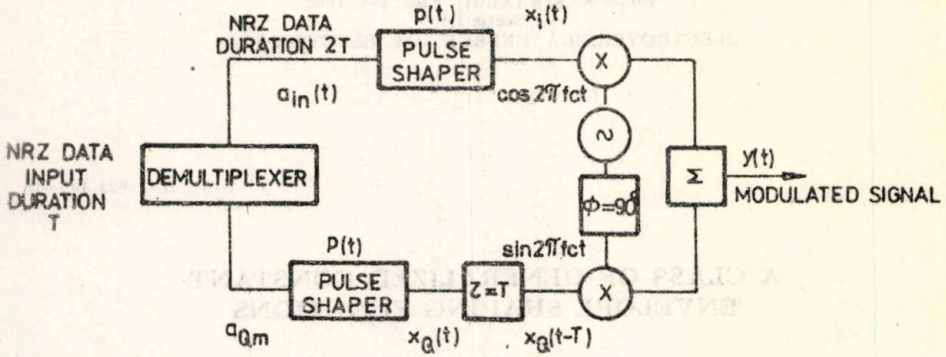

Fig. 2

where:

$$x_i(t) = \sum_{-\infty}^{+\infty} a_{nI}(t)p(t), \quad x_Q(t) = \sum_{-\infty}^{+\infty} a_{mQ}(t)p(t) \tag{2}$$

are the in phase and respectively quadrature pulse streams.

The condition, that should be fulfilled by the $p(t)$ function defined for the interval $[-T, T]$ and null for the rest for maintaining the feature of constant envelope is:

$$\begin{cases} p^2(t) + p^2(t-T) = 1, & 0 \le t \le T, \\ p^2(t) + p^2(t+T) = 1, & -T \le t \le 0. \end{cases} \tag{3}$$

2. Generalized Constant Envelope Functions

The constant envelope property (3) may be expressed by using a matrix approach. Let the matrix $[A]$ having the form:

$$[A] = \begin{bmatrix} p(t) & -p(t-T) \\ p(t-T) & p(t) \end{bmatrix}. \tag{4}$$

The transpose of $[A]$ will be designated by $[A]^*$.

We can easily verify that:

$$[A][A]^* = [I], \ [A]^* = [A]^{-1}, \ \det[A] = \det[A]^* = (\det A)^2 = 1. \tag{5}$$

The matrices satisfying these equalities are called orthogonals. But orthogonal matrices are also encountered in connection with mappings. A linear mapping of an Euclidean space into itself is called orthogonal if the lenghts of the vectors are not changed. We can easily verify that the matrix of an orthogonal mapping relative to a Cartesian basis is an orthogonal one. Consequently, due to the geometric meaning of the determinant of a matrix $[A]$, the pulse function $p(t)$ can have only the form:

$$p(t) = \cos \Phi(t). \tag{6}$$

We now proceed to derive the properties and a general form for the function $\Phi(t)$ which we suppose to be continuous and derivable. Introducing the relation (6) in (3), we easily deduce:

$$p(t - T) = \pm \sin \Phi(t) \tag{7}$$

and now the matrix $[A]$ has the form:

$$[A] = \begin{bmatrix} \cos \Phi(t) & -\sin \Phi(t) \\ \sin \Phi(t) & \cos \Phi(t) \end{bmatrix}. \tag{8}$$

It is a standard exercise to show that:

$$[A]^n = \begin{bmatrix} \cos n\Phi(t) & -\sin n\Phi(t) \\ \sin n\Phi(t) & \cos n\Phi(t) \end{bmatrix}. \tag{9}$$

Applying the expressions (6) for $p(t)$ and (7) for $p(t - T)$ to (3), we get:

$$[\cos \Phi(t - T) - \sin \Phi(t)][\cos \Phi(t - T) + \sin \Phi(t)] = 0. \tag{10}$$

Thus we have arrived at formulas which give the $\Phi(t)$ for $\forall k \in Z$:

$$\begin{cases} \Phi(t - T) - \Phi(t) = \pm \frac{\pi}{2} + 2k\pi, & \text{(a)}, \\ \Phi(t - T) - \Phi(t) = \pm \frac{\pi}{2} + 2k\pi, & \text{(b)}. \end{cases} \tag{11}$$

We are interested to solve the above equations. We suppose that $\Phi(t)$ can be a sum of two functions: the first is a linear function $\Phi_1(t)$ and the second, $\Phi_2(t)$, is a periodic one.

Applying the L a g r a n g e's theorem to (11 a) we obtain:

$$\Phi'(c) = (-4k \pm 1)\frac{\pi}{2T},$$

where $c \in (t - T,\ t)$ and therefore

$$\Phi_1(t) = (-4k' \pm 1)\frac{\pi t}{2T}, \quad \forall k' \in Z. \tag{12}$$

For $\Phi_2(t)$ we can verify that $\Phi_2(t) = \Phi_2(t - T)$. A short investigation of this function by taking into acount (6), (7), (11 a) leads to $\Phi_2(t) = \sin\frac{2\pi t}{T}$.

Considering the power series expansion of $\arcsin x$ function:

$$\arcsin x = x + \frac{1}{6}x^3 + \frac{3}{40}x^5 + \cdots \tag{13}$$

and putting $x = \sin\frac{2\pi t}{T}$ we obtain:

$$\frac{\pi t}{2T} = \frac{1}{4}\sin\frac{2\pi t}{T} + \frac{1}{24}\sin\frac{2\pi t}{T} + \frac{3}{160}\sin^5\frac{2\pi t}{T} + \cdots \tag{14}$$

For $k' = 0$ and keeping the first N terms of (14) it results that $\Phi(t)$ has the form:

$$\Phi(t) = \frac{\pi t}{2T} - \sum_{i=1}^{N} A_{2i-1}\sin^{2i-1}\frac{2\pi t}{T}. \tag{15}$$

Using the M o i v r e's identity:

$$[\cos\Phi(t) + \mathrm{i}\sin\Phi(t)]^n = \cos n\Phi(t) + \mathrm{i}\sin n\Phi(t), \tag{16}$$

for $n = 2i + 1$, it results:

$$\sin\Phi(t) =$$

(17)

$$= \frac{(-1)^{\frac{n+1}{2}}}{2^{n-1}}\left[\sin n\Phi(t) - \binom{n}{1}\sin(n-2)\Phi(t) + \binom{n}{2}\sin(n-4)\Phi(t) + \cdots\right].$$

Changing every term in (15) and taking into account the functions:

(18) $$1, \cos\frac{\pi t}{T}, \sin\frac{\pi t}{T}, \cos\frac{2\pi t}{T}, \sin\frac{2\pi t}{T}, \ldots, \cos\frac{n\pi t}{T}, \sin\frac{n\pi t}{T}, \ldots$$

(this function set forms an orthogonal system on the interval $[-T, T]$)we deduce for $\Phi(t)$:

(19) $$\Phi(t) = \frac{\pi t}{2T} - \sum_{i=1}^{N} \lambda_{2i-1} \sin\frac{(2i-1)2\pi t}{T}.$$

We conclude that this right hand side is a linear combination of even argument terms in $\sin(\cdots)$ of (18). The odd argument terms in cosine might be expected to be the solution of equation (11 b). This time the $\Phi(t)$ function has another linear part of (18) with odd argument. By the relation (11 b) it can easily verified that $\Phi(t) = \pm\frac{\pi}{4} + \Phi_3(t) + k\pi$ and we deduce (for $k = 0$) in the same manner the second form for $\Phi(t)$:

(20) $$\Phi(t) = \frac{\pi}{4}\left[1 - \sum_{i=1}^{M} \mu_{2i-1} \cos(2i-1)\frac{\pi t}{T}\right].$$

It can be noticed that the two forms proposed for $\Phi(t)$ are equal. This has been obtained by an adequately choice of transformation.

3. Particular Cases

1. $N = 0$, $k' = 0$ in (12), (15), (19); $\Phi(t) = \frac{\pi t}{2T}$, the MSK signal is obtained [3], [6].

2. $N = 1$, $k' = 0$ in (12), (14), (19); $\Phi(t) = \frac{\pi t}{2T} - \frac{1}{4}\sin\frac{2\pi t}{T}$, the SFSK (sinusoidal FSK) signal is obtained [2].

3. $N \geq 2$ represents the form proposed in [5].

4. $M > 1$ in (20); the class $\cos\Phi(t)$ of CSK modulation is obtained, [4].

4. Conclusions

A general form for constant envelope functions has been proposed. These functions has been showed to be an even argument sum of sine terms or an odd argument sum of cosine terms of an orthogonal basis. This form has been particularized for different modulation techniques met in the literature. In order to find new shaping functions the coefficients must be particularized.

Received, September 10, 1990

Polytechnic Institute, Jassy,
Department of Communications

REFERENCES

1. Alexandru N.D., Cotae P., *Telegraphy and Data Transmission* (in Romanian). Polytechnic Institute, Jassy, 1987.

2. Amoroso F., *Pulse and Spectrum Manipulation in the Frequency (Minimum) Shift Keying (MSK) Format.* IEEE Trans. Commun., **COM-24**, *8*, 381-384 (1976).

3. Simon M.K., *A Generalization of Minimum Shift Keying (MSK) Type Signaling Based Upon Input Data Symbol Pulse Shaping.* IEEE Trans. Commun., **COM-24**, *8*, 845-856 (1976).

4. Kalet I., *A Look at Crosstalk in Quadrature-Carrier Modulation Systems.* IEEE Trans. Commun., **COM-25**, *9*, 884-892 (1977).

5. Rabzel M., Pasupathy S., *Spectral Shaping in Minimum Shift Keying (MSK) – Type Signals.* IEEE Trans. Commun., **COM-26**, *1*, 189-195 (1978).

6. Pasupathy S., *Minimum Shift Keying: A Spectral Efficient Modulation.* IEEE Commun. Soc. Mag., **17**, 14-22 (1979).

7. Feher K., *Advanced Digital Communication.* Prentice-Hall, Inc., New Jersey, 1987.

O CLASĂ GENERALIZATĂ DE FUNCŢII DE ANVELOPĂ CONSTANTĂ

(Rezumat)

Prin utilizarea unei tratări matriceale a proprietăţii de anvelopă constantă a semnalelor modulate s-a dedus o clasă generală de funcţii pentru aceste semnale. Semnale modulate, ca de exemplu MSK, SFSK şi CSK, reprezintă cazuri particulare ale clasei de funcţii propuse.

BULETINUL INSTITUTULUI POLITEHNIC DIN IAŞI
Tomul XXXIX (XLIII), Fasc. 1–4, 1993
Secţia III
ELECTROTEHNICĂ. ENERGETICĂ. ELECTRONICĂ

D.C. 621.396.619

SOME GENERAL REMARKS ON SMOOTHED SHAPING FUNCTIONS

BY
PAUL COTAE and N.D. ALEXANDRU

1. Introduction

In order to reduce the bandwidth of quadrature modulated carrier signals, the shaping pulses must be smoothed, by requiring that the shaping functions have more continuous derivatives or by spreading the function over several symbol intervals. Several authors have dealt with this problem [1],...,[4] and many examples were proposed.

The conditions, that should be fulfilled by the $f(t)$ pulse shaping function defined for the interval $[-T,\ T]$ and null for the rest, are:

$$1^\circ \quad \begin{array}{ll} f^2(t) + f^2(t-T) = 1, & 0 \le t \le T, \\ f^2(t) + f^2(t+T) = 1, & -T \le t \le 0, \end{array} \tag{1}$$

for maintaining the feature of constant envelope [1].

$$2^\circ \quad f(-t) = f(t); \tag{2}$$

$f(t)$ should exhibit even symmetry arround the midpoint of the interval $[-T,\ T]$.

$$3^\circ \quad (1 - t/T)f(T-t) = 1 - (t/T)f(t); \tag{3}$$

$f(t)$ should have an odd symetry arround the midpoint of the interval $[-T,\ 0]$, $[0,\ T]$.

$$4^\circ \quad f^{(i-1)}(\pm T) = 0,\ (i = 1, 2, ..., N),\ [2]; \tag{4}$$

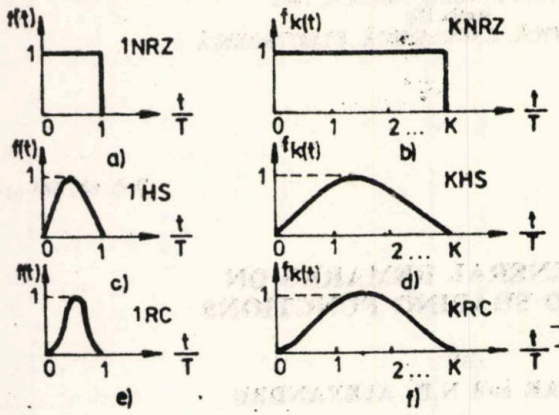

Fig. 1

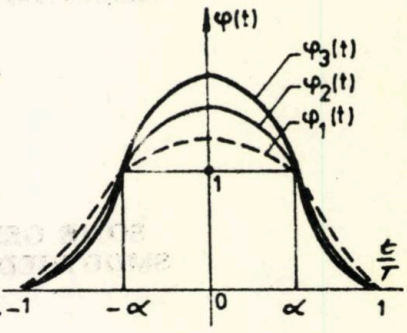

Fig. 2

(5) $$5^\circ \quad f'(t) \leq 0,\ 0 \leq t \leq T;\ f'(t) \geq 0,\ -T \leq t \leq 0.$$

Typical shaping functions are shown in Fig. 1. These functions can be described mathematically by:

(6) $$f(t) = \begin{cases} u(t) - u(t-T) = u(t), & 1 \text{ NRZ, (Fig. 1 } a); \\ u_T(t) \sin \frac{\pi t}{T}, & 1 \text{ HS, (Fig. 1 } c); \\ \frac{1}{2}(1 - \cos \frac{2\pi t}{T}) u_T(t), & 1 \text{ RC, (Fig. 1 } d), \end{cases}$$

where $u(t)$ is the step function, $u_T(t)$ is a rectangular pulse of duration T:

(7) $$u(t) = \begin{cases} 1, t \geq 0, \\ 0, t < 0, \end{cases} \quad u_T(t) = u(t) - u(t-T)$$

and the abreviations mean: 1 NRZ – non return to zero, 1 HS – half cycle sinusoid, 1 RC – raised cosine. When the shaping function is of duration KT, it can be described by:

(8) $$f_K(t) = \begin{cases} u(t) - u(t-KT) = u_{KT}(t), & \text{K NRZ, (Fig. 1 } b); \\ u_{KT}(t) \sin \frac{\pi t}{KT}, & \text{K HS, (Fig. 1 } d); \\ \frac{1}{2}(1 - \cos \frac{2\pi t}{T}) u_{KT}(t), & \text{K RC, (Fig. 1 } f). \end{cases}$$

The formulas (1) and (2) are satisfied if $f(t) = \cos \Phi(t)$.

2. Smoothed Shaping Functions

Given two well behaved complex valued functions $f(t)$ and $g(t)$ of variable t, their inner product is defined through the following integral:

$$(9) \qquad < f, g >= \int_{-\infty}^{+\infty} f(t)g^*(t)\mathrm{d}t.$$

For $\Phi(t)$ we propose the following form:

$$(10) \qquad \Phi_K(t) = \lambda_K < f_K, g_K >= \lambda_K \int_0^t f_K(\tau)g_K(\tau)\mathrm{d}\tau, \quad 0 \le t \le KT,$$

where $f_K(t)$, $g_K(t)$ were defined in (8), and λ_K is a suitable constant (s. (1)...(5)). The functions $\Phi(t)$ have been calculated in Table 1 for the values of λ_1 listed in Table 2.

It is to be noticed that we obtain $\Phi(t)$ functions characteristic for MSK, such as cos(cos), $\cos^3$ [3], SFSK [1] as well as a new function that is worth being taken into account:

$$(11) \qquad \Phi_1(t) = \frac{4\pi}{3}\int_0^t \frac{1}{4}(1-\cos 2\pi\tau)^2\mathrm{d}\tau = \frac{\pi t}{2T} - \frac{1}{3}\sin\frac{2\pi t}{T} + \frac{1}{24}\sin\frac{4\pi t}{T},$$

Table 1

$\Phi_1(t)=$ $\lambda_1\int_0^t f(\tau)g(\tau)\mathrm{d}\tau$	1 NRZ	1 HS	1 RC
1 NRZ	$\frac{\pi t}{2T}$ MSK	$\frac{\pi}{2}\cdot\frac{1-\cos(\pi t/T)}{2}$ cos(cos)	$\frac{\pi t}{2T} - \frac{1}{4}\sin\frac{2\pi t}{T}$ SFSK
1 HS	$\frac{\pi}{2}\cdot\frac{1-\cos(\pi t/T)}{2}$ cos(cos)	$\frac{\pi t}{2T} - \frac{1}{4}\sin\frac{2\pi t}{T}$ SFSK	$\frac{\pi}{4}(1 - \frac{3}{2}\cos\frac{\pi t}{T} + + \frac{1}{2}\cos^3\frac{3\pi t}{T})$ $\cos^3$
1 RC	$\frac{\pi t}{2T} - \frac{1}{4}\sin\frac{2\pi t}{T}$ SFSK	$\frac{\pi}{4}(1 - \frac{3}{4}\cos\frac{\pi t}{T} + + \frac{1}{2}\cos^3\frac{3\pi t}{T})$ $\cos^3$	$\frac{\pi t}{2T} - \frac{1}{3}\sin\frac{2\pi t}{T} + + \frac{1}{24}\sin\frac{4\pi t}{T}$ RCSK

Table 2

Modulation	MSK	cos(cos)	SFSK	$\cos^3$	RCSK
λ_1	$\frac{\pi}{2}$	$\frac{\pi}{2}$	π	$\frac{3\pi}{4}$	$\frac{4\pi}{3}$

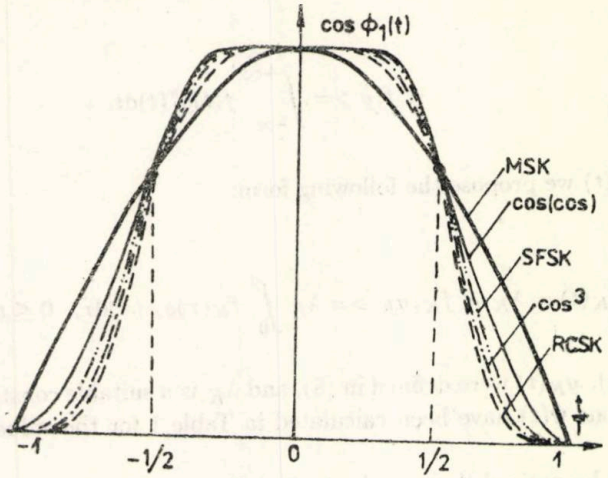

Fig. 3

named RCSK. These functions are illustrated in Fig. 3. The value of K being settled, we can obtain new functions with a well defined shape.

We consider the system of orthogonal functions:

$$1, \cos\frac{\pi t}{T}, \sin\frac{\pi t}{T}, \cos\frac{2\pi t}{T}, \sin\frac{2\pi t}{T}, \ldots, \cos\frac{n\pi t}{T}, \sin\frac{n\pi t}{T}, \ldots \tag{12}$$

defined on the interval $[-T, T]$. We will show that these smoothed shaping functions represent a linear covering of the system of functions (12) on the interval $[-T, T]$.

By linear covering we mean the numerable set of linear combinations forming a system:

$$\varphi_1(t), \varphi_2(t), \varphi_3(t), \ldots, \varphi_n(t) \tag{13}$$

that fulfil the conditions:

$$1.\ \varphi_n(x) \geq 1, \quad x \in (-\alpha, \alpha),$$
$$2.\ 0 \leq \varphi_n(x) \leq 1, \quad x \in [-1, -\alpha) \cup (\alpha, 1],$$

as in Fig.2.

The existence of the function system (13) implies that the system (12) is a closed one. Let us suppose another function $f(t)$ might exist which is orthogonal with all the functions of the system (12). So, there is at least one point $x_0 \in [-T, T]$ so that $f(x_0) \neq 0$ and, without loosing anything of their generality, we may suppose that $f(x_0) = 2c > 0$.

Let us now consider the inner product $< f, \varphi_n >$. Acccording to our supposition $< f, \varphi_n >= 0$, as $\varphi_n(t)$ is a linear combination of the function system **(12)**, that is:

$$\varphi_n(x) = \sum_K \left(a_K \sin \frac{K\pi t}{T} + b_K \cos \frac{K\pi t}{T} \right), \tag{14}$$

and $f(x)$ is orthogonal with all these functions. On the other hand however:

$$< f, \varphi_n >= \int_{-1}^{+1} f(x)\varphi_n(x)\mathrm{d}x \geq \int_{-\alpha}^{+\alpha} f(x)\varphi_n(x)\mathrm{d}x > c \neq 0$$

which refutes the previous supposition. For $\varphi_n(t)$ we propose the form:

$$\varphi_n(t) = \Phi_K^n(t). \tag{15}$$

It is easily to verify that $\varphi_n(t)$ is a linear combination of (12) and these functions represent a linear covering of the interval $[-T, T]$. For $\alpha = T/2$ and $K = 1$, $n = 1$, the obtained functions are illustrated in Fig. 3. All values for λ_1 satisfy the inequality $\lambda_1 > 1$.

3. Conclusions

Generalized forms have been proposed for smoothed shaping functions. They can be used if the coefficients of these functions are adequatly particularized. If the inner product is calculated, we obtain the exact values of these coefficients. It has been proved that these functions represent a linear covering on the $[-T, T]$ interval.

Received, September 10, 1990

Polytechnic Institute, Jassy,
Department of Communications

REFERENCES

1. A m o r o s o F., *Pulse and Spectrum Manipulation in the Minimum (Frequency) Shift Keying (MSK) Format.* IEEE Trans. Commun., **COM-24**, 381-384 (1976).

2. K a l e t I., *A Look at Crosstalk in Quadrature-Carrier Modulation System.* IEEE Trans. Commun., **COM-25**, 884-892 (1977).

3. K o r n I., *Digital Communications.* Van Nostrand Reinhold, NY, 1985.

4. F e h e r K., *Advanced Digital Communications.* Prentice–Hall, Inc., Englewood Cliffs, NJ, 1987.

CÂTEVA OBSERVAŢII GENERALE ASUPRA FUNCŢIILOR „NETEDE"

(Rezumat)

Se prezintă o serie de proprietăţi ale funcţiilor „netede" utilizate în telecomunicaţii. Se definesc o serie de funcţii elementare uzuale. Prin utilizarea produsului scalar al acestor funcţii se regăsesc numeroase exemple propuse în literatura de specialitate. Se propune o nouă funcţie RCSK. Se demonstrează că aceste funcţii constituie o acoperire liniară a intervalului $[-T,T]$.

BULETINUL INSTITUTULUI POLITEHNIC DIN IAŞI
Tomul XXXIX (XLIII), Fasc. 1–4, 1993
Secţia III
ELECTROTEHNICĂ. ENERGETICĂ. ELECTRONICĂ

D.C. 621.315.05

CHARACTERISTIC OUTPUT AND SEMI-INFINITE DISTRIBUTED SYSTEMS

BY
IRINEL CASIAN

1. Introduction

The expression for the fundamental matrix:

$$[H](s,x) = \exp\{([F_0]+[F_1]s+[F_2]s^2)x\} = [I] + ([F_0]+[F_1]s+[F_2]s^2)x + \tag{1}$$
$$+([F_0]+[F_1]s+[F_2]s^2)\frac{x^2}{2!}+\cdots$$

is an entire function of s (analytic for all finite value of s) for all finite x. It is evident, however, that if x is allowed to become infinite, the series may diverge for all finite values of s and the transfer functions would not exist. If the equations represent the behavior of a physical system which might be semi-infinite, we require that the transfer functions exist as $x \to \infty$, since a finite output is to be expected as $x \to \infty$. This requires that certain terms in $\exp\{([F_0]+[F_1]s+[F_2]s^2)x\}$ vanish as $x \to \infty$ in such a manner that the transfer functions continue to exist. As we shall subsequently discover, this implies a particular relationship between the dynamic variables at every point in the system. We shall denote this relationship as the *constraint of characteristic output.*

2. Equation of Characteristic Constraint

To approach the problem we transform the matrix $[F_0]+[F_1]s+[F_2]s^2$ into a diagonal one by means of a similarity transformation:

$$[F_0]+[F_1]s+[F_2]s^2 = [T](s)[\Lambda](s)[T]^{-1}(s), \tag{2}$$

where $[\Lambda](s)$ is a diagonal matrix and $[T](s)$ represents the matrix of the transformation.

$[T](s)$ is the matrix of vectors $[T_i](s)$ (the ith column of $[T](s)$) for which:

$$[F_0] + [F_1]s + [F_2]s^2 = \lambda_i[T_i], \tag{3}$$

where $\lambda_i = \lambda_i(s)$ are assumed to be distinct eigenvalues of the matrix $[F_0]+[F_1]s+[F_2]s^2$, that is, the roots of the characteristic equation:

$$|[I] - [F_0] - [F_1]s - [F_2]s^2| = 0. \tag{4}$$

We can now write the solution of the homogeneous form:

$$\frac{\mathrm{d}[Q]}{\mathrm{d}x} = ([F_0] + [F_1]s + [F_2]s^2)[Q] \tag{5}$$

as:

$$[Q](s,x) = \exp\{[T](s)[\Lambda](s)[T]^{-1}(s)x\}[Q](s,0). \tag{6}$$

By expanding in series the exponential we may write:

$$\begin{aligned}\exp\{[T](s)[\Lambda](s)[T]^{-1}(s)x\} &= [T](s)[T]^{-1}(s) + [T](s)[\Lambda](s)[T]^{-1}(s)x + \\ &+\frac{1}{2!}[T](s)[\Lambda](s)[T]^{-1}(s)x[T](s)[\Lambda](s)[T]^{-1}(s)x + \ldots = \\ &=[T](s)\left\{[I] + [\Lambda](s)x + [\Lambda]^2(s)\frac{x^2}{2!} + \ldots\right\}[T]^{-1}(s).\end{aligned}$$

Hence:

$$[Q](s,x) = [T](s)\mathrm{e}^{[\Lambda](s)x}[T]^{-1}(s)[Q](s,0) \tag{7}$$

so that:

$$[H](s,x) = [T](s)\mathrm{e}^{[\Lambda](s)x}[T]^{-1}(s). \tag{8}$$

If we define a new set of dynamical variables by:

$$[P](s,x) = [T]^{-1}(s)[Q](s,x), \tag{9}$$

expression (7) becomes:

$$[P](s,x) = e^{[\Lambda](s)x}[P](s,0).$$

Thus the transfer function from $P_i(s,0)$ to $P_i(s,x)$ is given by $e^{\lambda_i(s)x}$ since $[\Lambda]$ is a diagonal matrix.

If $e^{\lambda_i(s)x}$ is the transfer function of a physical quantity, it must be analytical to the right of some line $\sigma = \sigma_a$ (the abscissa of absolute convergence) in the plane $s = \sigma + j\omega$ for all positive (not merely finite) values of x. Thus a necessary condition for $e^{\lambda_i(s)x}$ to be a physical transfer function is the existence of a real number σ_a such that $e^{\lambda_i(s)x}$ be analytical for any s with $\Re e(s) > \sigma_a$ for all (not merely finite) positive values of x. In other words, it is necessary that:

$$\lim_{x\to\infty} e^{\lambda_i(s)x}$$

be analytical for $\sigma = \Re e(s)$ sufficiently large. This further requires that $\lambda_i(s)$ be nonpositive for real s. Hence those eigenvalues $\lambda_i(s)$ which are positive for large σ cannot appear in the matrix $e^{[\Lambda](s)x}$. Accordingly, the components of $[P]$ corresponding to these eigenvalues must be identically zero in the semi-infinite system.

Let us assume that m eigenvalues $\lambda_1(s), \lambda_2(s), ..., \lambda_m(s)$ are positive for sufficiently large positive values of s. Then, the corresponding components $P_1(s,x), ..., P_m(s,x)$ must be identically zero. Thus:

$$[P](s,x) = \begin{bmatrix} P_1(s,x) \\ \vdots \\ P_m(s,x) \\ \hline P_{m+1}(s,x) \\ \vdots \\ P_n(s,x) \end{bmatrix} = \begin{bmatrix} [0] \\ \hline [\overline{P}](s,x) \end{bmatrix}.$$

But:

$$[P](s,x) = [T]^{-1}(s)[Q](s,x) = \begin{bmatrix} [W_1](s) \\ [W_2](s) \end{bmatrix} [Q](s,x) = \begin{bmatrix} [0] \\ \hline [\overline{P}](s,x) \end{bmatrix},$$

where $[W_1](s)$ is the matrix consisting of the first m rows of the inverse of the matrix $[T](s)$, the first m columns of which correspond to the m unallowed eigenvalues.

Hence, in a physical system, it is necessary to have:

$$[W_1](s)[Q](s,x) = [0], \quad (\forall x). \tag{10}$$

This is the general form of the *equation of characteristic constraint.*

3. Example

For the transmission-line we have [1]:

$$[F_0]+[F_1]s=\begin{bmatrix} 0 & -(ls+r) \\ -(cs+g) & 0 \end{bmatrix},$$

where: r – series resistance, [Ω/m], l – series inductance, [H/m], g – shunt (leakage conductance), [S/m], c – shunt capacitance, [F/m]. Hence the characteristic equation is given by:

$$\begin{vmatrix} \lambda & ls+r \\ cs+g & \lambda \end{vmatrix}=0.$$

Then:

$$\lambda_1=-\sqrt{(ls+r)(cs+g)}=-\sqrt{zy}, \quad \lambda_2=\sqrt{(ls+r)(cs+g)}=\sqrt{zy},$$

where $z=ls+r$ and $y=cs+g$.

We now calculate the matrix $[T](s)$, using (3), which for $i=1$ gives:

$$\begin{bmatrix} 0 & -z \\ -y & 0 \end{bmatrix}\begin{bmatrix} T_{11} \\ T_{21} \end{bmatrix}=\sqrt{zy}\begin{bmatrix} T_{11} \\ T_{21} \end{bmatrix},$$

so that:

$$T_{21}=\sqrt{\frac{y}{z}}T_{11}=\frac{T_{11}}{Z_0},$$

where $Z_0=\sqrt{z/y}$. Also, for $i=2$:

$$\begin{bmatrix} 0 & -z \\ -y & 0 \end{bmatrix}\begin{bmatrix} T_{12} \\ T_{22} \end{bmatrix}=\sqrt{zy}\begin{bmatrix} T_{12} \\ T_{22} \end{bmatrix},$$

so that $T_{22}=-(T_{12}/Z_0)$. Setting $T_{11}=T_{12}=1$, we have

$$[T]=\begin{bmatrix} 1 & 1 \\ \frac{1}{Z_0} & -\frac{1}{Z_0} \end{bmatrix} \text{ and } [T]^{-1}=\begin{bmatrix} \frac{1}{2} & \frac{Z_0}{2} \\ \frac{1}{2} & -\frac{Z_0}{2} \end{bmatrix}.$$

Thus, since $[Q]=[T][P]$, from (9) we obtain:

$$\begin{bmatrix} V(s,x) \\ I(s,x) \end{bmatrix}=\begin{bmatrix} 1 & 1 \\ \frac{1}{Z_0} & -\frac{1}{Z_0} \end{bmatrix}\begin{bmatrix} P_1(s,x) \\ P_2(s,x) \end{bmatrix},$$

i.e.,

$$V(s,x)=P_1(s,x)+P_2(s,x) \quad I(s,x)=\frac{1}{Z_0}P_1(s,x)-\frac{1}{Z_0}P_2(s,x).$$

Note that P_1 is the well-known incident voltage and P_2 is the reflected voltage. In semi-infinite line, P_2 (corresponding to $\lambda_2=\sqrt{(ls+r)(cs+g)}$), must be absent, i.e., *there must be no reflected wave.*

The requirement that $P_2=0$ for all x means that:

$$V(s,x)-Z_0(s)I(s,x)=0$$

everywhere along the transmission line. This is the *constraint of characteristic output.*

Received, December 10, 1990

Polytechnic Institute,
Jassy, Department of
Applied Electronics

REFERENCES

1. R o s m a n H., *Propagation des ondes de tension et de courant le long d'une ligne non-homogène linéaire.* Bul. Inst. Polit., Jassy, **XXXII (XXXVI)**, *1-4*, s.III, 7-11 (1987).

SISTEME DISTRIBUITE SEMI-INFINITE ŞI „TERMINAŢIA CARACTERISTICĂ"

(Rezumat)

Plecând de la reprezentarea matriceală a sistemelor distribuite se introduc, pe o altă cale decât cea clasică, noţiunile de undă incidentă şi undă reflectată, în legătură cu condiţiile la limită ale sistemelor semi-infinite. În acelaşi context se introduce şi noţiunea de „terminaţie caracteristică".

BULETINUL INSTITUTULUI POLITEHNIC DIN IAŞI
Tomul XXXIX (XLIII), Fasc. 1–4, 1993
Secţia III
ELECTROTEHNICĂ. ENERGETICĂ. ELECTRONICĂ

C.D. 621.316

SUR L'INVERSION DES POLYNÔMES D'APPROXIMATION DES CARACTÉRISTIQUES DES ÉLÉMENTS NONLINÉAIRES

PAR
MARIANA BUZDUGA et VALENTIN BUZDUGA

1. Introduction

En nombreux cas pratiques où la caractéristique nonlinéaire d'un élément de circuit (résistence, bobine ou condensateur) est approximée par un polynôme incomplet du troisième degré, du type:

$$y(x) = a_1 x + a_3 x^3, \quad x \in \mathbf{R}, \tag{1}$$

apparait la nécessité d'obtenir la relation $x(y)$, c'est-à-dire l'inverse de la fonction $y(x)$.

Pour les éléments fréquemment utilisés en pratique dont les caractéristiques sont approximées par un polynôme du type (1), on peut rencontrer, quant aux signes des coefficients, les cas suivants:

a) a_1, $a_3 > 0$ pour des caractéristiques concaves. Exemples: $i(u)$ pour des résistances nonlinéaires du type diodes ou transistors; $u(i)$ pour des résistances nonlinéaires du type régulateurs de tension; $i(\psi)$ ou $H(B)$ pour des bobines à noyau ferromagnétique; $u(q)$ pour des condensateurs à diélectrique nonlinéaire; $C(u)$ pour la capacité nonlinéaire de la jonction $p-n$.

b) $a_1 < 0$, $a_3 > 0$ pour des caractéristiques en N ou S. Exemples: $i(u)$ pour la diode Tunnel, ou $u(i)$ pour le tube à neon.

c) $a_1 > 0$, $a_3 < 0$ pour des caractéristiques en N renversé. Exemples: la caractéristique $i_g(u_a)$ ou $u_g > u_a$, qui met en évidence l'effet dinatron dans les triodes.

Dans ce qui suit on analyse les conditions d'existence et d'obtention des fonctions inverses $x(y)$.

2. Détermination de la fonction $x(y)$

Soit un polynôme incomplet du troisième degré, du type (1), avec a_1, a_3 réels.

Dans les cas où a_1 et a_3 ont le même signe, la fonction (1) s'annule dans l'origine où elle a encore un point d'inflexion; elle est strictement croissante (respectif décroissante) (Fig. 1) et admet une inverse dans tout le domaine de définition.

Conformément aux formules de C a r d a n l'inverse de la fonction est:

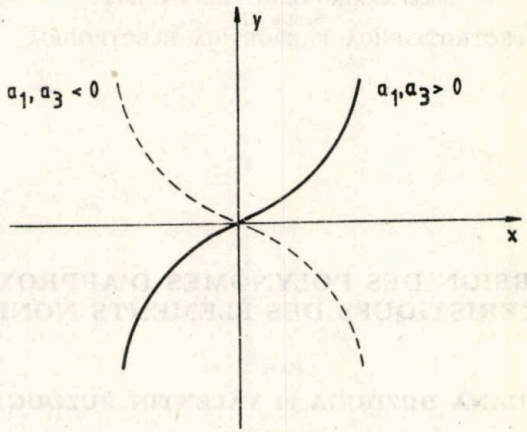

Fig. 1

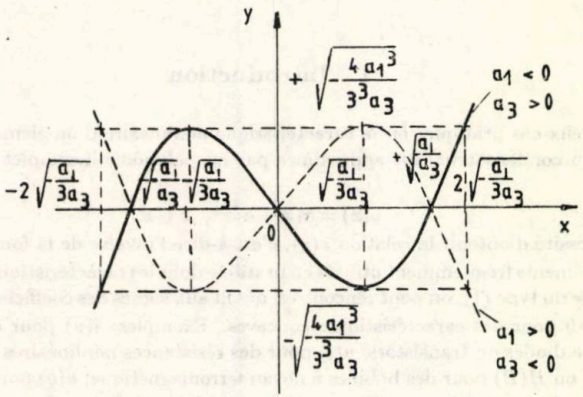

Fig. 2

$$x = \sqrt[3]{\frac{y}{2a_3} + \sqrt{\frac{y^2}{4a_3^2} + \frac{a_1^3}{27a_3^3}}} + \sqrt[3]{\frac{y}{2a_3} - \sqrt{\frac{y^2}{4a_3^2} + \frac{a_1^3}{27a_3^3}}} \tag{2}$$

et elle est réele car le discriminant est positif:

$$\frac{y^2}{4a_3^2} + \frac{a_1^3}{27a_3^3} > 0. \tag{3}$$

Si a_1 et a_3 ont des signes différents la fonction (1) a des extrêmes situés en $x_e = \pm\sqrt{-a_1/3a_3}$ ayant les valeurs $y_e = \pm\sqrt{-4a_1^3/27a_3}$, des zéros en $x = 0$ et $x_0 = \pm\sqrt{-a_1/a_3}$ et un point d'inflexion dans l'origine (Fig. 2).

La fonction n'admet pas une inverse sur tout le domaine de définition, n'étant pas monotone, mais elle admet des fonctions inverses sur les intervalles de monotonie, qu'on peut déterminer à l'aide des formules de C a r d a n, c'est-à-dire:

$$(4)\qquad \begin{cases} x_1 = \sqrt[3]{\frac{y}{2a_3} + \sqrt{\frac{y^2}{4a_3^2} + \frac{a_1^3}{27a_3^3}}} + \sqrt[3]{\frac{y}{2a_3} - \sqrt{\frac{y^2}{4a_3^2} + \frac{a_1^3}{27a_3^3}}}, \\ x_2 = \varepsilon \sqrt[3]{\frac{y}{2a_3} + \sqrt{\frac{y^2}{4a_3^2} + \frac{a_1^3}{27a_3^3}}} + \varepsilon^2 \sqrt[3]{\frac{y}{2a_3} - \sqrt{\frac{y^2}{4a_3^2} + \frac{a_1^3}{27a_3^3}}}, \\ x_3 = \varepsilon^2 \sqrt[3]{\frac{y}{2a_3} + \sqrt{\frac{y^2}{4a_3^2} + \frac{a_1^3}{27a_3^3}}} + \varepsilon \sqrt[3]{\frac{y}{2a_3} - \sqrt{\frac{y^2}{4a_3^2} + \frac{a_1^3}{27a_3^3}}}, \end{cases}$$

ε étant la racine cubique primitive de l'unité:

$$(5)\qquad \varepsilon^2 + \varepsilon + 1 = 0,$$

ce qui est équivalent à:

$$(6)\qquad \varepsilon_1 = \frac{-1 + i\sqrt{3}}{2} = \cos\frac{2\pi}{3} + i\sin\frac{2\pi}{3}, \quad \varepsilon_2 = \frac{-1 - i\sqrt{3}}{2} = \cos\frac{4\pi}{3} + i\sin\frac{4\pi}{3}.$$

La nature des racines dépend du signe du discriminant (3), à savoir:

a) Pour les intervalles $x < -2\sqrt{-a_1/3a_3}$ et $x > 2\sqrt{-a_1/3a_3}$ la fonction $y(x)$ a des valeurs, en module, plus grandes que ses extrêmes locales:

$$(7)\qquad |y| > \sqrt{-\frac{4a_1^3}{27a_3}}$$

et le discriminant (3) a des valeurs positives. En conséquence, dans ces intervalles $y(x)$ admet une seule fonction inverse réele, x_1, les deux autres (x_2, x_3) étant des fonctions complexes.

b) Pour l'intervalle $x \in (-2\sqrt{-a_1/3a_3},\ 2\sqrt{-a_1/3a_3})$, $y(x)$ a des valeurs en module plus petites que ses extrêmes:

$$(8)\qquad |y| < \sqrt{-\frac{4a_1^3}{27a_3}}$$

En conséquence le discriminant a des valeurs négatives et les racines x_1, x_2, x_3 sont toutes les trois réeles.

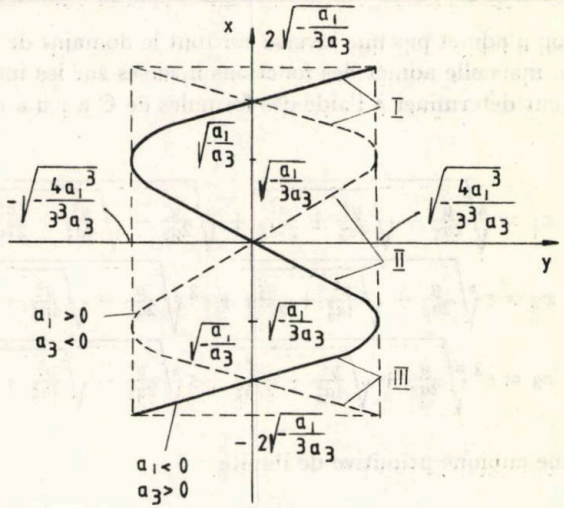

Fig. 3

Dans la Fig. 3 on a représenté les graphiques des inverses $x(y)$ qui correspondent à ce cas.

Il s'avère nécessaire à établir la correspondance qui existe entre les branches *I*, *II*, *III* du graphique et les expressions $x_1(y)$, $x_2(y)$, $x_3(y)$. Dans ce but on écrit les relations (4) sous une forme simplifiée. On introduit les notations:

$$\frac{y}{2a_3} \triangleq a, \quad \frac{y^2}{4a_3^2} + \frac{a_1^3}{27a_3^3} \triangleq -b^2, \quad a + \mathrm{i}b \triangleq z, \quad a, b \in \mathbf{R}. \tag{9}$$

Donc:

$$\begin{cases} x_1 = \sqrt[3]{a+\mathrm{i}b} + \sqrt[3]{a-\mathrm{i}b} = \sqrt[3]{z} + \sqrt[3]{\overline{z}} = \sqrt[3]{z} + \overline{\sqrt[3]{z}} = 2\Re e(\sqrt[3]{z}), \\ x_2 = \varepsilon\sqrt[3]{a+\mathrm{i}b} + \varepsilon^2\sqrt[3]{a-\mathrm{i}b} = \varepsilon\sqrt[3]{z} + \overline{\varepsilon}\sqrt[3]{\overline{z}} = \varepsilon\sqrt[3]{z} + \overline{\varepsilon\sqrt[3]{z}} = 2\Re e(\varepsilon\sqrt[3]{z}), \\ x_3 = \varepsilon^2\sqrt[3]{a+\mathrm{i}b} + \varepsilon\sqrt[3]{a-\mathrm{i}b} = \varepsilon^2\sqrt[3]{z} + \overline{\varepsilon^2}\sqrt[3]{\overline{z}} = \varepsilon^2\sqrt[3]{z} + \overline{\varepsilon^2\sqrt[3]{z}} = 2\Re e(\varepsilon^2\sqrt[3]{z}). \end{cases} \tag{10}$$

Le nombre complexe z peut être écrit encore sous la forme:

$$z = a + \mathrm{i}b = \sqrt{a^2+b^2}(\cos\varphi + \mathrm{i}\sin\varphi) \tag{11}$$

où

$$\varphi = \operatorname{arctg}\frac{b}{a}. \tag{12}$$

Alors:

$$\sqrt[3]{z} = \sqrt[6]{a^2+b^2}\cos\left(\frac{\varphi+2k\pi}{3}+\mathrm{i}\frac{\varphi+2k\pi}{3}\right), \quad (k=0,1,2,...). \tag{13}$$

Les solution x_1, x_2, x_3 sont, respectivement, pour les trois valeurs ci-dessous de k:

a) $k=0$

$$\begin{cases} x_1^{(0)} = 2\Re e(\sqrt[3]{z}) = 2\sqrt[6]{a^2+b^2}\cos\frac{\varphi}{3} \overset{\Delta}{=} x_a, \\ x_2^{(0)} = 2\Re e(\varepsilon\sqrt[3]{z}) = 2\sqrt[6]{a^2+b^2}\cos\left(\frac{\varphi}{3}+\frac{2\pi}{3}\right) \overset{\Delta}{=} x_b, \\ x_3^{(0)} = 2\Re e(\varepsilon^2\sqrt[3]{z}) = 2\sqrt[6]{a^2+b^2}\cos\left(\frac{\varphi}{3}+\frac{4\pi}{3}\right) \overset{\Delta}{=} x_c; \end{cases} \tag{14}$$

b) $k=1$

(15)

$$x_1^{(1)} = 2\sqrt[6]{a^2+b^2}\cos\left(\frac{\varphi}{3}+\frac{2\pi}{3}\right) = x_b, \quad x_2^{(1)} = 2\sqrt[6]{a^2+b^2}\cos\left(\frac{\varphi}{3}+\frac{4\pi}{3}\right) = x_c,$$

$$x_3^{(1)} = 2\sqrt[6]{a^2+b^2}\cos\frac{\varphi}{3} = x_a.$$

c) $k=2$

$$\begin{aligned} x_1^{(2)} &= 2\sqrt[6]{a^2+b^2}\cos\left(\frac{\varphi}{3}+\frac{4\pi}{3}\right) = x_c, \quad x_2^{(2)} = 2\sqrt[6]{a^2+b^2}\cos\frac{\varphi}{3} = x_a, \\ x_3^{(2)} &= 2\sqrt[6]{a^2+b^2}\cos\left(\frac{\varphi}{3}+\frac{2\pi}{3}\right) = x_b. \end{aligned} \tag{16}$$

On observe que quelconque soit k les trois solutions réeles de la fonction $y(x)$ sont les mêmes, quelque soit leur indexation.

Pour établir la correspondance entre les solutions x_a, x_b, x_c et les branches I, II, III du graphique (Fig.3) il faut établir une relation d'ordre entre elles. Sachant que x_a, x_b, x_c sont continues sur leurs domaines de définition, il suffit de comparer les valeurs particulières que celles-ci prennent dans un point de la variable y. Soit ce point $y=0$. Dans le cas $a_1<0$, $a_3>0$ on obtient:

$$\lim_{y\to 0}\varphi = \lim_{y\to 0}\operatorname{arctg}\frac{\sqrt{-\frac{y^2}{4a_3^2}-\frac{a_1^3}{27a_3^3}}}{\frac{y}{a_3}} = \frac{\pi}{2}, \tag{17}$$

compte tenu que le numérateur est toujours positif, donc on est situé dans les quadrants I et II; pour $a_1 > 0,\ a_3 < 0$

$$\lim_{y \to 0} \varphi = \frac{\pi}{2}, \tag{18}$$

avec la même conclusion. Dans tous les deux cas:

$$\sqrt[6]{a^2 + b^2} = \sqrt[6]{\frac{y^2}{4a_3^2} - \frac{y^2}{4a_3^2} - \frac{a_1^3}{27a_3^3}} = \sqrt{-\frac{a_1}{3a_3}} \tag{19}$$

et on a aussi:

$$\begin{cases} x_a = 2\sqrt{-\frac{a_1}{3a_3}} \cos\frac{\varphi}{3} = 2\sqrt{-\frac{a_1}{3a_3}} \cos\frac{\pi}{6} = \sqrt{-\frac{a_1}{a_3}}, \\ x_b = 2\sqrt{-\frac{a_1}{3a_3}} \cos\left(\frac{\varphi}{3} + \frac{2\pi}{3}\right) = 2\sqrt{-\frac{a_1}{3a_3}} \cos\frac{5\pi}{6} = \sqrt{-\frac{a_1}{a_3}}, \\ x_c = 2\sqrt{-\frac{a_1}{3a_3}} \cos\left(\frac{\varphi}{3} + \frac{4\pi}{3}\right) = 2\sqrt{-\frac{a_1}{3a_3}} \cos\frac{3\pi}{2} = 0, \end{cases} \tag{20}$$

donc x_a représente l'expression analytique de la branche notée par I, x_c celle de la branche II et x_b celle de la branche III du graphique.

Les fonctions $x_a(y), x_b(y), x_c(y)$ sont définies dans le même domaine de variation de y où elles sont continues.

c) Dans les points $x = \pm\sqrt{-a_1/3a_3}$, respectivement $y = \pm\sqrt{-4a_1^3/27a_3}$, le discriminant (3) est nul et les racines x_1 et $x_2 = x_3$ sont réeles toutes les trois.

Dans le cas $a_1 > 0,\ a_3 < 0$ on a:

$$x_c = x_a = \sqrt{-\frac{a_1}{3a_3}},\ \text{pour}\ y = \sqrt{-\frac{4a_1^3}{27a_3}}, \tag{21}$$

respectivement

$$x_c = x_b = -\sqrt{-\frac{a_1}{3a_3}},\ \text{pour}\ y = -\sqrt{-\frac{4a_1^3}{27a_3}}; \tag{22}$$

pour $a_1 < 0,\ a_3 > 0$ on a

$$x_c = x_a = \sqrt{-\frac{a_1}{3a_3}},\ \text{pour}\ y = -\sqrt{-\frac{4a_1^3}{27a_3}}, \tag{23}$$

respectivement

$$x_c = x_b = -\sqrt{-\frac{a_1}{3a_3}}, \text{ pour } y = \sqrt{-\frac{4a_1^3}{27a_3}}. \tag{24}$$

Dans les points de frontière entre les domaines analysés, c'est-à-dire en $x = \pm 2\sqrt{-a_1/3a_3}$, quand $y = \pm\sqrt{-4a_1^3/27a_3}$, le discriminant (3) est nul.

Pour $a_1 < 0$, $a_3 > 0$ on a

$$x_a\left(+\sqrt{-4a_1^3/27a_3}\right) = 2\sqrt{-a_1/3a_3} = x_1\left(\sqrt{-4a_1^3/27a_3}\right) \tag{25}$$

et pour $a_1 > 0$, $a_3 < 0$,

$$x_a\left(-\sqrt{-4a_1^3/27a_3}\right) = 2\sqrt{-a_1/3a_3} = x_1\left(-\sqrt{-4a_1^3/27a_3}\right). \tag{26}$$

D'une manière similaire, dans le point $x = -2\sqrt{-a_1/3a_3}$ on a, pour $a_1 > 0$, $a_3 < 0$,

$$x_b\left(+\sqrt{-4a_1^3/27a_3}\right) = -2\sqrt{-a_1/3a_3} = x_1\left(\sqrt{-4a_1^3/27a_3}\right), \tag{27}$$

et pour $a_1 < 0$, $a_3 > 0$,

$$x_b\left(-\sqrt{-4a_1^3/27a_3}\right) = -2\sqrt{-a_1/3a_3} = x_1\left(-\sqrt{-4a_1^3/27a_3}\right). \tag{28}$$

Les relations (25)...(28) montrent que la fonction inverse du polynôme (1), dans les domaines $|x| > 2\sqrt{-a_1/3a_3}$, se continue avec la branche III, respectivement I, du domaine $|x| < 2\sqrt{-a_1/3a_3}$.

3. Conclusions

Pour les caractéristiques des éléments de circuit nonlinéaires qu'on peut représenter par des polynômes incomplets du troisième degré de la forme (1), on considère, d'habitude, que l'expression de la fonction inverse a la forme:

$$x(y) = b_1 x - b_3 x^3, \tag{29}$$

ce qui implique, en réalité, une nouvelle approximation de la caractéristique inverse par un polynôme incomplet du troisième degré, dans un domaine limité de variation de y. Ce procédé introduit une erreur supplémentaire.

Afin d'éviter ces erreurs on déduit les expressions des fonctions inverses du polynôme (1) en fonction du signe des coefficients, dans les intervalles de motonie des fonctions. On démontre aussi la continuité des branches de l'inverse dans les points extrêmes des intervalles étudiés.

Reçue le 15 juillet 1992

Institut Polytechnique, Jassy,
Chaire de Mesures électriques

BIBLIOGRAPHIE

1. S a v i n Gh., R o s m a n H., *Circuite electrice neliniare şi parametrice.* Ed. Tehnică, Bucureşti, 1973.
2. C h u a L.O., *Introduction to Nonlinear Network Theory.* Mc.Graw Hill, NY, 1969.

ASUPRA INVERSĂRII POLINOAMELOR DE APROXIMARE A CARACTERISTICILOR ELEMENTELOR NELINIARE

(Rezumat)

Se analizează condiţiile de existenţă şi de obţinere a funcţiilor inverse ale caracteristicilor neliniare, aproximate prin polinoame incomplete de gradul III, de tipul (1), funcţie de semnul coeficienţilor a_1, a_3, pe baza relaţiilor lui C a r d a n.

BULETINUL INSTITUTULUI POLITEHNIC DIN IAŞI
Tomul XXXIX (XLIII), Fasc. 1–4, 1993
Secţia III
ELECTROTEHNICĂ. ENERGETICĂ. ELECTRONICĂ

D.C. 621.391

ON GENERATING RANDOM VARIABLES WITH GAUSSIAN DISTRIBUTION

BY
RADU URSULEAN and I. SUCHAR

1. Generating Random Variables as Analog Signals

When testing systems one can use random numbers obtained by means of mathematical methods which generate such numbers using relative simple algorithms [1], [8]. This task can be done using a computer or a dedicated hardware. Random numbers can also be generated for certain types of spread-spectrum signals and in this case there are used the so called pseudo-random binary sequences. These sequences are obtained as digital signals by means of shift registers with feedback taken using XOR gates, as in Fig. 1. The feedback is chosen so that the

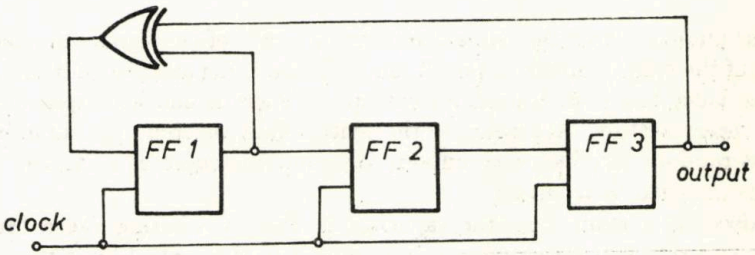

Fig. 1

length of the sequence is the greatest possible for a given number p of flip-flops of the shift register. The feedback for a certain length of the sequence is determined using a so called generator polynomial [2]. The length of the sequence can be furthermore increased combining two such shift registers by means of a demultiplexer, as shown in [3] or an XOR gate as in [7]. The pseudo-random sequences obtained using the mentioned above methods have uniform distribution and are also known as pseudo-white noise. There are integrated circuits that can generate pseudo-white noise both in audio and radio frequencies domains using the same method. Sometimes analog signals are needed and this can be easily achieved using a D/A converter if the desired distribution is an uniform one. Unfortunately generating other distributions as analog signals is a difficult task because rather complicated functional transforms are needed [4]. Such transforms are expensive to perform when dealing with analog signals because of the precision needed for

them; using a computer for the functional transform and then the resulting digital signals to be converted using a D/A converter is also expensive because of the computer itself.

Taking into account the fact that for generating the gaussian distribution as an analog signal, a simple method is proposed in [5], this paper intends to demonstrate why the signals generated using that method have indeed gaussian distribution, and, another thing, that the author of [5] fails to tell us how to choose the parameters in order to obtain a given mean and standard deviation and a very good concordance with the theoretical distribution.

2. A Method for Generating the Gaussian Distribution

In [5] K o r n proposes the following simple method for generating the gaussian distribution: a pseudo-random binary sequence is generated and than this signal is "filtered" by means of a low-pass filter, usually a RC network as in Fig. 2.

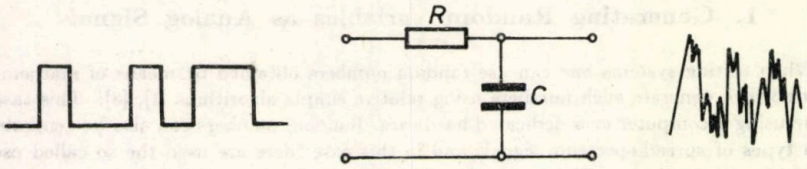

Fig. 2

The quality – from the statistical point of view – of the signal obtained at the output of the simple circuit in Fig. 2 can be tested using samples of it and passing a concordance test (Chi-Square, for example). There is another explanation that makes useless testing. According to the central limit theorem, [6], summing independent random variables with uniform distribution generates a random variable that has gaussian distribution.

Indeed, in certain cases the capacitor in Fig. 2 is acting like a "summing device" and the distribution obtained according to the central limit theorem is a gaussian one. There are a few parameters that must be taken into account in order to be sure that the signal generated using a simple circuit like the one in Fig. 2 (or another with the same transfer function) has the ability to provide the desired signal from the statistical point of view.

Firstly, is worth remembering that every pseudo-random binary sequence that is the input signal of the above mentioned circuit, has the following properties: a) the signal represents a succession of pulses lasting T seconds (the elementary interval of time) or multiples of T and in this intervals only two states are possible: 0 and 1 (low voltage and high voltage respectively); b) the number of intervals during a whole period is $N = 2^p - 1$, where p is the number of flip-flops that are used in the shift register; c) if N_0 and N_1 are the number of 1-s and 0-s during a whole period, then $N_0 + 1 = N_1$; d) if we define a "state" as the sum of elementary time intervals when the signal has the value 1 or 0, then the total number of states

is 2^{p-1}; e) during a period $1/2$ of the states have T seconds, $1/2^2$ have $2*T$ seconds, $1/2^3$ have $3*T$ seconds and there are only two states lasting $p*T$ and $(p-1)*T$ seconds.

It is well known that charging the capacitor in Fig. 2 can be made according to the following equation:

$$u(t) = U[1 - \exp(-t/RC)], \tag{1}$$

where U is the amplitude of the pulse. The value of the voltage across the capacitor when descharged is:

$$u(t) = U_0 \exp(-t/RC), \tag{2}$$

where U_0 is the initial value of the voltage across the capacitor. The relations (1) and (2) are graphically represented in Fig. 3.

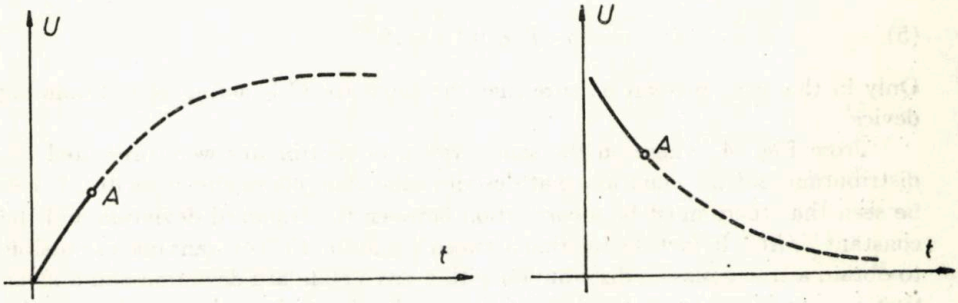

Fig. 3

In order to achieve the summing needed for a gaussian variable, the longest state of the pseudo-radom sequence (that is $p*T$ for 1 and $(p-1)*T$ for 0) must not exceed the point A on the characteristics in Fig. 3, so that the curve can be approximated with a line. That means:

$$p*T \ll 0.1*t_0, \tag{3}$$

where t_0 is obtained solving the following equation:

$$u(t_0) = 0.9*U, \tag{4}$$

or, to put it another way,

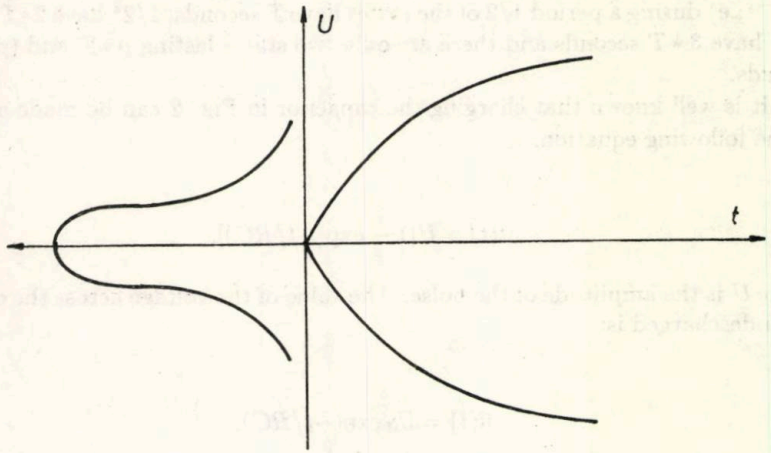

Fig. 4

(5) $$p * T \ll 0.1 * \ln 10^{RC}.$$

Only in this way one can be sure that the capacitor C is acting as a "summing device".

From Fig. 4, where on the same system of coordinates were presented the distribution and the equation that describes the charging of the capacitor, it can be seen that there must be a correlation between the standard deviation and the constant T/RC. In fact the relation between T and the RC constant makes possible to obtain a true gaussian distribution with a given standard deviation and a mean that is – as a voltage – the half of the amplitude of the pulses of the pseudo-random sequence. This mean of the distribution is assured by the fact that, as mentioned above, the time that an one is generated during a whole period of the pseudo-random sequence, equals the time when a zero is generated.

3. A Computer Simulation

In order to verify the correctness of the above mentioned conditions a program that simulates the pseudo-random binary sequence, the charging and the discharging of the capacitor was written. Running the program led us to the following conclusions:

1° The optimum value for T/RC is 0.1 – in this case the Chi-Square test showed the greatest "goodness of fit" – and this can be seen from the histogram in Fig. 5 *a*; choosing a much smaller value but the same amplitude of the pulse (for example $T/RC = 0.02$) makes the distribution asymmetrical as shown in Fig. 5 *b*. A bigger value for T/RC ($T/RC = 1$ for example) trucates the histogram as shown in Fig. 5 *c*.

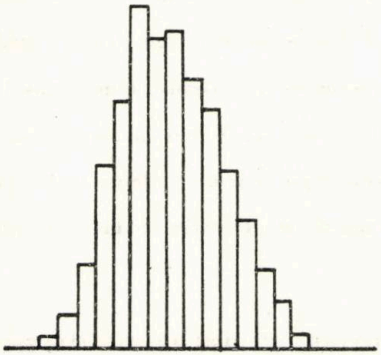

Fig. 5 *a*

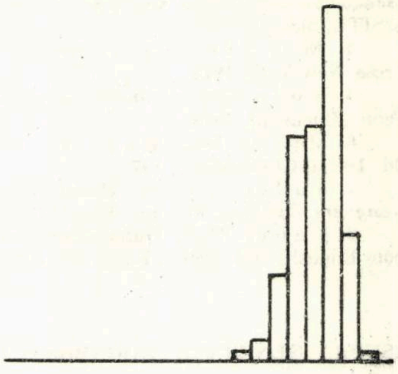

Fig. 5 *b*

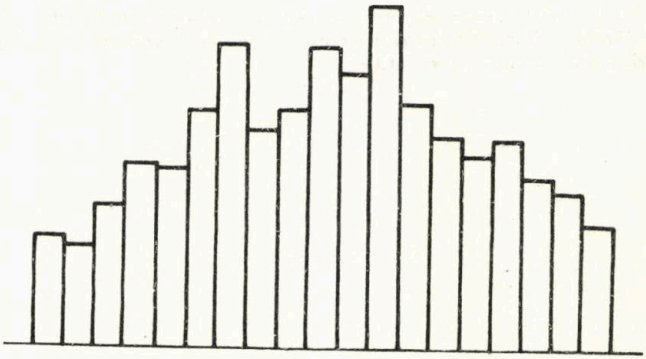

Fig. 5 *c*

2° No matter the shape of the histogram, when (5) is fulfilled, the mean is always half of the amplitude of the pulse; when (5) doesn't hold (when dealing with asymmetrical histograms) the mean has a different value. A mean value equal to 0 can be obtained using a sequence with equal amplitudes but different signs for 1 and 0.

3° The calculated correlation coefficient between T/RC and the obtained standard deviation was 0.9888, another confirmation that our initial supposition was true.

Received, December 16, 1991

Polytechnic Institute, Jassy,
Department of Electrotechnics
and Electrical Machines

REFERENCES

1. V ă d u v a I., *Modele de simulare cu calculatorul.* Ed. Tehn., Bucureşti, 1977.
2. S p ă t a r u Al., *Teoria transmisiunii informaţiei. Coduri şi decizii statistice.* Ed. Tehn., Bucureşti, 1971.

3. U r s u l e a n R., G r i g o r a ş V.A., *Metodă de generare a secvenţelor binare pseudoaleatoare.* In the vol. „Realizări în domeniul electronicii profesionale", Scient. Session, ICSITE, Snagov, 1985.

4. M i r h a m G.A., *Simulation. Statistical Foundations and Methodology.* Academic Press, New York, 1972.

5. K o r n G.A., *Simularea şi măsurarea proceselor aleatoare* (transl. from English). Ed. Tehn., Bucureşti, 1969.

6. M i h o c Gh., M u j a A., D i a t c u E., *Bazele matematice ale teoriei fiabilităţii.* Ed. Dacia, Cluj-Napoca, 1976.

7. A n d e r s o n L.H., *Uniting Number Generators for Long Bit Patterns.* In *Electronics Designers Casebook*, McGraw-Hill, 1979.

8. K n u t h D.E., *Tratat de programarea calculatoarelor. Algoritmi seminumerici* (transl. from English). Ed. Tehn., Bucureşti, 1983.

ASUPRA GENERĂRII VARIABILELOR ALEATOARE CU DISTRIBUŢIE GAUSSIANĂ

(Rezumat)

Se prezintă o modalitate de generare a variabilelor aleatoare cu distribuţie normală precum şi condiţiile ce trebuie îndeplinite pentru a obţine o bună concordanţă cu repartiţia teoretică şi anumite valori pentru parametrii repartiţiei.

BULETINUL INSTITUTULUI POLITEHNIC DIN IAŞI
Tomul XXXIX (XLIII), Fasc. 1–4, 1993
Secţia III
ELECTROTEHNICĂ. ENERGETICĂ. ELECTRONICĂ

D.C. 518.8

A HIGHLY PARALLEL ARCHITECTURE WHICH EFFICIENTLY OPERATE WITH BOOLEAN FUNCTIONS

BY
DORU-FLORIN CHIPER

1. Introduction

In a previous paper [4], we have presented a parallel manner of operating with Boolean functions. In what follows it is proposed a parallel architecture which supports efficiently this parallel manner of operating. The proposed architecture form an array processor which operates in bit-serial word-parallel manner. The overall organization of the specialized array processor together with its instruction set is presented. The proposed architecture is vary suited to VLSI implementation.

2. The Presentation of the Proposed Architecture

One of the basic limiting factor of the von N e u m a n n architectures consists in the so call von N e u m a n n bottleneck, which appears at the communication channel level between the memory and the processing elements. So, is very natural to couple as strong as possible the processing elements with the memory cells to obtain higher processing speeds. For this reason the proposed architecture is based on a such idea.

The proposed architecture represents an array processor which operates in bit-serial word-parallel manner. Array processors belog to the SIMD cathegory of computer organization. This kind of architectures is characterized by a SIMD orientation of the data and instructions streams. (All the processors execute the same instruction but over their own data items from their memory modules). In many applications it is necessary to have a mechanism to activate or deactivate some PE. In the proposed architecture it is implemented a such mechanism based on the presence of a Tag register. The results yield by the processing elements which correspond to a zero in the Tag register can not be stored in their memory modules.

3. The General Organization of the Parallel Processing System

An overview of the parallel processing system is presented in Fig. 1. The main modules which form the parallel processing system are: the Master Processor, the Control Unit, the Processor Array and the I/O processor.

The Master Processor is represented by an usual computer. It assures the interface with the user, sends instructions to the Control Unit and control the I/O operations together with the I/O Processor. The Master Processor communicate with the Array Processor by several registers map in the memory address space of the Master Processor.

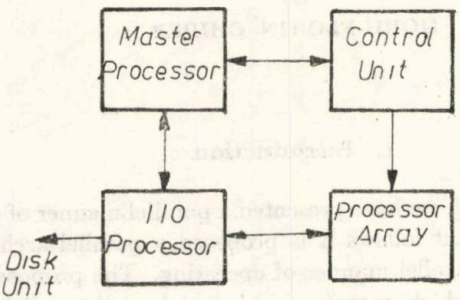

Fig. 1.– Overview of the Parallel Processing System.

The Control Unit sends the bit-slice address for all memory words and the function code for the BFG unit (Boolean Function Generator unit). It controls the Read and Write operations.

During the programs execution it sends the control signals to the all PE (processing elements). It contains several registers and a number of counters which together with the Address Processor are used to implement the loops and form the bit-slices address.

3.1. The I/O Processor

The parallel processing systems are characterized by the appearance of the I/O bottleneck which occurs at the I/O channel level. (This means that the processing speed is limited by the I/O channel bandwidth). To avoid this situation we have to attach an I/O processor to the parallel system. We can thus obtain a fast transfer between the Disk Unit and the Array Processor and between the Master Processor and the Array Processor. The I/O processor have to be designed to allow the data arrangement corresponding to the new format. It consider the I/O data flip-flops as a set of I/O registers. It selects this I/O data flip-flops as a set of registers of 64 bits each, because the data bus between the I/O processor and the Array Processor has 64 bits width. This registers are selected by an I/O data address sent by the I/O processor. The I/O registers addresses are generated by the Address Processor from the I/O Processor. The I/O Processor can be equipped with a

Buffer Memory which permits to I/O Processor to operate in pipeline manner with the Array Processor. The I/O Processor communicates with the Master Processor by several registers mapped in the memory address space of the Master Processor.

The programs are executed as follows: a) part of the program instructions are executed sequential by the Master Processor; b) the other part is executed in parallel by the Array Processor.

The sequential part executes the operations with scalers and controls the I/O operations. The Master Processor loads and reads the I/O registers and the I/O registers and the Control Unit executes the microoperations which achieve the data transfers between PE and I/O registers. The I/O registers can be loaded using the data from the files under the I/O Processor control. The Master Processor controls the data transfer operations sending the necessary instructions to I/O Processor.

4. The Proposed Array Processor Architecture

The overall organization of the proposed Array Processor is presented in Fig. 2. For every memory or „Word" we have associated a PE which operates with one bit from its memory module. The Tag register is used to implement an activation mechanism based on the Tag values stored in the Tag register. If we have a zero in the Tag register then the corresponding PE will be deactivated. That means that the transfer of the result to its memory module will be inhibited. The Array Processor works in bit-serial manner. As a consequence the Array Processor memory which is a RAM one will be accessed „perpendicularly" to their normal usage. The Control Unit (CU) sends a bit address to the memory and all the bits with that address will be accessed. As compared with an ordinary sequential computer we have still an advantage because the number of bits from a word is largely smaller than the number of words from the memory.

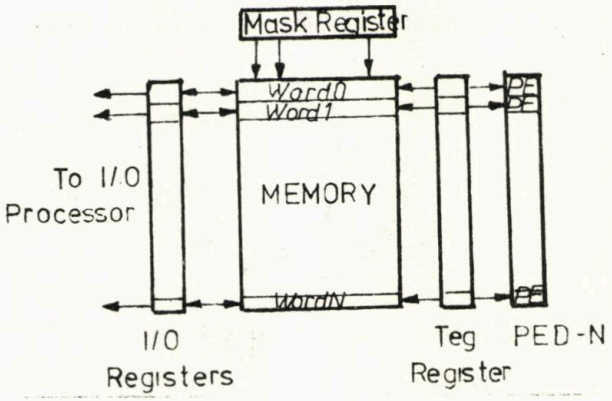

Fig. 2.– The Array Processor Architecture.

An Array Processor which operate in bit-serial mode works with data items organized in fields. Each field is formed of one or several bit-slices. All the memory modules receive the same address from the CU. So, the same bit from all the memory modules (or „words") is accessed. All these bits form a bit-slice. One of the basic task of the CU is to transform the operation with fields in operation with bit-slices. The mask register can be used to select certain bit-slices.

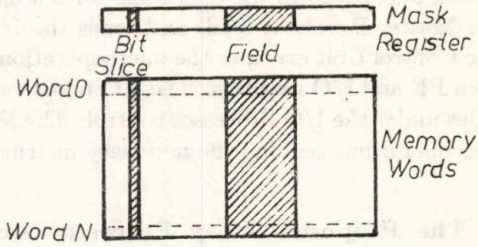

Fig. 3.– Bit-slices and fields.

4.1. The Architecture of a PE together with its Memory Module

In Fig. 4 is presented a processing element (PE) together with its memory module. The processing element consists of a Boolean Function Generator (BFG) and two registers of one bit, the tag register T and the Result register R. The Boolean Function Generator can be implemented with a PROM or a PLA. The BFG implements the 16 BFG functions which consists of elementary logical function. The BFG function cod is sent by the Control Unit. The Tag register together with the associated gates and control signals WR and WRALL implement the mentioned mechanism of PE selection.

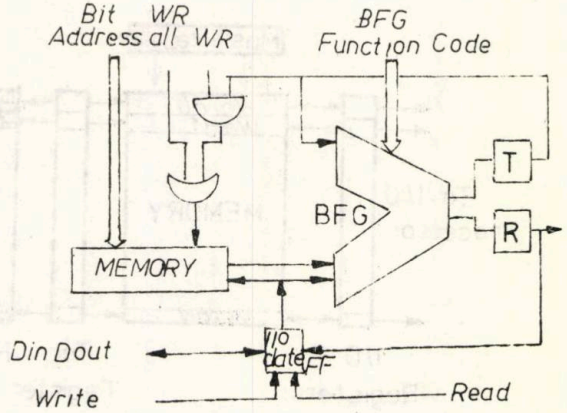

Fig. 4.– A PE and its Memory module.

There are two kind of instructions:

1. Tag-masked instructions for which are activated only the selected PE by means of the tag registers. The selected PE are those with the tags from the Tag register set. Only for these PE the result is stored in their memory module when the control signal WR is activated.

2. Non-masked instructions which are executed by all the processing elements. When the control signal WRALL is activated all the PE results are stored in there memory modules no matter are the tags set.

Associated with every PE we have a memory module. This is a RAM memory for which the data pass is one bit width. At a time only one bit is selected by the bit address sent by the Control Unit.

For every PE we have a I/O data register of one bit which is used for the data transfers between I/O processor and the Array processor. The I/O one bit registers are grouped in 64 bits registers. Each register is selected using a I/O register address sent by the I/O processor. The I/O data bus is 64 bits wide. The control signals READ and WRITE are sent by the I/O processor, too.

5. The Array Processor Instruction Set

The instruction set of the Array Processor implements the elementary logical operations with the registers contents and the data items from the memory, data items organized as bit-slices. There are two kinds of instructions: a) without parameters – the operands are located in registers and the result is placed also in one of the PE registers; b) with one parameter – these instructions use the content of one register as one operand and the other is represented by a bit-slice from the memory.

The majority of the instructions are in two variants: tag masked and not tagmasked, as it was mentioned above.

5.1. The BFG Functions

The BFG implements 16 different functions. These functions are listed below:

Moves and Exchange

LDRMA	Load R from M, all	$R' < -M$
LDRMT	Load R from M, tag-masked	Where T=1 do $R' < -M$ elsewhere $R'=R$
LDRTA	Load R from T, all	$R' < -T$
LDTMA	Load T from M, all	$T' < -M$
LDTRA	Load T from R, all	$T' < -R$
XCGRT	Exchange R with T	$R' < -T$ and $T' < -R$

Logical Functions

ANDTRA	And T with R, all	$T' < -T$ AND R
ANDTMA	And T with M, all	$T' < -T$ AND M
AND RMT	And R with M, tag-masked	Where T=1, $R' < -R$ AND M elsewhere $R' = R$
ORRMT	Or R with M, tag-masked	Where T=1, $R' < -R$ OR M elsewhere $R' = R$

ORTRA	Or T with R, all	$T' < -T$ OR R
XORRMT	Xor R with M, tag-masked	Where T=1, $R' < -R$, XOR M elsewhere $R' = R$
XORRTA	Xor R with T, all	$R' < -R$, XOR T

Set, Clear, Complement

SETT	Set Tag register	T=1
CLRR	Clear R registers	R=0
CMPT	Complement Tag register	
CMPR	Complement R register	

6. The Parallel Manner of Operation with Boolean Functions

We shall briefly present the parallel manner of operation with boolean functions.

6.1. The Case of Completely Defined Boolean Functions

In a previous paper [4] it was shown that every completely defined function can be represented by the binary n-tuple:

$$m_1 = (a_1^1 a_2^1 ... a_i^1 ... a_N^1),$$

with $N = 2^{k-1} - 1$ and $a_i = 1$ for $i \in M_1$ or $a_i = 0$ otherwise, where $M_1 = \{n_1^1, ..., n_i^1, ..., n_n^1\}$ is the ordered set of state numbers for which the function f takes the value 1.

These binary numbers can be stored in the memory of a parallel Array Processor as bit-slices. The manner of operating with this representation is derived from the isomorphism based on the function $\varphi_1^* : F_B \to N$ with $\varphi_1^*(f) = m_1$, which has the following properties:

1. $\varphi_1^*(f)$ is bijective; 2. $\varphi_1^*(f_1 f_2) = \varphi_1^*(f_1) \& \varphi_1^*(f_2)$; 3. $\varphi_1^*(f_1 + f_2) = \varphi_1^*(f_1) | \varphi_1^*(f_2)$,

where $f_1 f_2$ and $f_1 + f_2$ are the logical product and the logical sum of the two functions, and $\varphi_1^*(f_1) \& \varphi_1^*(f_2)$, $\varphi_1^*(f_1) | \varphi_1^*(f_2)$ are the bitwise AND and inclusive OR operations applied to the "mark" binary numbers for f_1 and f_2.

6.2. The Case of Partially Defined Functions

Each partially defined function will be represented by a binary number v_f with 2^{N-1} bits, where N represents the number of the input variables of that function, and a mask m_f which will define the positions of the don't care values of the function. Thus:

$$f(x_1, ..., x_N) = (v_f, m_f),$$

where $v_f = (v_1 v_2 ... v_{2N})$, $m_f = (m_1 m_2 ... m_{2N})$, with

$$v_i = \begin{cases} 0 & \text{if } s_i \in M_0 \text{ or corresponds to a don't care value of the function } f, \\ 1 & \text{if } s_i \in M_1 \end{cases}$$

and

$$m_i = \begin{cases} 1 & \text{if } s_i \in M_0 \text{ or } M_1, \\ 0 & \text{if } f(s_i) = X \text{ (a don't care value).} \end{cases}$$

These two binary vectors can be stored in the memory of a parallel array processor as bitslices. If the number of bits of the binary vectors v_f and m_f exceeds the number of the Array Processor memory "words" then these binary vectors are stored as several consecutive bitslices. If the number of bits of these binary words is not a multiple of N, where N is the number of the Array Processor memory "words", then these binary vectors, m_f and v_f, are completed with 0. Using this representation, we have established the following operating rules with the base logical operators which permit to operate in parallel with Boolean functions.

For the AND operator we have established the following rule:

$$f(A,B) = A \wedge B = (v_{A\wedge B}, m_{A\wedge B}),\ v_{A\wedge B} = v_A \& v_B|_{m_{A\wedge B}},$$

$$m_{A\wedge B} = m_A \& m_B + \tilde{v}_B \& m_B + \tilde{v}_A \& m_A,$$

where "&", "+", and "~" are the bitwise AND, OR, and NOT operators, respectively.

In the case we choose the logical value 0 to represent in v_f the don't care values, the binary word $v_{A\wedge B}$ will be obtained by the bitwise AND operation with the binary words v_A and v_B, but only for the positions in which $(m_{A\wedge B})_i = 1$ (positions where the logical function AND will have defined values).

This operating rules will be implemented as follows. First the binary vector $m_{A\wedge B}$, which has the role of a mask which we shall call "selector", will be obtained in the Tag register, using the operations from the last relation with binary vectors v_A, v_B, m_A, m_B which are stored as bitslices in the memory of the array processor. Then, the binary vector $v_{A\wedge B}$ will be obtained very natural using the tag-masked AND function of the BFG applying the second relation.

Similarly we can operate with logical operators OR, XOR and NOT.

For the logical OR operator we have the next operating rules:

$$f(A,B) = A \vee B = (v_{A\vee B}, m_{A\vee B}),\ v_{A\vee B} = v_A + v_B|_{m_{A\vee B}},$$

$$m_{A\vee B} = m_A \& m_B + v_A \& m_A + v_B \& m_B.$$

For the logical XOR operator we have the following relations:

$$f(A,B) = A \oplus B,\ v_{A\oplus B} = v_A \oplus v_B|_{m_{A\oplus B}},\ m_{A\oplus B} = m_A \& m_B.$$

For the logical NOT operator we have the following relations:

$$f(A) = \overline{A},\ v_{\overline{A}} = \tilde{v}_A|_{m_A},\ m_{\overline{A}} = m_A.$$

7. VLSI Implementation of the Processor Array

Due to his highly regular structure the proposed array processor is very suited to VLSI implementation. For this architecture the distinction between the memory and the processing elements is not so distinct. With the today's technologies the memory and the processing elements can be implemented with the same technology. So, we can integrate the whole processor array architecture on the same chip. This means that the use of VLSI technologies will bring extraordinary advantages for a such processor.

We shall analyze bellow the consequences of processing elements and memory modules integration from the point of view of the number of gates and the number of pins per chip.

The number of pins per chip is in principal determined by the control signals for I/O registers, the instruction code for the Array Processor, the bitslice address signals and the address signals used to select the I/O registers. We shall consider that the data channel width for I/O registers is of b bits. In this case the number of pins per chip can be calculated using the data from Table 1.

Table 1

Specification	Number of pins
Bit-slices address	$\log_2 M$
I/O data bus	b
I/O read, write	2
I/O data address	$\log_2 N/b$
Chip select	1
Array Processor Instruction Code	k
Power, Ground, Clock	3

It results the next relation for NPC (number of pins per chip):

$$\text{NPC} = \log_2 N/b + \log_2 F + \log_2 M + b + 6,$$

with: N – the PE number, M – the memory "word" length and F – the number of the Array Processor instructions.

For $b = 64$ (I/O registers data bus width), $M = 512$ bits, $F = 32$ and $N = 1024$ PE per chip results:

$$\text{NPC} = 64 + \log_2 1024/64 + \log_2 512 + \log_2 32 + 6 = 88 \text{ pins per chip.}$$

We can observe that the NPC value is determined in principal by the I/O data bus width value b. We can significant reduce the number of pins per chip if we choose $b = 32$. But in this case the I/O data transfer rate is slower.

The number of gates necessary to implement the processing elements can be calculated with the following relation:

$$NG = f * 2^{f+k1+1},$$

with: NG – the number of gates, f – the number of flip-flops necessary to implement one PE, $k1$ – the number of bits necessary to specify the BFG function. This represents an upper bound because this relation can be used in the case when we use a ROM to implement the BFG. If we use a PLA to implement the BFG the number of cells can be reduced considerably.

In our case we have chosen $N = 1024$ processing elements, $f = 2$ flip flops necessary to implement one PE and $k1 = 4$ bits necessary to select one of the 16 BFG functions. In this case results:

$$NG = 2^{10} * 2 * 2^7 = 2^{18} \text{ memory cells.}$$

If we associate to every PE a memory module with the word length of M bits and we shall choose $M = 512$ bits then the number of cells necessary to implement the memory modules can be calculated with:

$$\text{NMC}=M * N = 2^9 * 2^{10} = 2^{19} \text{ memory cells.}$$

Assuming that using the current technology we can implement chips with 2^{20} cells (which is a very realistic hypothesis) results that we can implement easily 1024 PE, each of them with a memory module of 512 bits on a single chip.

A circuit board with 80 chips can contains 64 such VLSI chips together with additional chips such as address decoders for I/O registers and buffers. As a consequence a such board can contains 64*1024 PE, which means a great processing power. We can thus operate with Boolean functions with 20 arguments in a very short time, using a module formed by such a single board, considering the proposed data organization and using the proposed method. This module can be designed as a custom one, which can be attached to a general Associative Computer because its operating manner is compatible with that of a such computer.

8. Conclusions

A highly parallel architecture which can efficiently supports a new manner of operating with Boolean functions is proposed. The main elements which form this architecture are presented and its principal blocks are described. It was presented the main instruction set and the working manner of the proposed architecture. As it was argued in this paper the proposed array processor is very suited for VLSI implementation.

Received, August 5, 1992

Polytechnic Institute, Jassy,
Department of
Applied Electronics

REFERENCES

1. B a t c h e r K.E., *Bit-Serial Parallel Processing systems.* IEEE Trans. on Computers, **C-31**, 377-384 (1982).

2. B a t c h e r K.E., *Design of a Massively Parallel Processor.* IEEE Trans. on Computers, **C-29**, 836-840 (1980).

3. B a t c h e r K.E., *The Multiplicational Access Memory in STARAN.* IEEE Trans. on Computers, **C-26**, *2*, 174-177 (1977).

4. C h i p e r D., *A Parallel Manner of Operating with Boolean Functions.* Bul. Inst. Polit., Iaşi, **XXXVIII (XLII)**, *1-4*, s.III (1992) (in print).

O ARHITECTURĂ CU GRAD RIDICAT DE PARALELISM CE OPEREAZĂ EFICIENT CU FUNCŢII BOOLEENE

(Rezumat)

Se prezintă o arhitectură paralelă, cu un grad ridicat de paralelism, ce urmăreşte implementarea eficientă a unei noi metode de operare cu funcţii Booleene. Se expun principalele elemente ce formează sistemul de procesare paralelă propus şi se descriu principalele blocuri componente. A fost prezentat, de asemenea, setul de instrucţiuni al procesorului matriceal, procesor ce formează partea principală a sistemului de procesare paralelă conceput. Se prezintă argumente ce pledează în favoarea implementării eficiente a procesorului matriceal astfel conceput în tehnologie VLSI.

BULETINUL INSTITUTULUI POLITEHNIC DIN IAŞI
Tomul XXXIX (XLIII), Fasc. 1-4, 1993
Secţia III
ELECTROTEHNICĂ. ENERGETICĂ. ELECTRONICĂ

D.C. 621.317.336

CONSIDERATIONS CONCERNING THE THERMIC REGIME IN THE MEASUREMENT PROCESS OF RESISTANCES

BY
N. DAMEAN

1. Introduction

It is known that there are a lot of methods of measurement of the resistances which can be realized either in d.c. or in a.c.

The resistance of a passive receiver in d.c. is defined as the ratio between the continuous voltage U applied to the receiver and the current I which passes through it:

$$R = \frac{U}{I} = \frac{P}{I^2},$$

where P is the power consumed by receiver.

In a.c. it is defined as the ratio between the active power P consumed by receiver and the square of the effective current I which passes through it:

$$R = \frac{P}{I^2}.$$

The methods of measurement of the resistances in d.c. are the most used.

All these methods are influenced by the thermic effect of the current.

The thermic effect produces a dynamic behaviour of the resistance, during the process of measurement. In other words, this behaviour consists of the variation of the resistance depending on time. In what follows this effect will be studied.

2. Mathematical Approach

It is considered a resistor realized as a very long wire in comparison with its circular cross-section A and with the radius r.

In what follows it will understand that A is both the area of the cross-section and the surface of it, the true meaning resulting from the context in which is used.

The wire, through which flows a d.c., I, in the time $t > 0$, is oriented along the x-axis having its extremities in the points of abscissa 0 and l_0.

In accordance with the J o u l e law, in wire is generated the amount of heat:

$$G = \frac{W}{Vt} = \frac{P}{V} = \frac{\omega I^2}{A^2}, \tag{1}$$

on the time and volume unit.

In the relation (1) ω, P, W, V represent: the resistivity of the wire, the power consumed by resistor, the energy consumed by it and the volume of the wire which constitutes the resistor, respectively.

It is considered, for simplicity, that the dependence of ω versus the time can be neglected (for example for the wire made by platinum – iridium).

Initially the following hypotheses may be accepted: a) the lateral surface of the wire is perfectly thermic insulated so that no heat passes across the lateral surface; b) at any instant each cross-section of the wire is an isothermal surface (the latter assumption is plausible when the dimensions of cross-section of the wire are small in comparison with its length, as it was considered).

The electric current generates heat which produces the growth of the temperature of the wire, through conduction (when the transfer of the thermic energy is produced because the collisions among the molecules in movement or because the free electrons from metals) as well as through convection (when the transfer of the thermic energy is produced through a fluid current) in the exterior medium at the temperature T_0. The convection can be realized through the surfaces of the bases only, according to hypothesis a).

One considers the process of conduction of the heat in an homogeneous and izotropic solid (a wire in this case) with the initial length l_0.

Let ρ, c and λ the mass density, heat capacity and (inner) heat conductivity, respectively, of the material of the wire.

The coefficients ρ, c and λ are, in general, functions of position, i.e. $\rho = \rho(x)$, $c = c(x)$, $\lambda = \lambda(x)$, $x \in [0, l_0]$, unless the medium is homogeneous (the case considered here) when these ones may be considered as constants. (These coefficients are also functions of temperature but this dependence may be neglected if the variation of temperature under consideration is not too significant. All these quantities are assumed to be time independent as well).

For common solids at ordinary temperatures the values C_p and C_v, the heat capacity at constant pressure and at constant volume, respectively, differ very

little (C_p being at most with 5% greater than C_v), so it is possible to consider $C_p = C_v = C$.

Suppose that within the wire there exist a source generating heat (through electrical process) which is characterized by a function of both position and time, $G = G(x,t)$, giving the amount of heat generated per unit of time and per unit of volume.

With the goal to obtain a partial differential equation for the temperature $T = T(x,t)$ it is necessary to establish the heat energy balance for an arbitrary control volume $V_o = A\mathrm{d}x$ within surrounding of the point x in the time interval from t to $t + \mathrm{d}t$.

In [2], [5] it was obtained the following partial differential equation, named heat equation:

$$T_t - aT_{xx} = g(x,t), \quad x \in (0, l_0), \quad t > 0, \tag{2}$$

where:

$$g = \frac{G}{c\rho} \quad \text{and} \quad a = \frac{\lambda}{c\rho}. \tag{3}$$

The coefficient a is called the temperature conductivity.

The initial condition takes the form:

$$T(x,0) = T_0, \quad x \in [0, l_0], \tag{4}$$

and the boundary condition:

$$\lambda \frac{\partial T(x,t)}{\partial \nu} + \alpha T(x,t) = \alpha T_0, \quad x = 0 \text{ or } l_0, \quad t > 0, \tag{5}$$

where $\partial/\partial\nu$ denotes the outward normal derivative on the boundary of $[0, l_0]$. Here α is the so-called heat transfer coefficient, those value varying significantly with the state, shape and temperature of the boundary surface and depending considerably on the surroundings.

As it was seen the one-dimensional heat equation (2) describes the heat conduction in a wire on the condition that its lateral surface is rendered imprevious to heat (hypothesis a)). If this condition is not satisfied and there is an exchange of heat between the boundary surface of the wire and the surroundings at the temperature T_0 (a realist case) it is not necessary to use a three-dimensional model as might seem at first sight.

It shows that the one-dimensional model is sufficient if it retains the assumption b), (which now, however, is not so convincing as before). Namely, the description of the thermal behaviour of the lateral surface can be amalgamed into the differential equation and the boundary condition for the lateral surface drops out. One obtains a somewhat more complicated equation but again only in one spatial variable.

Let dQ_0 denote the amount of heat generated by thermic effect of electric current in the volume $V_0 = Adx$ during the infinitesimal time interval dt, dQ_1 – the outflow of heat through the ends and lateral surface of volume V_0, and finally dQ_2 – the increase (decrease) of heat which brings about an increase (decrease) in temperature of V_0. The heat energy conservation law yields:

$$dQ_0 - dQ_1 = dQ_2. \tag{6}$$

For dQ_0 it results:

$$dQ_0 = dt \int_{V_0} G(x,t)dV. \tag{7}$$

To evaluate dQ_1 and dQ_2 it is necessary to apply two well-known experimental laws of physics [6].

Let $q = q(x,t)$ denote the heat flux density vector, that is, the vector whose direction coincides with that of the heat flow, namely with the direction of decreasing temperature, and the magnitude of which is equal to the amount of heat passing out, per unit time, through a surface of a unit area perpendicular to heat flow. The relation between q and T is given by the well known F o u r i e r law:

$$q = -\lambda \operatorname{grad} T. \tag{8}$$

The amount of heat flowing, per unit time, across a unit area having a unit normal vector $\boldsymbol{\nu}$ is equal to the projection of the vector $\mathbf{q}$ on the vector $\boldsymbol{\nu}$ namely:

$$q_\nu = \boldsymbol{\nu}\mathbf{q} = -\lambda \frac{\partial T}{\partial \nu}. \tag{9}$$

This scalar quantity is called the heat flux density in the direction $\boldsymbol{\nu}$. It is positive or negative according to the heat flows in the direction of $\boldsymbol{\nu}$, i.e. $\partial T/\partial \nu < 0$, or in the opposite direction, i.e. $\partial T/d\nu > 0$.

Using (8) and (9) it results:

$$dQ_1 = -\lambda dt \int_{V_0} T_{xx} dV + \alpha dt \int_{\partial V_0} [T(x,t) - T_0] dS, \tag{10}$$

where the first term corresponds to the outflow of heat through the ends of V_0 and the latter to the outflow of heat through the lateral surface of the volume V_0.

The second law leads to the conclusion that the change $\mathrm{d}Q$ of heat in a matter of mass m is proportional (through c) to m and the temperature variation $\mathrm{d}T$:

$$\mathrm{d}Q = cm\,\mathrm{d}T. \tag{11}$$

In the considered case (11) leads to:

$$\mathrm{d}Q_2 = \int_{V_0} c\rho\,\mathrm{d}T\mathrm{d}V.$$

Using the expression:

$$\mathrm{d}T(x,t) = \mathrm{d}t\frac{\partial T(x,t)}{\partial t}$$

it results:

$$\mathrm{d}Q_2 = \mathrm{d}t\int_{V_0} c\rho\frac{\partial T}{\partial t}\mathrm{d}V. \tag{12}$$

From (6), (7), (10), (12), and since V_0 is arbitrary it results:

$$T_t - aT_{xx} + \gamma(T - T_0) = g(x,t), \tag{13}$$

where $\gamma = \alpha p/c\rho A$, p is the perimeter of the cross-section, a and g being given in (3).

The Eq. (13) describes the dependence of temperature $T(x,t)$ versus space coordinate x and time t, for a resistor realized as a thermic non-insulated wire through which flows the constant current I.

The solution of this equation is [3]:

$$T(x,t) = T_0 + \frac{\omega I}{\alpha p A}\left[1 - \exp\left(-\frac{\alpha p}{c\rho A}t\right)\right].$$

If r is the ray of the cross-section of the wire, it results:

$$T(t) = T_0 + \frac{\omega I^2}{2\alpha\pi^2 r^3}\left[1 - \exp\left(-\frac{2\alpha}{c\rho r}t\right)\right], \quad \text{with} \quad T(0) = T_0.$$

It follows that:

$$\lim_{t\to\infty} T(t) = T_0 + \frac{\omega I^2}{2\alpha\pi^2 r^3} = T_\infty$$

and

$$\Delta T = T_\infty - T_0 = \frac{\omega I^2}{2\alpha\pi^2 r^3}. \tag{14}$$

Consequently the resistance of the wire has a dynamic behaviour being a function of time:

$$R = R(t) = \frac{\omega l}{A} = \frac{\omega l_0(1+\beta\Delta T)}{A}, \tag{15}$$

where $l = l(t)$, β, represent the length of the wire and the coefficient of linear dilatation of the wire, respectively.

Using (14) and (15) it results:

$$R(t) = \frac{\omega l_0}{A}\left\{1+\beta\frac{\omega I^2}{\alpha\rho A}\left[1-\exp\left(\frac{-2\alpha}{c\rho r}t\right)\right]\right\},$$

$$\lim_{t\to\infty} R(t) = \frac{\omega l_0}{\pi r^2}\left(1+\frac{\beta\omega I^2}{2\alpha\pi^2 r^3}\right) = R_0\left(1+\frac{\beta\omega I^2}{2\alpha\pi^2 r^3}\right) = R_\infty, \quad R(0) = \frac{\omega l_0}{A} = R_0$$

and

$$\Delta R = R_\infty - R_0 = R_0\frac{\beta\omega I^2}{2\alpha\pi^2 r^3}. \tag{16}$$

Therefore the maximum error determined by the thermic effect of the electric current is:

$$\varepsilon,[\%] = \frac{\Delta R}{R(0)}\cdot 100 = \frac{\beta\omega I^2}{2\alpha\pi^2 r^3}\cdot 100. \tag{17}$$

3. Numerical Approach

It may be observed that among all coefficients used in above relations, the coefficient α depends of the most parameters as: geometric shape of the wire, the speed of the fluid where is situated, the properties of this fluid, the difference of temperature, $T(x,t)-T_0$.

Studying the tables from [4], [8], considering that the wire is in air and the free convection of the heat, it gets:

$$\alpha = 293.74\sigma\Delta T^{1/4}, \tag{18}$$

where the coefficient σ is a function of θ, with $\theta = \frac{1}{2}[T(x,t)+T_0]$.

Using the least squares methods [1], it results:

$$\sigma = 2.7035\times 10^{-6}\theta^2 - 3.2817\times 10^{-3}\theta + 3.5719. \tag{19}$$

Therefore it uses the following algorithm for the computing of ΔT:

1. Start.
2. Read ω, I, r, e, ΔT_0, π.
3. Initialization $\Delta T=\Delta T_0$.
4. Compute σ with (19).
5. Compute α with (18).
6. Compute ΔT with (14).
7. If $|\Delta T-\Delta T_0|>e$ it puts $\Delta T_0=\Delta T$ and jump at 4; if $|\Delta T-\Delta T_0|<e$ it results ΔT. Stop.

In what follows two applications of this algorithm are given .

3.1. The Thermic Analysis of the Heater Wire of an Thermoelement

The wire is made from constantan having the following characteristics: $r=4.10^{-6}$ m; $l_0=10^{-2}$ m; $R_0=95$ Ω. The wire is situated in a medium with the temperature $T_0=25^{\circ}$C.

Using the above algorithm, the results from Table 1 are obtained.

Table 1

I, [A]	ΔT, [°C]	I, [A]	ΔT, [°C]
.001	.46	.06	362.
.005	6.04	.07	478.18
.01	18.41	.08	610.89
.025	81.55	.09	758.49
.05	262.45	.1	916.9

With the goal to obtain the dependence $\Delta T=\Delta T(I)$ some least squares algorithms may be used. A polynomial dependence is obtained. It will not be a square one as is considered generally.

3.2. The Thermic Analysis of a Resistance Temperature Detector

Let be such a resistance temperature detector Pt 100 realized as a wire with the characteristics: $r=5\times10^{-6}$ m; $l_0=71.4\times10^{-3}$ m; $R_0=100$ Ω [7]. It is situated in a medium with the temperature $T_0=200^{\circ}$C.

Using the above algorithm, the results from Table 2 are obtained.

Table 2

I, [A]	ΔT, [°C]	ε, [%]	I, [A]	ΔT, [°C]	ε, [%]
.001	.0913	.0167	.011	4.2391	.7757
.002	.2768	.0506	.012	4.8733	.8918
.003	.5296	.0969	.013	5.5402	1.0139
.004	.8393	.1535	.014	6.2389	1.1417
.005	1.1996	.2195	.015	6.9685	1.2752
.006	1.6061	.2939	.016	7.7283	1.4143
.007	2.0556	.3761	.017	8.5175	1.5587
.008	2.5456	.4658	.018	9.3354	1.7084
.009	3.0739	.5625	.019	10.181	1.8632
.01	3.6391	.6659	.02	11.055	2.023

In view to obtain the dependences $\Delta T(I)$ and $\varepsilon(I)$ some least squares algorithms are used. These will conduct to two polynomial dependences. In the Table 2 it was presented the maximum error ε computed with relation (17).

4. Conclusions

It was presented some aspects concerning the thermic effect of electric current in the measurement of the resistances. The obtained algorithm was tested in two usual applications. The results are in concordance with the experimental ones.

Annex

Units of Measure and Numerical Values for the Constants Used:

Material	λ J/ms°C	ω Ωm	ρ kg/m^3	β 1/°C	c J/kg°C
Constantan (0.60 Cu, 0.40 Ni)	23	$.49\times10^{-6}$	8900	2×10^{-5}	405
Platinum	134	$.11\times10^{-6}$	21450	1.83×10^{-9}	134

Received, November 16, 1992

Polytechnic Institute, Jassy,
Department of Electrical Measurements

REFERENCES

1. Aïvazian S., Énukov I., Méchalkine L., *Eléments de modélisation et traitement primaire des données.* Mir, Moscou, 1986, 226-231.
2. Bajpai A.C., Mustoe L.R., Walker D., *Advanced Engineering Mathematics.* John Willey and Sons, Ltd., London, 1977, 238-270.
3. Barták J., Herrmann L., Lovicar V., Vejvoda O., *Partial Differential Equations of Evolution.* Ellis Harwood, England, 1991, 171-196.
4. Cornwell K., *The Flow of Heat in SI Units.* Van Nostrand Reinhold Company, Ltd., England, 1977, 113-148, 237.
5. Lin C.C., Segel L.A., *Mathematics Applied to Deterministic Problems in the Natural Sciences.* SIAM, Philadelphia, 1988, 114-181.
6. Martinet J., *Eléments de thermocinétique (conduction de la chaleur), technique et documentation.* Lavoisier, Paris, 1989, 5-27, 52, 257-259.
7. Tse F.S., Morse I.E., *Measurement and Instrumentation in Engineering.* Marcel Dekker, Inc., New York, 1989, 370-372, 532-539.
8. Washburn E.W., *International Critical Tables of Numerical Data.* Physics, Chemistry and Technology, McGraw-Hill Book Company Inc., New York, 1926-1930.

CONSIDERAŢII PRIVIND REGIMUL TERMIC ÎN PROCESUL DE MĂSURARE A REZISTENŢELOR

(Rezumat)

Sunt prezentate câteva aspecte legate de efectul termic al curentului electric care se manifestă la măsurarea rezistenţelor. Este pusă în evidenţă comportarea dinamică a rezistenţei în cursul procesului de măsurare.

Algoritmul stabilit a fost testat pentru două aplicaţii practice, rezultatele obţinute fiind în concordanţă cu observaţiile experimentale.

BULETINUL INSTITUTULUI POLITEHNIC DIN IAŞI
Tomul XXXIX (XLIII), Fasc. 1–4, 1993
Secţia III
ELECTROTEHNICĂ. ENERGETICĂ. ELECTRONICĂ

C.D. 621.317.083.4

MÉTHODE DE ZÉRO ET APPAREIL POUR LA MESURE DES PARAMÈTRES DES BOBINES LINÉAIRES

PAR

ADRIAN CREŢU, RADU COCIU, ELENA CREŢU et LIVIA COCIU

1. Introduction

Dans ce qui suit on étudie un nouveau procédé et on réalise un appareil (brevété en Roumanie) destiné pour la mesure des bobines linéaires, en tenant compte des recherches antérieures [1],...,[3].

2. Le schéma structural de mesure

La structure et les blocs fonctionnels qui sont à la base du procédé proposé et étudié dans ce qui suit sont présentés dans la Fig. 1.

Le schéma de mesure proprement dit contient un circuit résonant complètemment apériodique (C.R.C.A.), un converteur de résistance négative (C.R.N.) et deux converteurs courant–tension, A_2 et A_3. Les circuits d'entrée sont connectés en série aux branches inductive-active, respectivement capacitive-active, du circuit résonant. Le C.R.C.A. est constitué d'une branche inductive-active, obtenue par la connexion en série de la bobine dont les paramètres vont être mesurés, au converteur C.R.N. et de la résistance variable, R_L, connectée en dérivation à une branche capacitive-active, obtenue par le connexion en série d'un condensateur fixe, C, présumé sans pertes et de la résistance réglable, R_C; les noeuds M et N sont des points virtuels de masse. L'accord du C.R.C.A. est effectué par le réglage simultané des résistances $R_L = R_C$ (potentiomètre double à précision adéquate). Au préalable, l'effet de la résistance r_x de la bobine est annulé par l'intermédiaire du C.R.N.

Au moment de la résonance apériodique dans le C.R.C.A. est accomplie la condition bien connue [1]:

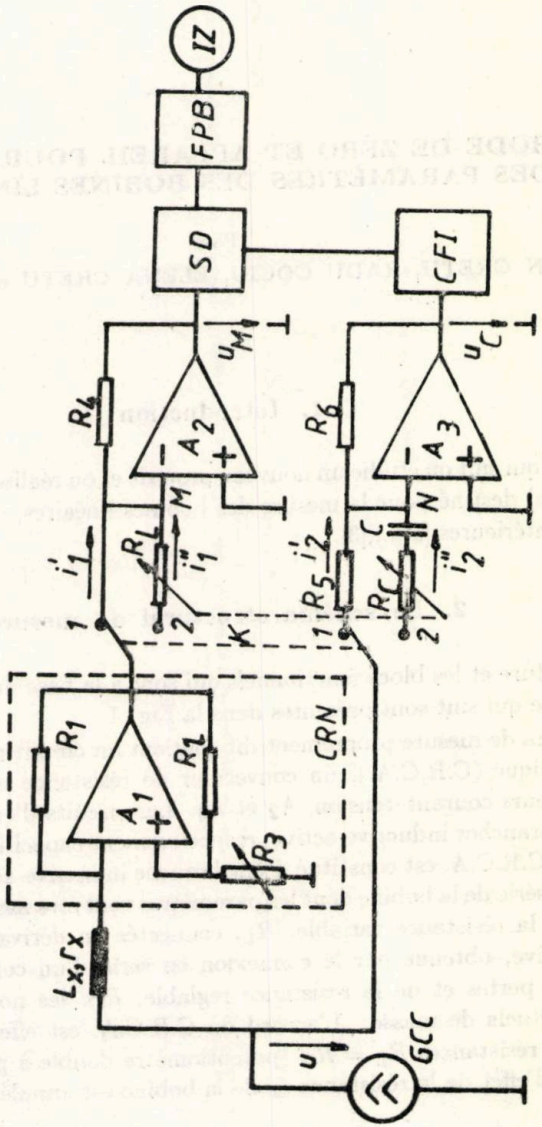
IZ
FPB
SD
CFI
u_M
u_C
R_4
R_6
A_2
A_3
M
N
i'_1
i''_1
R_L
i'_2
i''_2
R_5
R_C
C
1
2
K
R_1
R_1
A_1
R_3
CRN
L_x, r_x
u
GCC

Fig. 1

$$R_L = R_C = \sqrt{\frac{L_x}{C}}, \tag{1}$$

où R_L et R_C représentent les résistances totales des branches inductive-active et capacitive-active du C.R.C.A.

Par suite de [1] il résulte que l'indication de la résonance complètement apériodique par la détection du moment où les courants i_1 et i_2, appartenant aux deux branches du C.R.C.A., sont en quadrature, présente des avantages nets par rapport au procédé bien connu [9], de réalisation de la résonance complètement-apériodique par le controle de la concordance des phases de la tension et du courant du circuit résonant considéré.

En même temps, dans une Note antérieure [2] on a prouvé que, dans le moment de la résonance complètement-apériodique dans un C.R.C.A., les courants i_1 et i_2 qui circulent par les branches du circuit sont toujours symphasiques; la réciproque est vraie si les résistances totales des deux branches sont rigoureusement égales, leurs valeurs en satisfaisant simultanément la relation (1).

Ces conclusions ont permis l'élaboration de la méthode de zéro qui se trouve à la base du fonctionnement du schéma de mesure proposé dans la Fig. 1.

En outre des éléments mentionnés ci-dessus le schéma proposé contient: un synchrodétecteur, S.D., un filtre passe-bas, F.P.B., un circuit formateur des impulsions rectangulaires, C.F.I., un instrument magnéto-électrique, I.Z., à rôle de détecteur de zéro, un générateur de courant, G.C., et un commutateur bipolaire, K, à deux sections.

La mesure des paramètres L_x, r_x d'une bobine linéaire implique deux étapes:

a) Dans la première étape, pour la mesure de la résistance r_x, le commutateur K est connecté dans la position 1. On règle la résistance R_3 du schéma du C.R.N., jusqu'à ce que la déviation de I.Z. s'annule. En ce moment la tension aux bornes de la branche inductive et le courant i sont en quadrature; la résistance totale de cette branche devient égale à zéro:

$$r_x + r = 0, \tag{2}$$

où:

$$r = -R_3 \frac{R_1}{R_2} \tag{3}$$

constitue la résistance négative du C.R.N.

De (2) et (3) il en résulte la valeur de la résistance r_x à mesurer:

$$r_x = R_3 \frac{R_1}{R_2} = \text{const.} \cdot R_3. \tag{4}$$

En effet, lorsque le commutateur K se trouve en position 1, on applique au circuit de mesure du S.D. le signal sinusoïdal u'_M, obtenu à la sortie du converteur courant–tension A_2:

$$u'_M = -R_6 i'_2 = -\frac{R_6}{R_5} u. \tag{5}$$

On applique au circuit de commande du S.D. un signal rectangulaire, symphasique avec u_C, obtenu à la sortie du converteur A_3:

$$u'_C = -R_6 i'_2 = -\frac{R_6}{R_5} u, \tag{6}$$

où i'_2 est le courant par la résistance R_5, symphasique avec la tension u appliquée aux bornes de la branche inductive-active du C.R.C.A. L'expression de la déviation de l'instrument magnéto-électrique I.Z. est, en cette première étape:

$$\alpha = S_{DS} U'_M \cos(\widehat{\underline{U}'_M, \underline{U}'_C}). \tag{7}$$

En tenant compte de (4), celle-ci devient:

$$\alpha = S_{DS} U'_M \cos(\widehat{\underline{I}'_1, \underline{U}}), \tag{8}$$

où S_{DS} représente la sensibilité globale du S.D. Il en résulte de (8) que la déviation α s'annule quand le déphasage entre les signaux i_1 et u devient 90°, moment qui coïncide au celui d'annulation de la résistance totale de la branche inductive-active du C.R.C.A. On réalisé l'annulation de cette résistance par le réglage de la résistance négative r du C.R.N. (en réglant la résistance R_3 à un rapport R_1/R_2= =const.) à une valeur égale à celle de la résistance à mesurer, (v. r_x (2)).

On peut étalonner directement la résistance R_3 par les valeurs de la résistance de pertes de la bobine à mesurer, en adoptant pour le rapport des résistances R_1/R_2 des valeurs adéquates, en fonction des gammes de mesure imposées.

b) Dans la deuxième étape, en gardant la résistance du C.R.N. à la valeur (4), résultée dans la première étape, on passe le commutateur K en position 2. Par conséquence on connecte en série la résistance réglable R_L dans la branche inductive du C.R.C.A. et dans la branche capacitive-active, le condensateur fixe C, supposé sans pertes et la résistance réglable R_C, couplée mécaniquement à R_L, en résultant:

$$R_L = R_C = R. \tag{9}$$

On règle simultanément les résistances $R_L = R_C$ jusqu'à une nouvelle annulation de la déviation α de I.Z. Ce moment coïncide avec la réalisation de la résonance complètement-apériodique dans le C.R.C.A. Dans ce moment est satisfaite la condition (1). En tenant compte de (9) il résulte la valeur de l'inductance L_x de la bobine à mesurer:

$$L_x = R^2 C. \tag{10}$$

En effet, quand le commutateur K se trouve en position 2, le signal sinusoïdal

$$u''_M = -R_4 i''_1 \tag{11}$$

est appliqué au circuit de mesure du S.D. Celui-ci se trouve en opposition de phase avec le courant i''_1 de la branche inductive-active du C.R.C.A. En même temps on applique au circuit de commande un signal rectangulaire, symphasique avec le signal sinusoïdal:

$$u''_C = -R_6 i''_2, \tag{12}$$

qui se trouve en opposition de phase avec le courant i'_2 de la branche capacitive-active du C.R.C.A.

Il résulte de (7), en tenant compte de (11) et (12), l'expression de la déviation α de I.Z.:

$$\alpha = S_{DS} U''_M \cos(\widehat{\underline{U}''_M, \underline{U}''_C}) = S_{DS} U''_M \cos(\widehat{\underline{I}''_1, \underline{I}''_2}). \tag{13}$$

Par conséquence, dans cette nouvelle situation, la déviation α s'annule au moment où les courants qui circulent par les deux branches du C.R.C.A. sont en quadrature, c'est-à-dire dans le moment où la résonance complètement-apériodique dans ce circuit est réalisée.

3. Erreurs de mesure

Les erreurs de mesure de la résistance de pertes r_x sont déterminées, ainsi qu'il résulte de la rélation (4), par les erreurs du C.R.N. et celles de détermination du moment de la quadrature des signaux $\underline{U}$ et $\underline{I}$. Dans le cas du schéma proposé ces derniers sont pratiquement négligeables. En effet, on peut calculer la sensibilité de mesure de la résistance r_x, définie par le rapport entre la variation de la déviation α de I.Z. et la variation de la résistance r du C.R.N., en utilisant l'équation de fonctionnement (8), que l'on peut écrire sous la forme:

$$\alpha = S_{DS}U_M \cos(\widehat{\underline{U}_1, \underline{I}_1'}) = S_{DS}U_M \frac{r_x + r}{\sqrt{(r_x + r)^2 + \omega^2 L_x^2}}. \tag{14}$$

Supposant que le signal u_M est gardé constant en alimentant le schéma à l'aide d'un générateur de courant G.C., la sensibilité de mesure de la résistance r_x (conformément à la définition donnée ci-dessus) résulte de l'équation (14). Son expression finale est:

$$S_{\alpha r} = \frac{\mathrm{d}\alpha}{\mathrm{d}r}\bigg|_{U_M=\text{ct.}} = S_{DS}U_M \frac{\omega^2 L_x^2}{[(r_x + r)^2 + \omega^2 L_x^2]^{3/2}}. \tag{15}$$

Au moment de la quadrature des signaux $\underline{U}$ et $\underline{I}$ ($r_x + r = 0$; $\alpha = 0$), la sensibilité du schéma de mesure obtenue de (15), compte tenu de la condition (2), a la valeur:

$$S_{\alpha r_0} = S_{DS} \frac{U_M}{\omega L_x}. \tag{16}$$

Vu que la sensibilité globale S_{DS} du S.D. dépend, surtout (v. (5)), de la sensibilité de mesure de l'instrument magnéto-électrique utilisé (en fonction de la précision imposée, celui-ci peut être un microampermètre ou un galvanomètre à grande sensibilité) il résulte de (16) que les erreurs de détermination du moment de la quadrature des signaux $\underline{U}$ et $\underline{I}$ sont pratiquement négligeables pour un domaine très vaste des valeurs des paramètres de la bobine à mesurer.

Les erreurs de mesure de l'inductance L_x sont déterminées, surtout, par les erreurs de construction de la double résistance $R_L = R_C = R$ (potentiomètre double de précision ou boîte à décades, en fonction de la précision imposée au schéma et au condensateur fixe C). Les erreurs de la détermination (sensibilité) de la quadrature des courants $\underline{I}_1''$ et $\underline{I}_2''$ sont pratiquement négligeables; la sensibilité de mesure a dans ce cas l'expression (v. (1)):

$$S_{\alpha_0} = S_{DS}U_M \frac{2\omega C}{\omega^2 R^2 C^2 + 1}. \tag{17}$$

4. Conclusions

En utilisant les propriétés des circuits résonants complètement-apériodiques on propose et on étudie une nouvelle méthode de zéro pour la mesure des paramètres des bobines linéaires.

Le schéma proposé permet la mesure simple et rapide tant de la résistance qu'aussi de l'inductance des bobines linéaires, par un double procédé de zéro.

Les relations de calcul des paramètres r_x, L_x, très simples, sont indépendantes de la fréquence du signal d'alimentation, la valeur de celle-ci en affectant seulement la sensibilité de mesure du schéma (v. (16) et (17)).

Les appareils qu'on peut construire en utilisant le schéma présenté ci-dessous se caractérisent par un rapport performance-prix supérieur à celui réalisé au cas des appareils similaires utilisées dans l'étape actuelle (Henry-mètres, Q-mètres).

Étant donné que l'annulation de la déviation de l'indicateur de zéro s'effectue par le réglage d'une seule résistance, dans le cas de la mesure de r_x, et à l'aide d'un double potentiomètre, lors de la mesure de L_x, il y a la possibilité d'automatiser le procédé proposé.

Reçue le 15 janvier 1992

Institut Polytechnique, Jassy,
Chaire d'Electrotechnique
et Machines électriques

BIBLIOGRAPHIE

1. Creţu A., Creţu E., *About Resonance Indication in Complete-Aperiodic Parallel Circuits.* Bul. Inst. Polit., Iaşi, **XXXIII (XXXVII)**, *1-4*, s.III, 25-31 (1987).

2. Creţu A., Creţu E., Cociu R., *The Aperiodic Q-meter.* Bul. Inst. Polit., Iaşi, **XXIV (XXXVIII)**, *1-4*, s.III, 27-32 (1988).

3. Creţu A., Cociu R., *Metodă de zero şi aparat pentru măsurarea parametrilor bobinelor şi condensatoarelor liniare.* Brevet România, *100524* (1991).

4. Creţu A., *Detector-amplificator sensibil la fază.* Brevet R.S.R., *82632* (1983).

5. Creţu A., *Metodă şi aparat pentru indicarea rezonanţei în circuitele derivaţie complet-aperiodice.* Brevet R.S.R., *94116* (1987).

6. Creţu A., Cociu R., Creţu E., Cociu L., *Sur l'indication de la résonance dans les circuits électriques et son application dans la mesure des paramètres R, L, C.* Bul. Inst. Polit., Iaşi, **XXXV (XXXIX)**, *3-4*, s.III, 31-38 (1989).

7. Bulucea C., *Circuite integrate liniare.* Ed. Tehn., Bucureşti, 1976.

8. Goraş L., *Contribuţii la studiul şi utilizarea convertoarelor şi invertoarelor de impedanţă.* Thèse de doctorat, Inst. Polit., Iaşi, 1978.

9. Patachi N., *Q-metru aperiodic.* Brevet R.S.R., *67413* (1979).

METODĂ DE ZERO ŞI APARAT PENTRU MĂSURAREA PARAMETRILOR BOBINELOR LINIARE

(Rezumat)

Se propune şi se studiază o metodă de zero pentru măsurarea parametrilor bobinelor liniare cu pierderi, care, printr-un dublu procedeu de zero, simplu şi rapid, permite determinarea atât a rezistenţelor de pierderi cât şi a inductivităţilor bobinelor având schema echivalentă serie.

Aparatul (Q-metru aperiodic), având la bază metoda menţionată, cuprinde în esenţă un circuit rezonant derivaţie, complet-aperiodic, un convertor de rezistenţă negativă, două convertoare curent tensiune şi un detector sensibil la fază asociat cu un instrument magnetoelectric, cu rol de indicator de nul. Acest aparat, având toate blocurile funcţionale realizate cu amplificatoare operaţionale, permite măsurarea parametrilor bobinelor cu factor de calitate redus ($Q<1$) la frecvenţe joase şi audio. Relaţiile de calcul ale parametrilor de măsurat sunt extrem de simple, independente de valoarea frecvenţei semnalului de alimentare.

Întrucât anularea deviaţiei indicatorului de nul se efectuează prin reglarea unui singur parametru (un rezistor în cazul măsurării rezistenţei de pierderi şi un rezistor dublu, în cazul măsurării inductivităţii), există posibilitatea automatizării procedeului propus.

BULETINUL INSTITUTULUI POLITEHNIC DIN IAŞI
Tomul XXXIX (XLIII), Fasc. 1–4, 1993
Secţia III
ELECTROTEHNICĂ. ENERGETICĂ. ELECTRONICĂ

C.D. 621.317.39

SUR UNE MÉTHODE DE MESURE EN FLUX DU VOLUME DES GRUMES

PAR
C. SĂRMĂŞANU, M. CREŢU et LIVIU BRENIUC

1. Introduction

La mesure du volume de masse ligneuse en état brut (des grumes) est importante tant pour les producteurs que pour ceux qui la façonnent.

Les grandes quantités de bois dont on a besoin exigent l'évaluation très précise de la quantité et de la réduction du temps nécessaire pour cette opération. En utilisant la méthode de l'évaluation à l'aide des tables de cubage [1] on obtient des dates imprécises et on perd beaucoup de temps.

Nous nous proposons de présenter, ci-dessous, une méthode simple d'évaluation du volume de masse ligneuse brute (des grumes). Cette méthode est basée sur l'intercalation d'un „mesureur" directement sur la bande de transport, soit chez les producteurs lorsqu'on charge les grumes dans les moyens de transport, soit à la destination lorsqu'on les décharge.

Le „mesureur" de volume fournit des informations concernant la longueur et la section de la grume. Ces dates sont interprétées dans un organe de calcul, séparément, ou elles peuvent être utilisées comme des dimensions d'entrée pour une unité de calcul centralisé (calculateur de processus).

2. Principe de la méthode

En considérant l'objet à mesurer (la grume) de forme tronconique, son volume sera donné par la relation bien connue:

$$V = \frac{\pi l}{3}(R_1^2 + R_2^2 + R_1 R_2), \tag{1}$$

où: l représente la longueur, R_1, R_2 – les rayons des bases à ces deux extrémités, de sorte que:

$$V = \frac{l}{3}(S_1^2 + S_2^2 + \sqrt{S_1 S_2}), \tag{2}$$

où S_1, S_2 sont les surfaces des sections à ces deux extrémités. Donc, la mesure du volume suppose l'évaluation simultanée de la longueur et des sections S_1, S_2 de l'objet.

Etant donné que les grumes, surtout celles de bois dur, n'ont pas une forme homogène, l'évaluation peut être erronée. Par conséquent il est nécessaire d'évaluer la section et la longueur courante de l'objet à mesurer et de calculer le volume par une relation de la forme (Fig.1):

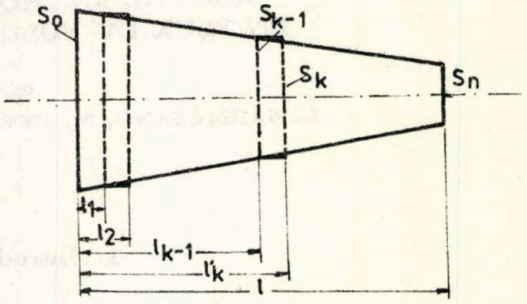

Fig. 1

$$V = \sum_{k=1}^{n} S_{k-1}(l_k - l_{k-1}), \tag{3}$$

où: S_{k-1} – la section courante, l_{k-1}, l_k – les longueurs courantes.

Le facteur de division, l_k, sera choisi de telle sorte que la variation de longueur $D_l = l_k - l_{k-1}$ détermine une variation négligeable de la section S_{k-1} ($S_{k-1} \approx S_k$).

2.1. Evaluation de la section courante

Pour évaluer la section courante de l'objet à mesurer, tout en mettant en évidence le manque d'homogénéité, on utilise un bloc avec 8 capteurs résistifs qui permettent l'interprétation des 8 cotes indépendantes de celui-ci, (R_i, $i = 1, ..., 8$), par rapport à un centre O situé au point de symétrie de la surface à mesurer.

À chaque côté R_i, ($i = 1, ..., 8$), correspond une section

$$S_i = \frac{\pi R_i^2}{8}, \quad (i = 1, ..., 8), \tag{4}$$

de sorte que la section courante sera donnée par la relation:

$$S_k = \sum_{i=1}^{8} S_i = \frac{\pi}{8} \sum_{i=1}^{8} R_i^2, \quad (i = 1, ..., 8). \tag{5}$$

On peut constater que l'aire de la section courante, S_k, est approximée avec l'aire des 8 secteurs circulaires, S_i. En supposant le centre de la section de la grume de forme convexe (Fig. 2) les différences possibles entre la section courante, S_k, réele et la surface approximative, S_k, vont se compenser réciproquement.

Les 8 capteurs résistifs sont disposés sur les côtés d'un cadre octogonal situé dans un plan perpendiculaire sur l'axe de la bande transporteuse.

Les palpeurs P_i, $(i = 1, ..., 8)$, qui représentent la partie mobile, peuvent glisser dans le plan de la section sur une direction radiale, suivant les variations de la côté R_i par rapport avec le centre de la surface active.

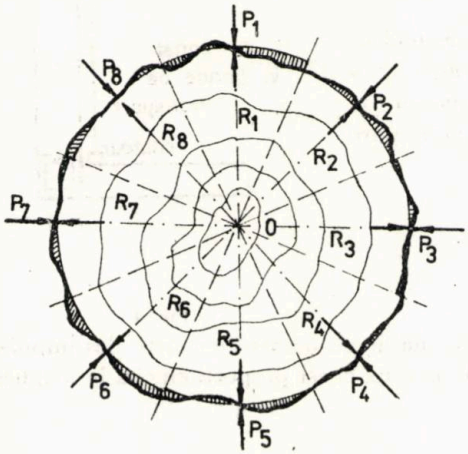

Fig. 2

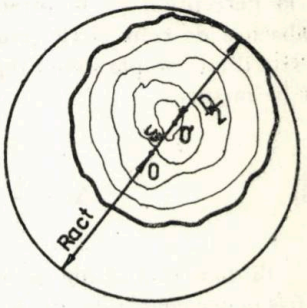

Fig. 3

Compte tenu que l'objet à mesurer peut apparaître dans une autre zone que celle active (le centre O du cadre des palpeurs), l'erreur peut augmenter avec la croissance de la distance ε entre le centre O et le centre O' de la section courante de la grume (Fig. 3). De la Fig. 3 résultent les conditions limite nécessaires pour une évaluation correcte:

$$\text{(6)} \qquad \text{a)} \quad \frac{D_k}{2} + |\varepsilon| \leq R_{\text{act}},$$

afin que l'objet à mesurer ne sorte pas de la surface active à mesurer, et:

$$\text{(7)} \qquad \text{b)} \quad |\varepsilon| \leq \frac{D_k}{2} - \frac{D_m}{2},$$

où D_k est le diamètre dans la section courante S_k et R_{act} – le rayon du cercle qui correspond à la surface active à mesurer de sorte qu'aucun palpeur ne perde pas le contact avec la grume, D_m – le diamètre minimum qui peut être mis en évidence.

Pour respecter ces conditions, avant de mesurer les grumes on les passe par un dispositif de guidage.

2.2. L'évaluation de la longueur

Si l'on considère la vitesse, a', de déplacement de la bande transporteuse constante, on peut mettre en évidence la longueur par un capteur de proximité photoélectrique qui saisit la pénétration et l'abandon de la surface active de l'objet à mesurer (Fig. 4).

La durée entre les fronts qui correspondent à la perception de la présence de l'objet et à l'absence de celui-ci (le palier de la tension de sortie d'un comparateur) représente une mesure de la longueur:

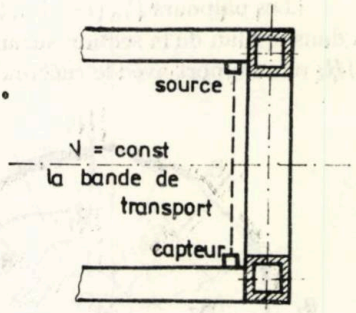

Fig. 4

$$\Delta t = \frac{l}{a}. \tag{8}$$

Si dans l'intervalle de temps Δt on charge un numérateur avec des impulses à fréquence constante, f_0, le numéro N de ceux-ci est proportionnel à la longueur courante:

$$N_{k_i} = \frac{l_k}{a} f_0. \tag{9}$$

3. La structure du système d'évaluation du volume

Le schéma de fonctionnement est présenté dans la Fig. 5. Les résistances R_i des 8 capteurs résistifs étant parcourues par des courant constants, I, générés par les sources de courant SCC, on peut définir les tensions:

$$U_i = IR_i. \tag{10}$$

Celles-ci sont amplifiées à l'aide de l'amplificateur A et converties numériquement à l'aide d'un converteur analogue–numérique CAN. La conversion analogue–numérique des signals fournis par les capteurs résistifs de mesure se réalise successivement, en contactant tour à tour les 8 entrées du signal au CAN par l'intermédiaire d'un multiplexeur MUX 8:1.

La commande du multiplexeur (les adresses A_0, A_1, A_2), le début de la conversion du CAN ainsi que la numération dans le numérateur de longueur N sont synchronisés par le microsystème de calcul.

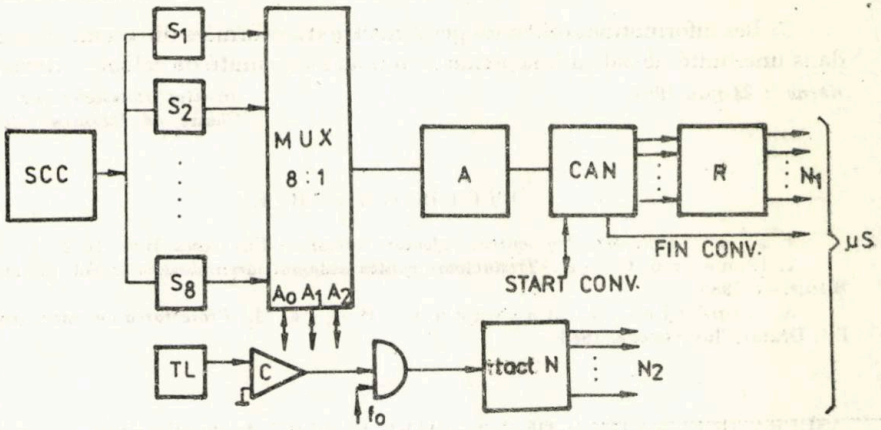

Fig. 5

Les deux mots digitals N_1, N_2 qui portent les informations concernant les rayons R_i, $(i = 1, ..., 8)$, et respectivement les longueurs courantes l_k, sont transformés par le système de calcul en suivant l'algorythme de principe de la méthode (v. rel. (3),...,(5)).

Si le CAN est du types à approximations successives, le temps de conversion spécifique pour une résolution de 8 bits est de 32 μs.

Si l'on considère aussi les temps MUX, qui représentent le retard du régistre tampon et les temps nécessaires à obtenir des informations par le système de calcul, le temps nécessaire pour une conversion ne peut pas dépasser 50 μs. Par conséquent le temps total de conversion atteindra 8×50 μs = 0,4 ms.

Pour une vitesse de la bande transporteuse de 0,5 m/s, le déplacement de celle-ci, pendant une conversion complète, est de 0,4 m/s $\times$0,5 mm m/s = 0,2 mm. Donc, on peut considérer que l'information reçue de tous les capteurs est transformée dans le même temps (en temps réel).

4. Conclusions

1. La méthode d'évaluation du volume en flux permet d'éliminer les temps morts nécessaires au calcul statistique.

2. En renonçant aux tables de cubage dans le calcul du volume (par la mesure directe de la longueur et de la section) par la méthode proposée on gagne du temps et on élimine certaines erreurs de mesure et de calcul.

3. L'évaluation de la section courante par la méthode de l'addition des secteurs correspondants à plusieur cotes distinctes, permet d'ignorer certaines fantes de mesure dues aux dérivations de la circonférence de la grume de forme circulaire.

4. Les erreurs de mesure, lorsqu'on réalise d'une façon satisfaisante le bloc de capteurs et le schéma électronique, sont de 3%, beaucoup moindres que celles obtenues par une évaluation directe.

5. Les informations obtenues peuvent être transformées directement, sur place, dans une unité de calcul indépendente ou dans une unité de calcul centralisée.

Reçue le 24 juin 1991

Institut Polytechnique, Jassy,
Chaire de Mesures électriques

BIBLIOGRAPHIE

1. * * * *Tabele de cubaj pentru exploatări forestiere.* Ed. Ceres, Buc., 1972.
2. Ionescu G. et al., *Traductoare pentru automatizări industriale.* Vol. I, Ed. Tehn., Bucureşti, 1985.
3. Căpăţînă O., Haşegan C., Puşcă M., *Proiectarea cu microprocesoare.* Ed. Dacia, Cluj-Napoca, 1983.

ASUPRA UNEI METODE DE MĂSURARE ÎN FLUX A VOLUMULUI LA BUŞTENI

(Rezumat)

Se propune o metodă de estimare în flux a volumului la buşteni, prin plasarea pe banda transportoare a unor senzori rezistivi. Informaţiile de la senzori sunt prelucrate de un microsistem de calcul. Metoda de calcul şi schema propusă oferă o eroare de estimare a volumului mai mică de 3%.

BULETINUL INSTITUTULUI POLITEHNIC DIN IAŞI
Tomul XXXIX (XLIII), Fasc. 1–4, 1993
Secţia III
ELECTROTEHNICĂ. ENERGETICĂ. ELECTRONICĂ

C.D. 538.551.21

SUR LES CONVENTIONS UNITAIRES POUR L'ÉNONCIATION DES ÉQUATIONS DES CIRCUITS ELECTRIQUES

PAR
AL. SIMION

1. Introduction

Dans la littérature de specialité roumaine on utilise d'habitude deux conventions afin d'associer les orientations des grandeurs électriques intervenant dans une branche de circuit (tension aux bornes, tension électromotrice (t.é.m.) et courant), en l'occurrence la convention du générateur et celle du récepteur. En fait, dans les équations qui décrivent les circuits électriques, l'une de ces grandeurs – la tension électrique – peut opérer soit avec le signe +, soit avec le signe –. L'option pour l'une de ces deux conventions est dictée par une hypothèse concernant le type de branche – réceptrice ou génératrice –, hypothèse qui a comme point de départ un raisonnement préliminaire concernant les grandeurs et les sens réels de la tension aux bornes, respectivement la t.é.m. dans la branche considérée. Parfois, après avoir opté initialement pour la convention récepteur, par exemple, il arrive qu'à la suite des calculs la branche s'avère être génératrice et *vice-versa*. De même, par exemple, si on ne connaît pas exactement la valeur de la t.é.m. dans une branche ou bien si on la considère comme étant variable, à ce moment-là le fait d'adopter une certaine convention pour la respective branche tout en adoptant une autre pour les autres branches du circuit (ou pour certaines d'entre elles) peut mener à des résultats erronés [1].

Le second théorème de K i r c h h o f f (la somme algébrique des t.é.m. tout au long d'une maille est égale à la somme algébrique des chutes de tensions le long de la même maille) suppose que le parcours de la maille peut être effectué de deux manières: par l'intérieur des sources (par la branche) mais aussi par l'extérieur. L'utilisation du même symbole, la flèche, pour la t.é.m. ainsi que pour le sens du courant constitue une inconséquence formelle susceptible de créer des confusions.

Lors de l'analyse du fonctionnemet des transformateurs électriques on adopte

pour l'un des deux circuits – le primaire – la convention de récepteur et pour l'autre circuit, le secondaire, la convention de générateur. Mais pour les transformateurs d'interconnexion entre des réseaux ou des transformateurs d'alimentation des machines électriques synchrones où asynchrones qui fonctionnent aussi en régime de récupération au réseau il y a des moments ou le changement des conventions pour écrire les équations des circuits s'impose afin de pouvoir vérifier le bilan des puissances. En plus, pour l'autotransformateur l'existence de deux conventions pour le même tronçon de circuit peut mener à des erreurs et à des difficultés inacceptables [2].

Dans l'étude des machines électriques synchrones, asynchrones et à courant continu, le fait de traiter séparément les deux régimes de fonctionnement, générateur où moteur, conduit à l'utilisation de deux équations différentes pour le même ensemble. En plus, pour écrire le régime de frein il faut faire appel à une troisième équation [3].

Les machines électriques utilisées dans les systèmes d'entraînement changent souvent leur régime de fonctionnement (moteur, générateur où frein) et la modélisation sur ordinateur de la machine – qui réclame aussi la vérification du bilan des puissances – n'est possible que si les équations changent de forme en fonction du régime concret de fonctionnement, ce qui engendre des difficultés au moment de l'application pratique.

Aux Etats Units et dans presque toute l'Europe occidentale on a adopté une manière unitaire pour écrire les équations des machines électriques. En Europe de l'Est le problème suscite encore des discussions [4], [5], [2].

Dans ce qui suit on propose nombre de conventions qui permettent d'écrire d'une façon unitaire les équations des transformateurs et des machines électriques.

2. Sens des grandeurs, conventions, exemples

a) On caractérise la résistance parcurue par le courant i, (Fig. 1 a), à l'aide de la tension aux bornes, u, répresentée à l'extérieur et orientée de a vers b. Les valeurs de ces grandeurs respectent la relation $u = Ri$.

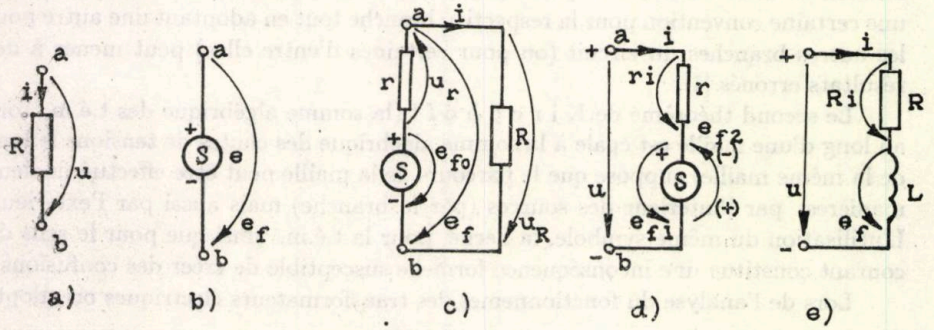

Fig. 1

b) On caractérise une source idéale, S, (la résistance interne étant nulle) par une tension électrique indiquée par une flèche extérieure orientée du pôle (+) vers le pôle (−), (Fig. 1 *b*), en renonçant à la flèche par l'intérieur pour éviter des confusions concernant le symbole du courant. Cette tension peut être denommée „tension électrique Faraday" (t.é.f.) où „tension électrique induite aux bornes" parce que d'habitude elle apparaît par suite de la variation du flux magnétique, sa valeur étant $e_f = +\mathrm{d}\psi/\mathrm{d}t$. Ultérieurement ce serait plus simple d'écrire cette expression en renonçant à l'indice f.

Une source réelle de tension peut être considérée équivalente avec l'ensemble d'une source idéale de tension (caractérisée par la t.é.f. de marche à vide e_{f0}, avec le sens indiqué par la flèche extérieure) et d'une résistance (interne), r, caracterisée par la tension aux bornes, u_r, ayant le même sens que le courant électrique, connectées en série (Fig. 1 *c*), tout en représentant cette résistance, par convention, à l'extérieur de la source.

La tension aux bornes de cette source réelle, notée par e_f, est illustrée par une flèche extérieure orientée de a vers b.

c) Une branche de circuit détachée d'un réseau qui peut contenir soit la source S connectée en série avec la résistance $r(R)$, soit un seul élément (source ou résistance) est caractérisée par le courant i (de a vers b) et par la tension aux bornes, u, indiquée par l'extérieur de a vers b (Fig. 1 *d*). En fonction de la polarité de la source on peut prendre en considération les deux cas pour les sens des tensions e_f, (e_{f1} où e_{f2}), mais dans les deux cas la flèche du courant et celle de la tension sortent de la même borne, c'est à dire a pour cette situation.

d) Pour appliquer les théorèmes de K i r c h h o f f il faut établir tout d'abord les sens des courants sur les branches du circuit, les sens des tensions entre les bornes a et b, associés de la manière indiquée dans la Fig. 1 *d*, et les sens des t.é.f. imposés par les polarités des sources sur les branches.

Le premier théorème (pour les courants) s'applique sous la forme suivante: la somme algébriques des courants des branches d'un noeud est nulle (on peut convenir que les courants représentés par des flèches dirigées vers le noeud soient positifs et les courants de sens contraires négatifs).

Le deuxième théorème (pour les tensions) est formulé tel qu'il suit: la somme algébrique des tensions sur les branches d'une maille du réseau est nulle. Pour appliquer ce théorème il faut considérer un sens pour le parcours sur la maille du réseau et suivre un tracé fermé, extérieur au circuit, qui englobe toutes les tensions des branches représentées par des flèches; les tensions dont les flèches ont le même sens que le sens du parcours sur la maille du réseau seront positives.

Les tensions aux bornes seront exprimées par les tensions sur les éléments de la branche. Par exemple, pour la maille de la Fig. 1 *c* on peut écrire: $e_f - u_R = 0$ si on considère le sens (a, e_f, b, R, a) ou $-u_r + e_{f0} - u_R = 0$ si on accepte le tracé (a, u_r, e_{f0}, b, R, a).

On peut écrire aussi soit $e_{f0} - u_r = e_f$, soit $e_{f0} - ri = e_f$ et donc la tension aux bornes d'une source qui débite sur le récepteur R sera égale avec la différence entre sa tension de marche à vide et la chute de tension sur la résistance inter-

ne. L'utilisation de la tension aux bornes, e_f, à la place de la t.é.m. signifie en fait l'introduction d'une grandeur mesurable à la place d'une grandeur existente (t.é.m.), mise en évidence par ses effets seulement.

Pour le circuit de la Fig. 1 *d* on peut écrire soit:

$$u - e_{f1} - ri = 0, \tag{1}$$

pour la polarité (+) et (−), de la source S, soit:

$$u + e_{f2} - ri = 0, \tag{2}$$

pour la polarité (−) et (+) de la même source.

e) Dans le cas d'une bobine, dont l'inductivité est L, alimentée par une source de tension sinusoïdale (harmonique), on peut associer le sens des grandeurs de la manière indiquée dans la Fig. 1 *e*, en tenant compte des relations:

$$u - e_f - Ri = 0, \quad u = e_f + Ri, \quad e_f = \frac{\mathrm{d}\psi}{\mathrm{d}t} = L\frac{\mathrm{d}i}{\mathrm{d}t}. \tag{3}$$

On peut utiliser des symboles analogues mêmes pour les sources à courant alternatif, y compris la polarité „+" et „−", puisque lors de la transcription des expressions instantannées de la t.é.f., il existe une possibilité d'erreur à savoir, l'introduction d'une valeur egale à π pour le déphasage.

f) Dans les circuits à courant continu on accepte (comme étant bien nécessaire) la représentation des tensions et des courants par des segments orientés sur un axe réel (diagramme vectoriel).

Si certaines grandeurs sont considérées positives, le vecteur sera orienté vers le „+" de l'axe et en sens contraire pour les grandeurs négatives. Par exemple, en considérant un accumulateur branché sur une source afin de le charger (Fig. 2 *a*), pour $U = 3$ V, $E_f = 2$ V, $r = 1\ \Omega$ l'équation $U - E_f - rI = 0$ conduit à $I = 1$ A, positif (v. le diagramme des grandeurs de la Fig. 2 *b*).

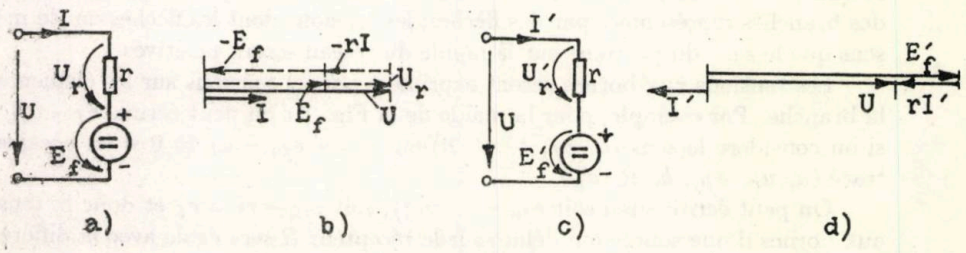

Fig. 2

. En substituant l'accumulateur précédent par un autre ayant $E'_f = 4$ V, l'équation $U - E'_f - rI' = 0$ conduit à $I' = -1$ A, et donc I' a le sens réel contraire par rapport au sens admis initialement (Fig. 2 *d*).

On observe donc qu'en acceptant les mêmes sens il résulte, pour le premier cas, des valeurs positives pour le courant I (ayant le même sens que la tension U), la puissance $P = UI$ étant positive, c'est-à-dire la branche est un récepteur; pour le deuxième cas, le courant I' est négatif, la puissance $P' = UI'$ est négative, la branche est donc un générateur.

g) La convention concernant les puissances dans les branches des circuits à courant continu a en vue, d'une part, les sens arbitraires acceptés pour les courants et les tensions aux bornes et d'autre part, l'orientation du courant et de la tension aux bornes sur le diagramme (le sens réel).

Pour les branches des circuits à courant continu il résulte quatre cas possibles (Tableau 1).

Tableau 1

Les sens des grandeurs	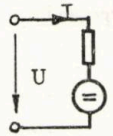 (+1)		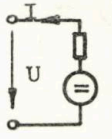 (-1)	
Le diagramme	(+1)	(-1)	(+1)	(-1)
Le type de la branche	Récepteur(+1) a)	Générateur(-1) b)	Génér. (-1) c)	Récep.(+1) d)

En tenant compte des sens des grandeurs sur les branches selon la Fig. 1 *d* il en résulte les cas a) et b) et donc la branche sera un récepteur si sur le diagramme le courant réel a le même sens que la tension et un générateur si leurs sens sont contraires.

h) La convention concernant les sens des puissances actives et réactives pour les circuits à courant alternatif qui fonctionnent en régime permanent sinusoïdal doit tenir compte des sens adoptés pour la tension et le courant et aussi du déphasage entre eux, φ.

Il y a huit situations possibles, présentées dans le Tableau 2.

Les régimes de récepteur des puissances active, P, ou réactive Q, (+1), respectivement les régimes de générateur de P ou Q, (−1), sont obtenus par la composition des sens du courant et de la tension par +1 si les flèches de la tension et du courant ont la même orientation rapportée à la borne supérieure gauche, par exemple; −1 si ces flèches ont une orientation différente avec les sens réels des composantes active

Tableau 2

Les sens des grandeurs	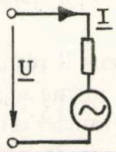 (+1)		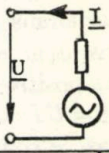 (-1)	
Le diagramme	I_a: (+1) a) I_r: (+1)	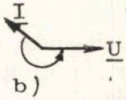 b) (-1)	(+1) e) (+1)	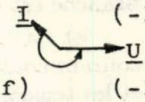 f) (-1)
Le type de la branche	Réc. P (+1) Réc. Q (+1)	Gén. P (-1) Gén. Q (-1)	Gén. P (-1) Gén. Q (-1)	Réc. P (+1) Réc. Q (+1)
Le diagramme	 I_a: (+1) c) I_r: (-1)	(-1) 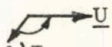 d)	 (+1) g) (-1)	(-1) 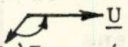 h) (+1)
Le type de la branche	Réc. P (+1) Gén. Q (-1)	Gén. P (-1) Réc. Q (+1)	Gén. P (-1) Réc. Q (+1)	Réc. P (+1) Gén. Q (-1)

I_a ou reactive I_r du courant, indiquées sur le diagramme tout en respectant la loi de composition pour la multiplication des nombres réels.

En acceptant les sens de la tension et du courant conformément à la Fig. 1 *d* on obtient les quatres situations de la première partie du Tableau 2, c'est-à-dire a),..., d).

i) Lors de l'analyse de certains circuits complexes de courant alternatif ou continu (Fig. 3), il est possible d'associer les sens des tensions et des courants (et il en est même souhaitable) d'une seule façon (Fig. 1 *d*).

Le calcul de ces circuits, en utilisant les théorèmes de K i r c h h o f f, fournit les informations concernant le caractère de chaque branche, récepteur ou générateur, pour P ou Q, selon ce qu'il en résultera du diagramme des grandeurs $\underline{U}_{ij}$ et $\underline{I}_{ij}$ (seules les quatre situations a),..., d) indiquées dans le Tableau 2 entrent en discussion).

Si on ne respecte pas cette convention il est possible d'aboutir à huit situations distinctes, (a),...,h) – Tableau 2), et l'analyse du bilan des puissances actives ou réactives sera d'autant plus difficile.

j) Au cas où un circuit contient seulement une source réelle branchée sur une impédance (ou même sur un autre source) – Fig. 4, l'analyse sera encore plus

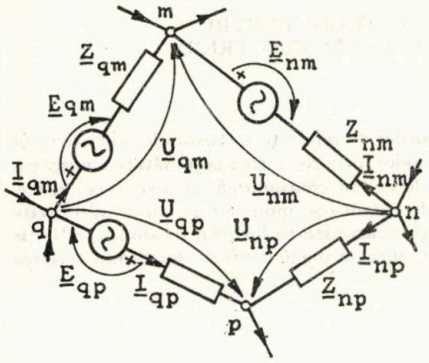

Fig. 3

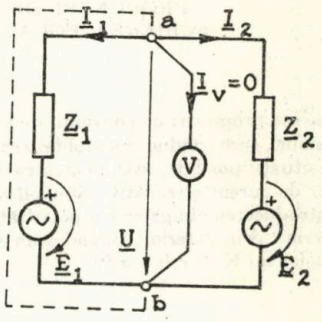

Fig. 4

difficile. Si cette maille est divisée en deux branches, (intérieure – qui contient la source; extérieure – qui contient le récepteur et éventuellement une autre source) il n'est plus possible d'associer les sens des grandeurs selon la même règle pour les deux branches sauf si on accepte la circulation par les deux branches des courants $\underline{I}_1$ et $\underline{I}_2$ de sens contraires. Pour atteindre ce but il faut introduire une branche fictive dont l'impédance est infinie (par exemple un voltmètre) entre les bornes a et b. Donc les points a et b en deviennent des noeuds et le calcul du circuit sera possible en utilisant les théorémes de K i r c h h o f f et la condition particulière $\underline{I}_v = 0$.

Il s'avère nécessaire à observer que les difficultés mises en évidence par l'analyse de ce dernier cas pourraient constituer l'obstacle majeur qui entrave l'utilisation d'une seule convention pour les sens des grandeurs dans des circuits électriques.

Dans un prochain article, on poursuivra l'utilisation des conventions dans l'étude des transformateurs et des machines électriques.

Reçue le 15 avril 1990

Institut Polytechnique, Jassy,
Chaire d'Électrotechnique
et de Machines électriques

BIBLIOGRAPHIE

1. M o c a n u C.I., *Teoria circuitelor electrice.* EDP, Bucureşti, 1979.
2. A n t i k I.V., *O vybore uslovno položitel'nyh napravlenyi napriaženyi i tokov pri analize raboty transformatorov.* Električestvo, *11*, 59-60 (1985).
3. C î m p e a n u A., *Maşini electrice.* Ed. Scrisul Românesc, Craiova, 1988.
4. M o r g a n T.A., *General Theory of Electrical Machines.* Ed. Heyden, London, 1979.
5. C h a t e l a i n J., *Machines électriques.* Presse Polytechnique Romandes, Laussane, 1988.

PROPUNERI DE CONVENŢII UNITARE PENTRU SCRIEREA ECUAŢIILOR CIRCUITELOR ELECTRICE

(Rezumat)

Se fac propuneri de convenţii de asociere a sensurilor de referinţă a tensiunilor şi curenţilor prin ramuri, care conduc la simplificarea analizei circuitelor, prin reducerea la jumătate a numărului de situaţii posibile, atât pentru cazul circuitelor de curent continuu cât şi pentru cel al circuitelor de curent alternativ. Simbolizarea surselor de curent continuu sau de curent alternativ prin introducerea obligatorie a polarităţilor la borne şi caracterizarea lor prin tensiunea la borne considerată prin exterior, ţinând seama de polarităţi, elimină unele confuzii, facilitând scrierea teoremelor lui K i r c h h o f f.

BULETINUL INSTITUTULUI POLITEHNIC DIN IAŞI
Tomul XXXIX (XLIII), Fasc. 1–4, 1993
Secţia III
ELECTROTEHNICĂ. ENERGETICĂ. ELECTRONICĂ

D.C. 621.313.333

ON THE EXPERIMENTAL TESTS RESULTS REGARDING THE UNDERSYNCHRONOUS CONDENSERS BRAKING OF THE ASYNCHRONOUS THREE-PHASE MOTOR

BY

MIRCEA-SORIN OPRIŞOR and SIMONA-ANA CABA

1. Introduction

The asynchronous form of the mechanical characteristic corresponding to the condensers braking regime has been established in [1], and the generalized form of the equation of the symmetrically three-phase asynchronous machine torque with variable frequency voltages have been determined. It has been shown that, from an economic point of view, it is favourable that the stator supplementary resistances and the condensers should be connected having regard to the diagram which requires the smallest overall sizes and determines minimum losses for the same braking torque.

The experimental tests have been made on an asynchronous motor ASI 112 M 28-2 of 4 KW, 2 860 rot/min., with $I_{1N} = 8.19$ A, $T_N = 11.35$ Nm, and without a fan. The torque has been determined by the calibrated dynamo method. In agreement with the conclusions in [1], all the tests have been accomplised for the star- or delta-connected condensers, with or without supplementary series resistances.

2. Experimental Tests Results

The variation curves of the phase voltage, function of speed and capacity of the used condensers, have been plotted in Fig. 1 a, b. For any connection diagram of the condensers, the phase voltage is relatively small, even at increased speeds. The introduction of the supplementary series resistances determines the diminishing of the voltage on the motor phase. The phenomenon is amplified with the increase of speed and E.M.F., due to the increase of the voltage drop on the series resistance. Also the phenomenon is more evident at the diagrams with increased values delta-connected condensers where the current tends to increase more rapidly with speed and is limited by the supplementary resistance. A similar limiting of the current

and phase voltage results, as well, in the case of the rotor resistance increase, but this affects the form of the mechanical characteristic.

The variation curves of the stator current I_1 vs. the speed and condensers capacity are represented in Fig. 2 a, b. For any connection diagram of the condensers and for a large range of speeds, one can notice the reduction of the current by the introduction of the supplementary series resistance. This is stronger in the case of the high value capacities and for the diagram with delta connected condensers, i.e., when the phase capacity reactance x_C is smaller; thus, a smaller voltage V_1 results. For increased speeds, the increase of the supplementary resistance produces a more rapid increase of the current due to the limitation of the voltage V_1. In such cases, the total impedance must be amplified by decreasing the capacity C.

In the high speeds domain, the current I_1, at a given speed, can be decreased, as well, by star-connecting the condensers. Consequently, generally speaking, for a given braking torque, the braking current can be smaller than the nominal current of the machine, I_{1N}. As the rotor current decreases at the same time with the stator one, in the case of the asynchronous motor, we can deduce that, under a proper adjustement, the condensers braking does not put special problems from a thermal point of view.

The families of mechanical braking characteristics obtained for the same stator diagrams as in Figs. 1 and 2, are represented in Fig. 3 a, b. One can notice that, for the same variation range of the phase capacity C, and for a given torque, in the case when the supplementary series resistance R_{1S} is increased, the variation domain of the speed moves downwards to the null speed. Also, for a given supplementary resistance, at the variation of the braking torque, the speed variation domain approaches the null one, either by the increase of the capacity C, or by switching the condensers from the star connection to the delta one. The decrease of the speed domain is also associated in both cases with its restriction.

Analysing the torque equation [1]:

$$T_b = \frac{2T_k\lambda^2(1+\gamma)}{\frac{\delta f_1^*}{\rho_2}\cdot\frac{s_k}{s}+\frac{\varepsilon\rho_2}{f_1^*}\cdot\frac{s}{s_k}+2\gamma}, \tag{1}$$

it is noticed that the magnitude of the braking torque T_b varies directly with the stator voltage V_1 (in the Eq.(1) $\lambda = V_1/V_{1N}$) and depends indirectly on the value both of the supplementary resistances R_{1S} and of the capacities C from the stator circuit. No matter what the condensers connection diagram is, the stator supplementary series resistance increases the braking torque, acting inversely to the increase of resistance from the phase:

$$\rho_2 = \frac{r_2}{r_2+R}. \tag{2}$$

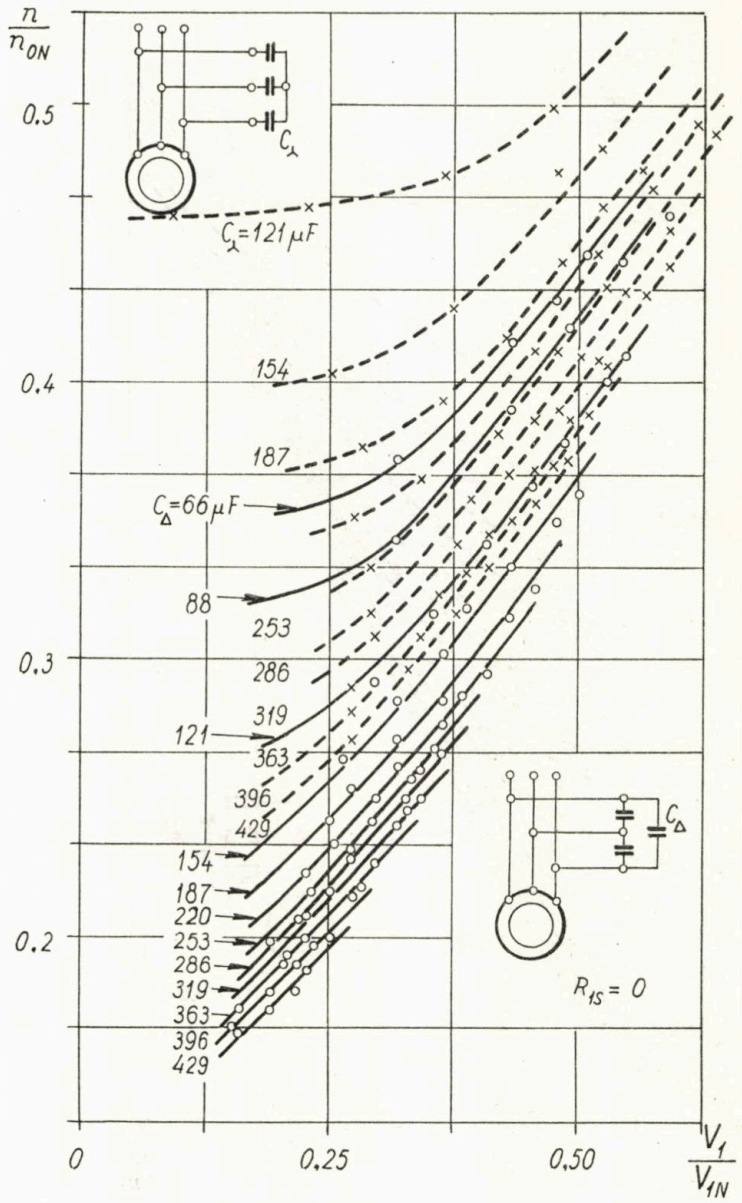
n/n0N
0.5
0.4
0.3
0.2
0
0.25
0.50
V1/V1N
CΔ
CΔ=121μF
154
187
CΔ=66μF
88
253
286
319
121
363
396
429
154
187
220
253
286
319
363
396
429
CΔ
RIS = 0

Fig. 1 *a*

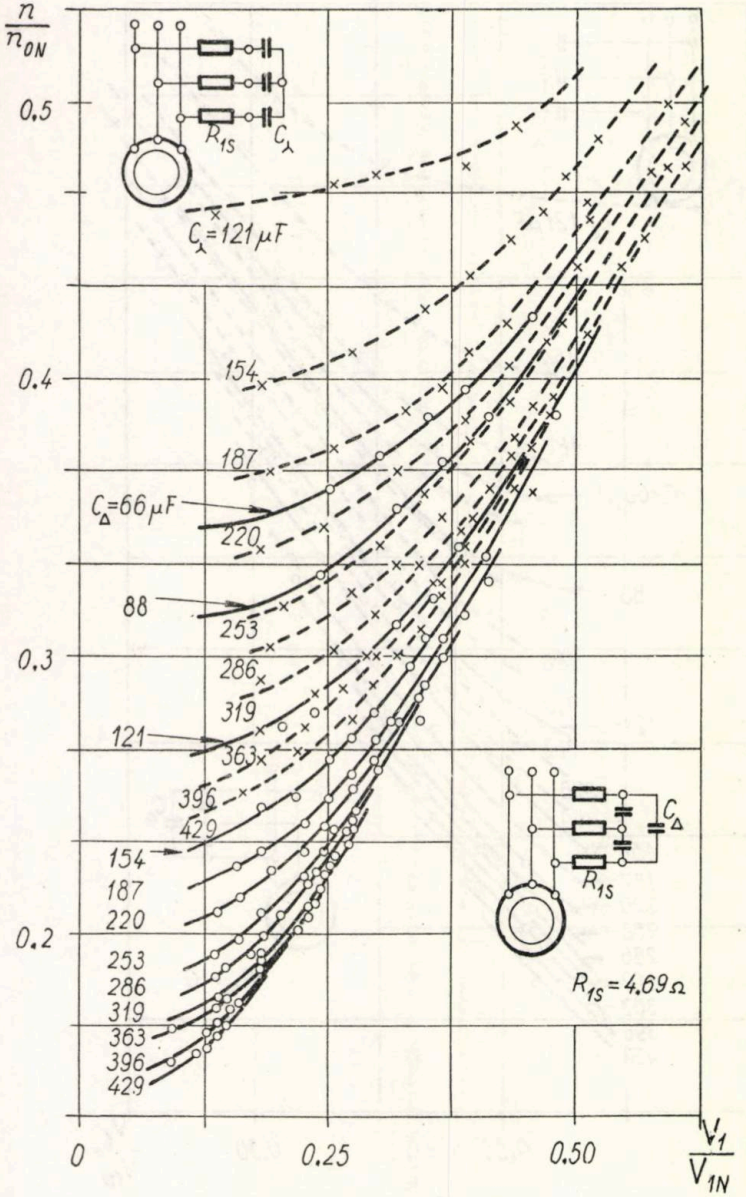
n/n0N
0.5
0.4
0.3
0.2
0
0.25
0.50
V1/V1N
R1S
CΔ
CΔ=121 μF
154
187
CΔ=66 μF
220
88
253
286
319
121
363
396
429
154
187
220
253
286
319
363
396
429
CΔ
R1S
R1S=4.69 Ω

Fig. 1 *b*

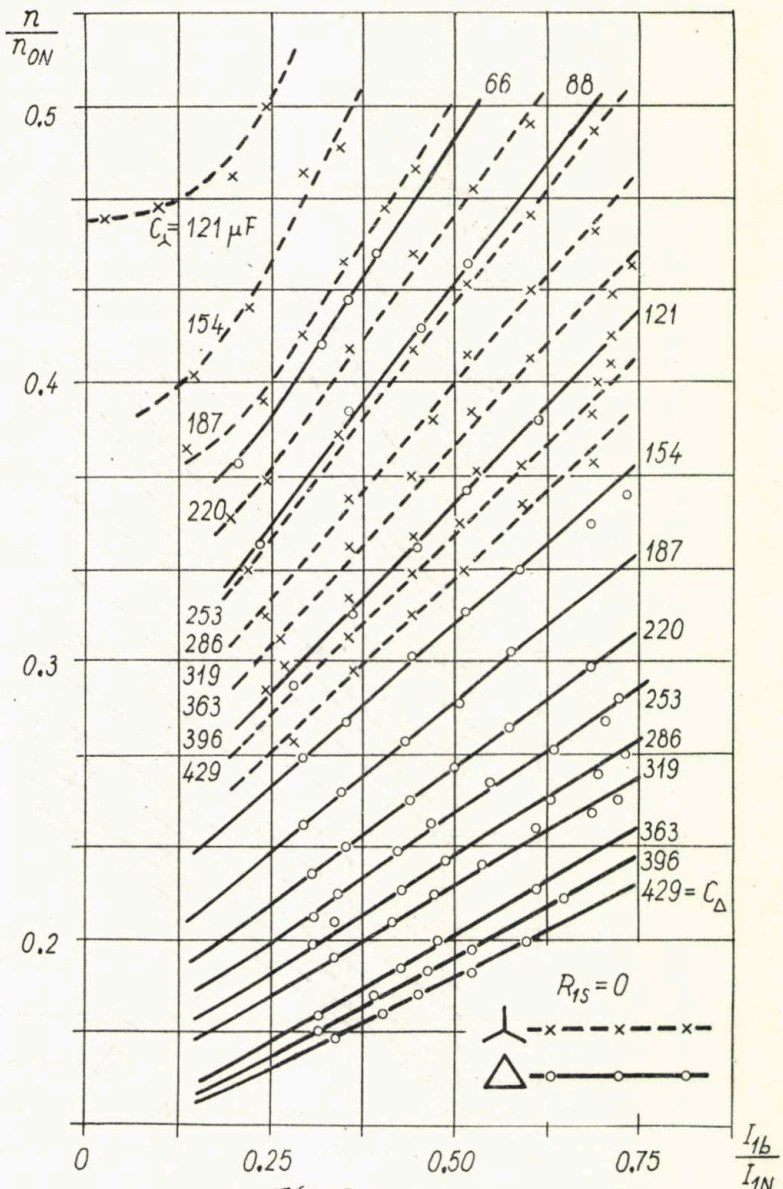
n/n_ON
0.5
0.4
0.3
0.2
0
0.25
0.50
0.75
I_1b/I_1N
66
88
C_Δ = 121 μF
154
187
220
253
286
319
363
396
429
121
154
187
220
253
286
319
363
396
429 = C_Δ
R_1S = 0

Fig. 2 a.

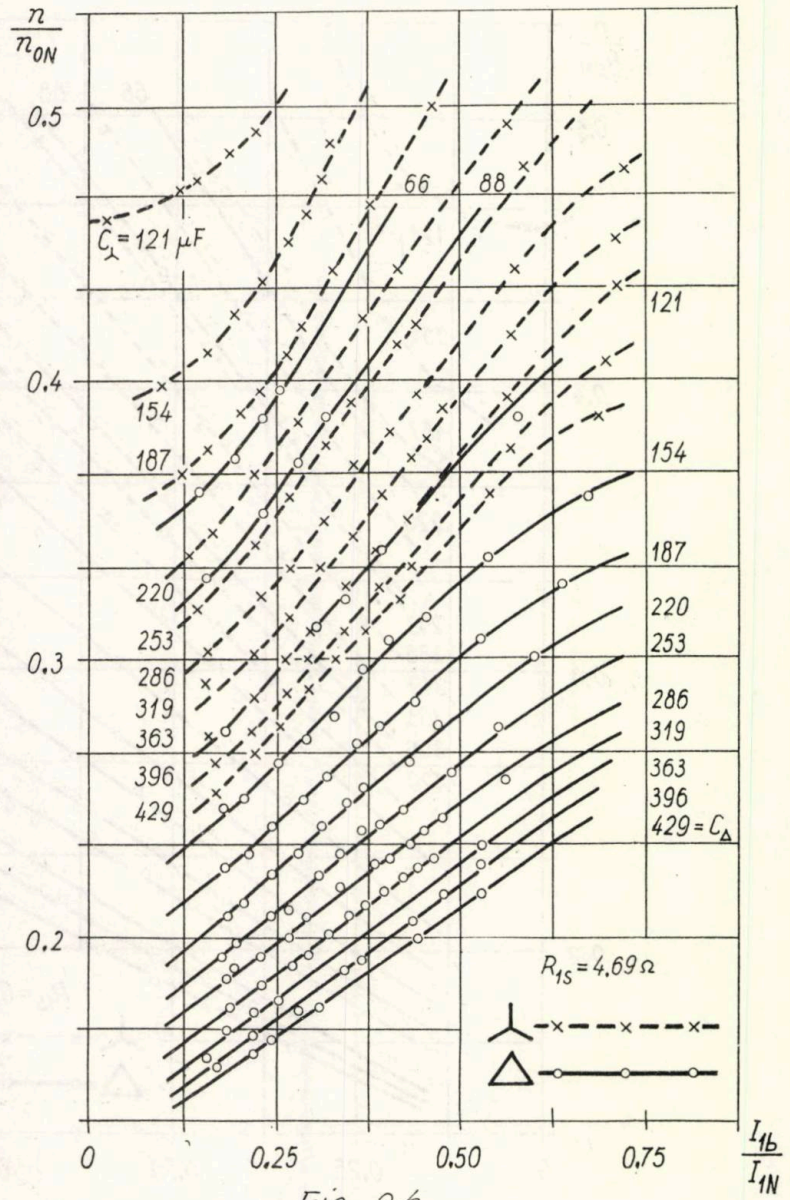
n/n0N
0.5
0.4
0.3
0.2
0
0.25
0.50
0.75
I1b/I1N
C= 121 μF
66
88
121
154
187
220
253
286
319
363
396
429 = CΔ
154
187
220
253
286
319
363
396
429
R1S = 4.69 Ω

Fig. 25

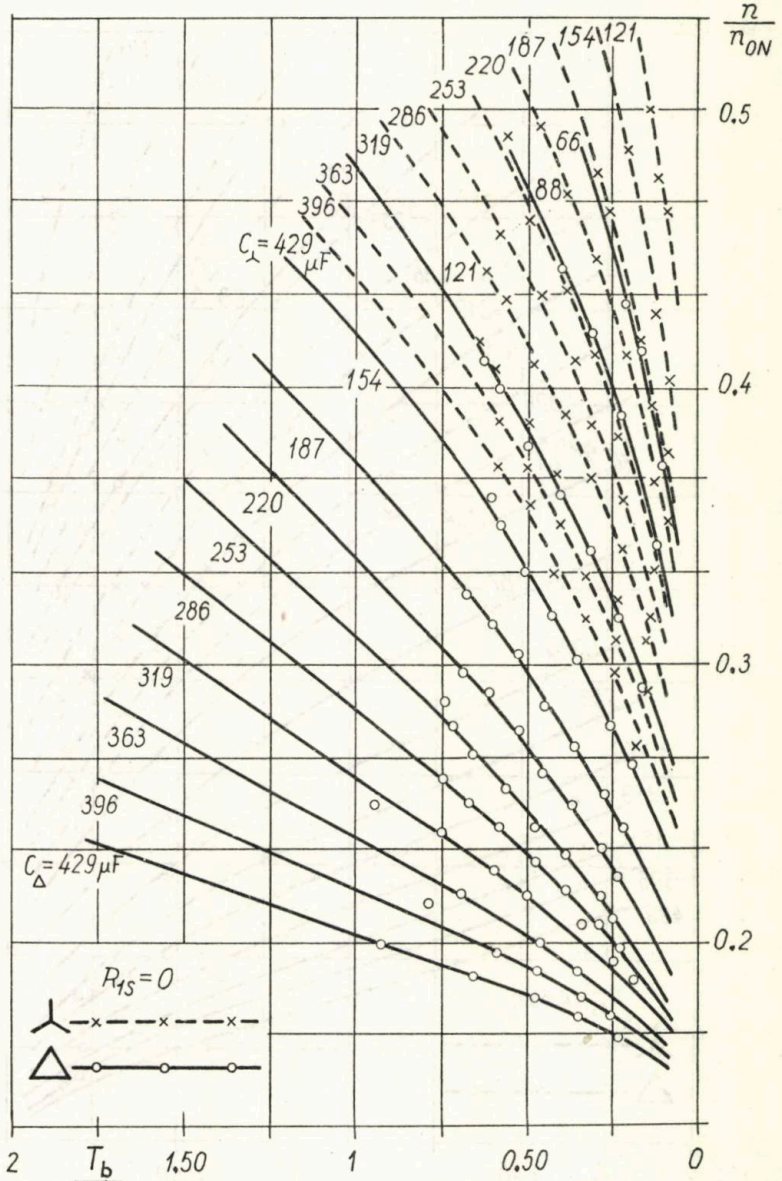
n/n_ON
0.5
0.4
0.3
0.2
187
154
121
220
253
286
319
363
396
66
88
C_Y = 429 μF
C_Δ = 429 μF
R_1S = 0
2
T_b/T_N
1.50
1
0.50
0

Fig. 3.a.

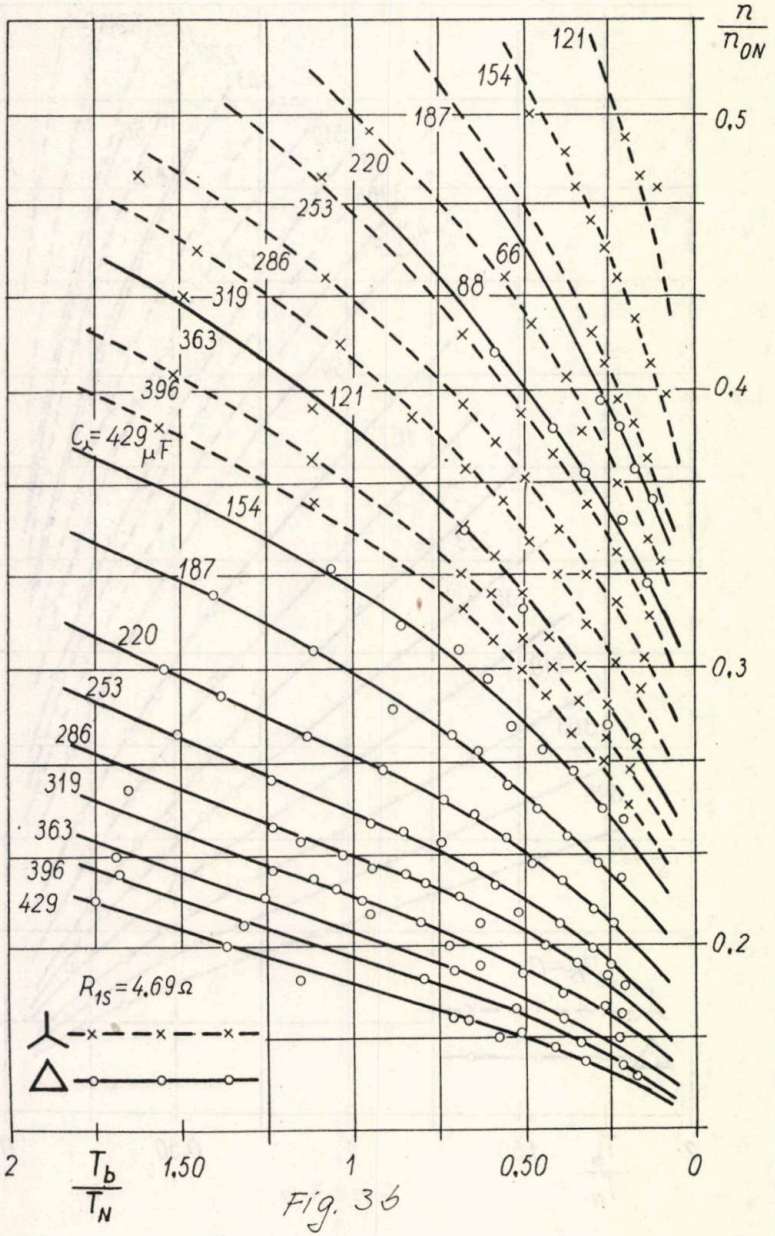
n/n0N
0,5
0,4
0,3
0,2
121
154
187
220
253
286
319
363
396
429
66
88
121
154
187
220
253
286
319
363
396
429
C= 429 μF
R1S = 4,69 Ω
2
Tb/TN
1,50
1
0,50
0

Fig. 36

This takes place as long as the stator current decreases with a relatively small value while the resistance R_{1S} is increased and when the voltage V_1 and the losses on R_{1S} are increased.

The increase of the connected capacity value on each phase determines the decrease of the free oscillation frequency of the stator voltage, $f_1^* = f_1/f_{1N}$, and, consequently, the increase of the braking slip s_b absolute value:

$$s = f_1^* s_b = \frac{f_1^* n_{0N} - n}{n_{0N}}. \tag{3}$$

Thus, it results an increase of the rotor current, at the same time, of the losses in the rotor and stator circuits, and of the braking torque, respectively. It is possible that in the case of high values of the condensers capacity [2], besides the diminishing of the stator current by the increase of the resistances R_{1S}, there could take place a demagnetization action of the increased rotor current which produces a more remarkable diminishing of the voltage and losses from the stator circuit, and of the braking torque, respectively.

The decrease and the restriction of the speed domain at the same time with the increase of R_{1S} or C, as well as the simultaneous increase of the braking torque determine the increase of the mechanical braking characteristic rigidity, of the static stability, of the constancy and precision of the adjustment, respectively. The phenomenon is ampler for the star-connected condensers diagram where these indexes are smaller in the absence of the stator supplementary resistance.

3. Operating Safety

Noticing from Fig. 3 that for $C < 121$ μF the braking is not set in the star-connected condensers diagram, the influence of the connection diagram and of the values of its parameters on the machine self-exciting conditions is rendered evident. Analysing the expressions of the limit self-exciting speeds [3]:

$$\omega_{k\max} = \omega_0 \left(1 + \frac{\rho_1}{\rho_2} \cdot \frac{r_2}{r_1}\right) \sqrt{\frac{x_C}{x_k}}, \quad \omega_{k\min} = \frac{\omega_0}{x_m} \sqrt{\frac{1}{2}\left(\frac{r_1}{\rho_1}\right)^2 - x_{1\sigma} x_C}, \tag{4}$$

where:

$$\omega_0 = 2\pi f_1, \quad \rho_1 = \frac{r_1}{r_1 + R_{1S}}, \quad x_k = X_1 - X_2 \frac{x_m^2}{(r_2/\rho_s s)^2 + X_2^2},$$

it is noted that the upper limit of the braking domain goes down at the same time with the decrease of the rotor supplementary resistance R (s. Eq. (2)), the increase of the stator supplementary resistance R_{1S}, the increase of the phase capacity C,

or the switch from the star-connected condensers to the delta-connected ones. As, generally speaking, $x_C > x_k$, the upper limit of the braking domain cannot go down the machine synchronism speed ω_0. The lower limit of the braking domain is not influenced by the magnitude of the rotor resistance and it is only a little influenced by the value of the stator supplementary resistance; on the other hand, it tends to values up to 10% from the synchronism speed (300 rot/min in the case of the used machine) when the phase-connected capacity is increased.

The most disadvantageous situation corresponds to the working machines with a high value potential-type torque, this being able to accelerate the machine up to speeds higher than $\omega_{k\max}$ before the self-excitation takes place. An incorrect braking entry control in a diagram having a diminished $\omega_{k\max}$ (increased stator resistance or decreased capacity reactance) greatly increases the danger of the regime unsetting. The increase of the operating safety imposes either the maintaining of the condensers to all operating regimes, fact which is not always necessary or admissible, or the pre-excitation of the machine by coupling to the supply network for a short time period (0.1...0.2 sec., according to [4]) after the condensers have been connected. In the last case, the supplementary series resistances also have the role of limiting the connection current load peak.

4. Economic Efficiency of the Proposed Solution

It is more difficult to make directly evident the economic efficiency of the installation as it depends on a series of particular factors for any operation system such as: the type of the working machine, the speed-time operating diagram, the productivity, the overall sizes of the movable or fixed elements, the area and the afferent buildings, etc. However, it is considered that the condensers braking is economic for the small and medium power asynchronous motors where the condensers batteries have smaller overall sizes.

The condensers braking is economic even when we have to adapt it on the existing installations, as it does not present oscillation phenomena, it is noiseless, it does not require special feed systems in d.c. (as the dynamic braking does) or for the control of the rotation direction (as the counter-current braking needs), and the static elements do not need a special maintenance; at the same time, it is efficient in a large range of speeds.

At the maintaining braking at high speeds, the economic efficiency of the installation is increased by star-connecting the condensers. In this case, the speed depends a lot on the magnitude of the braking torque, but the static stability is improved. The productivity of the installation is increased very much, especially for the hoisting machines where the lowering down of the load can be accomplished in smaller time intervals.

At the stop braking, the economic efficiency increases by the delta-connection of the condensers and by introducing of supplementary series resistances into the stator circuit. Both measures lead to marked increase of the braking torque, to the

creation of a greater independence of speed as compared to the torque magnitude and to the improvement of some adjustment indexes. A supplementary increase of the productivity is possible only by associating the condensers braking with the dynamic one [3], with the short-current one [5] or with the counter-current one [6].

The economic efficiency of the method is very good in the case when supplementary resistances are not introduced in the rotor circuit, being comparable with the one corresponding to the recuperative braking at nominal frequency. The supplementary resistance determines a marked increase of the method economic efficiency by the increase of the braking torque as well as by the dissipation of a quantity of the kinetic energy outside the motor.

5. Conclusions

Different braking diagrams by means of condensers are experimentally tried. In all the cases, the current and the phase voltage have admissible values, under the condition of a proper adjustment of the diagram and of the parameters values.

The method allows to obtain high braking torques under increased conditions of economic efficiency, stability and noiselessness.

The domain of the braking speeds is a very large one, and the adjustment is simple and economic.

The choosing of the diagram parameters depends on the braking torque and on the imposed speed domain. As, in the most cases, the condenser have, as well, the role of compensation for the power factor in the motor regime, their dimensioning should ensure $\cos\varphi = 1$ for the nominal parameters of this regime.

The operating safety is good and it can be simply ensured if the working speeds are in the self-excited domain of the machine, and the duration of the self-excited process is minimal.

In view to adopt the condensers braking and especially the mixed braking diagrams, or the diminished self-excited duration diagrams, we have to make careful analyses about the economic efficiency of the installation, specific for any given case.

Acknowledgements. The authors are indebted to Mr. subengineer V. Hriţcu, who effectively helped them for the experimental data, and to Professor M. Diaconescu, Polytechnic Institute, Jassy, who placed at theirs disposal the necessary testing machine.

Received, July 27, 1990

Polytechnic Institute, Jassy,
Department of
Utilizations, Drives
and Industrial Automation

REFERENCES

1. Oprişor M., Caba S., *Mathematical Model of the Subsynchronous Condensers Braking of the Asynchronous Three-Phase Motor.* Bul. Inst. Polit., Iaşi, **XXXVII (XLI)**, *1-4*, s.III, 63-70 (1991).

2. Petrow L.P., *Tormoznye charakteristiki asinchronnyh dvigatelei v generatornom režime s kondensatornym vozbuždeniem.* Vestnik Elektropromyshlennosti, **31**, 7, 47-52 (1960).

3. Petrov L.P., Bushtyan L.V., *Kharakteristiky asinchronnyh k.z. dvigatelei pri kondensatornom tormoženyi s aktivnymi nagruzočnymi soprotivlenyami.* Izv. V.U.Z., Elektromekhanika, **12**, *8*, 829-836 (1969).

4. Kashkalov V.I., Davidovič V.S., *O kondensatornom tormoženii asinchronnogo elektroprivoda mehanizmov podyema.* Prom. Energ., **12**, 47-49 (1971).

5. Căluianu D., Ailoaie Gh., Ceangă M., *Frînarea motoarelor asincrone trifazate cu ajutorul condensatoarelor.* Commun. at the Scient. Ses. of the Univ. of Galatzi, 1960.

6. Rashkovicz, M.P., Shaparev, N.K., Shklovskii, B.I., *Rasčet emkosti dlya skhemy dvukhstupenčatogo tormoženyia asinchronnyh korotkozamknutih dvigatelei.* Elektrotehnika, **42**, *8*, 27-28 (1971).

7. Oprişor M., *Schema optimă pentru frînarea de oprire cu condensatoare a motorului asincron.* Lucr. Conf. Naţion. de Electrot. şi Energ., Timişoara, 17-18 sept., 1982, **6**, 131-140.

REZULTATELE ÎNCERCĂRILOR FRÂNĂRII SUBSINCRONE CU CONDENSATOARE A MOTORULUI ASINCRON TRIFAZAT

(Rezumat)

Sunt prezentate curbele, ridicate experimental, de variaţie a tensiunii pe fază şi curentului statoric, precum şi familiile de caracteristici mecanice de frânare, obţinute pentru diferite scheme statorice la un motor asincron trifazat cu colivie. Se arată că în domeniul subsincron soluţia cu maximum de eficienţă corespunde condensatoarelor conectate în triunghi şi înseriate cu rezistenţe suplimentare. Sunt analizate siguranţa în funcţionare şi economicitatea soluţiei. Concluziile formulate urmăresc să stabilească condiţiile în care se poate extinde rapid în practică această metodă de frânare cu calităţi superioare.

BULETINUL INSTITUTULUI POLITEHNIC DIN IAŞI
Tomul XXXIX (XLIII), Fasc. 1-4, 1993
Secţia III
ELECTROTEHNICĂ. ENERGETICĂ. ELECTRONICĂ

C.D. 621.316.728

L'AUGMENTATION DE LA VITESSE DE CALCUL DANS LES PROBLÈMES D'OPTIMISATION DU RÉGLAGE TENSION–PUISSANCE RÉACTIVE

PAR
GH. CÂRŢINĂ et VIRGIL ALEXANDRESCU

1. Introduction

Le réglage optimal tension–puissance réactive est l'un des principaux problèmes rencontrés par les ingénieurs d'études des réseaux électriques. Depuis le début des années 60 la plupart des méthodes d'optimisation nonlinéaire ont été expérimentées pour le resoudre.

Dans ce qui suit on propose de resoudre le problème d'optimisation du plan des tensions d'un réseau électrique à puissances actives fixées aux noeuds en utilisant la méthode des gradients conjugués. De plus, on prouve que certaines simplifications dans le calcul de la matrice hessienne conduit à une sensible augmentation de la vitesse de calcul sans nuire à la précision de la méthode.

L'état d'un réseau électrique en régime permanent est complètement défini lorsque l'on connaît le module V_i et la phase θ_i de la tension en chaque noeud i. Les puissances actives et réactives injectées au noeud i s'expriment par des relations de la forme:

$$P_i = G_{ii}V_i^2 + V_i \sum_{\substack{k=1 \\ k\neq i}}^{n} V_k(G_{ik}\cos\theta_{ik} + B_{ik}\sin\theta_{ik}), \quad (i \neq e); \tag{1}$$

$$Q_i = -B_{ii}V_i^2 + V_i \sum_{\substack{k=1 \\ k\neq i}}^{n} V_k(B_{ik}\cos\theta_{ik} - G_{ik}\sin\theta_{ik}), \quad (i \neq e), \tag{2}$$

où G_{ik}, B_{ik} sont des constantes pour le réseau considéré, P, Q, V et θ sont des vecteurs de dimension $n-1$, ayant, respectivement, pour composants P_i, Q_i, V_i et θ_i.

Dans ces conditions soit le problème d'optimisation [1]:

$$\min p(P,Q,\theta,V) = \min \sum_{i=1}^{n} P_i(\theta,V), \tag{3}$$

avec les restrictions

$$\Delta P_i = P_i(\theta,V) - P_i = 0, \quad (i = \overline{2,n}), \tag{4}$$

$$\Delta Q_i = Q_i(\theta,V) - Q_i = 0, \quad (i = \overline{m+1,n}), \; g_i(\theta,V) = 0, \tag{5}$$

où

$$\underline{P}_i \le P_i \le \overline{P}_i, \tag{6}$$

$$\underline{Q}_i \le Q_i \le \overline{Q}_i, \tag{7}$$

$$\underline{V}_i \le V_i \le \overline{V}_i. \tag{8}$$

Dans les relations ci-dessus $i = 1$ est le noeud d'équilibre (générateur); $\overline{2,m}$ – les noeuds générateurs; $\overline{m+1,n}$ – les noeuds récepteurs. Pour ce qui suit il est utile d'introduire les notations:

$$V' = [\theta_2 ... \theta_n \; V_{m+1} ... V_n]_t, \tag{9}$$

$$X = [P_2 ... P_n \; Q_{m+1} ... Q_n]_t. \tag{10}$$

2. Optimisation du plan des tensions

Si l'on considère comme variables d'optimisation les tensions dans les noeuds générateurs, la fonction L a g r a n g e du modèle (3)...(10) a pour expression

$$\Phi = p(X,V') + \sum_{i=2}^{n} \lambda_i [P_i(V') - P_i] + \sum_{i=m+1}^{n} \mu [Q_i(V') - Q_i], \tag{11}$$

dont les dérivées par rapport à $V_g = [V_1 ... V_m]_t$ ont la forme générale (le gradient réduit) [2]:

$$\left[\frac{\partial \phi}{\partial V_g}\right] = \left[\frac{\partial P_1}{\partial V_g}\right] + \left[\frac{\partial X}{\partial V_g}\right] \begin{bmatrix} \lambda \\ \mu \end{bmatrix}, \text{ avec} \tag{12}$$

$$\begin{bmatrix} \lambda \\ \mu \end{bmatrix} = -[J]_t^{-1} \left[\frac{\partial P_1}{\partial V'}\right]. \tag{13}$$

Afin de déterminer le minimum des pertes de puissance active, $p(V_g)$, à l'aide des composants du gradient réduit (rel. (12)), on utilise l'algorithme des gradients conjugués. Pour la fonction objectif (3) la méthode des gradients conjugués consiste dans la détermination d'un point de l'itération $k+1$ [2]:

$$V_g^{(k+1)} = V_g^{(k)} + \alpha^{(k)} d^{(k)}, \quad (k = 0, 1, 2, ...), \tag{14}$$

le long d'une direction

$$d^{(k)} = -g^{(k)} + \beta^{(k)} d^{(k-1)}, \quad (k = 1, 2, ...), \tag{15}$$

$$d^{(0)} = -g^{(0)}. \tag{16}$$

Dans ces relations le pas de déplacement

$$\alpha^{(k)} = -\frac{< g^{(k)},\ d^{(k)} >}{< d^{(k)},\ H^{(k)} d^{(k)} >}, \tag{17}$$

et le coefficient

$$\beta^{(k)} = \frac{< g^{(k)},\ g^{(k)} >}{< g^{(k-1)},\ g^{(k-1)} >}, \tag{18}$$

sont déterminés à partir des conditions d'optimisation le long de la direction $d^{(k)}$, de façon que les directions successives soient conjuguées. Le critère d'arrêt est soit la norme du gradient, soit $V_g \leq \overline{V}_g$ (les bornes des tensions).

Le terme général de la matrice hessienne, $H^{(k)}$, qui intervient dans le calcul du pas de déplacement, (rel. (17)), est de la forme:

$$\frac{\partial \phi}{\partial V_{gi} \partial V_{gj}} = G_{ij} \cos\theta_{ij} (\lambda_i + \lambda_j) + B_{ij} \sin\theta_{ij} (\lambda_i - \lambda_j), \tag{19}$$

où les coefficients λ_i, nommés facteurs de pénalité, sont calculés avec la relation (13). Pour les valeurs usuelles, le rapport entre le premier et le deuxième terme de la relation (19) est de l'ordre $3 \cdot 10^3$. Donc, dans le calcul de la matrice hessienne on peut ignorer le terme en B_{ij} sans trop affecter la convergence de la méthode d'optimisation.

3. Exemple de calcul

La méthode proposée a été testée pour différents réseaux, avec un nombre de noeuds allant de 3 à 100. Les calculs ont été effectués avec la méthode précise et avec celle simplifiée, en ignorant

le deuxième terme de la relation (19). Il en a résulté que dans le cas de la méthode simplifiée la précision du calcul n'est pas affectée, mais la vitesse de calcul a augmenté sensiblement.

À titre d'exemple sont présentés les résultats du calcul pour un réseau à 220 KV dont les principaux caractéristiques sont données dans le Tableau 1.

Tableau 1

Les caractéristiques du réseau considéré

La ligne	Z, [Ω]	Y, [S]
(1,2)	8,375+j50,5	$j3{,}47.10^{-4}$
(2,3)	6,700+j43,4	$j2{,}78.10^{-4}$
(1,3)	5,36 +j32,5	$j2{,}23.10^{-4}$

En utilisant la méthode des gradients conjugués, dans la première itération on trouve

$$d^{(0)}=-g^{(0)}=[0{,}005269 \quad 0{,}04125]_t.$$

Le calcul des direction de déplacement ($\partial\phi/\partial V_{gi}$) doit être effectué d'une manière autant que précise possible, autrement les erreurs peuvent être très grandes.

Tableau 2

Les résultats du calcul

Valeurs calculées	La méthode précise	La méthode simplifiée
α	64,383842	64,364671
$\Delta V=[\Delta V_1 \ \Delta V_3]_t$, [KV]	$[0{,}339 \ \ 2{,}655]_t$	$[0{,}339 \ \ 2{,}654]_t$
V, [KV]	$[230{,}339 \ \ 230{,}655]_t$	$[230{,}339 \ \ 230{,}654]_t$

4. Conclusions

Pour la détermination du plan optimal des tensions d'un réseau électrique la méthode des gradients conjugués s'avère très efficace. L'optimum est atteint généralement dans 4...7 itérations. On gagne dans la vitesse de calcul si l'on ignore les termes en B_{ij} de la matrice hessienne.

Reçue le 10 avril 1992

Institute Polytechnique, Jassy,
Chaire d'Energétique

BIBLIOGRAPHIE

1. C â r ţ i n ă Gh., *Minimisation des pertes de puissance active dans les réseaux à haute tension.* Bull. ASE/UCS, **76**, *13*, 746-749 (1985).

2. C â r ţ i n ă Gh., *Sur les possibilités d'utilisation de la matrice jacobienne.* Bul. Inst. Polit., Iaşi, **XXXV (XXXIX)**, *1-2*, s.III, 77-82 (1989).

CREŞTEREA VITEZEI DE CALCUL ÎN PROBLEMELE DE OPTIMIZARE A REGLAJULUI TENSIUNE–PUTERE REACTIVĂ

(Rezumat)

Se arată că prin simplificarea calculului matricei hessienne din metoda gradienţilor conjugaţi creşte sensibil viteza de calcul fără a se pierde din precizie.

BULETINUL INSTITUTULUI POLITEHNIC DIN IAŞI
Tomul XXXIX (XLIII), Fasc. 1–4, 1993
Secţia III
ELECTROTEHNICĂ. ENERGETICĂ. ELECTRONICĂ

D.C. 621.315.05

REMARKS ABOUT THE STUDY OF SELF-COMPENSATED OVERHEAD LINES WITH BUNDLED CONDUCTORS

BY
M. GAVRILAŞ

1. Introduction

At present bundled conductors are used for rated voltages superior to 220 KV to limit radio interference and power loss due to corona effect. Their geometrical parameters (n – number of subconductors in bundle; R – radius of circle on which subconductors are or bundle radius) generally coincide with the minimum values determined by electrical or mechanical requirements.

The literature [1] has recently proposed certain applications of bundled conductors for rated voltages inferior to 220 KV, using bundling parameters superior to their present day values. Thus, it suggests a possible development of overhead lines with up to 10 (110 and 220 KV), 12 (500 KV) or even 18 (750 KV) subconductors in bundle. This method is called "deep bundled conductors" and it is intended to increase the surge impedance loading of the line.

The literature up today reffered to this method only in connection with one-circuit overhead lines. In this paper we intend to analyze the influence of "deep bundled conductors" on the geometrical characteristics of self-compensated overhead lines (SCOL), which use two three-phase circuits and a phase shift between voltages of these circuits.

2. Principle of "Deep Bundled Conductors"

The principle of "deep bundled conductors" intends to use more efficiently the surface of subconductors placed in the electric field of the line.

For a given number of subconductors per phase, their surface will be used better if the electric charge is uniformly distributed on them and the voltage gradient is close by its critical value.

Form the viewpoint of carring capacity of the line these conditions provide the maximum value of the natural load that can be obtained using a certain number of subconductors, of a given total cross section. This aim can be attained by

simultaneously increasing of the number of subconductors and of the bundle radius following the equation [1]:

$$R = \left[\frac{D_{\text{eq}}}{\sqrt{nr_0}} \exp\left(-\frac{U_{fn}}{nr_0 E_{\text{adm}} k_{ut}}\right)\right]^{\frac{n}{n-1}}. \tag{1}$$

Here the subconductor's surface using coefficient (k_{ut}) takes the desired value. The other quantities from this equation represent: U_{fn} – phase-to-ground rated voltage; E_{adm} – critical value of the voltage gradient on surface of subconductors (approximately 20 KV/cm); r_0 – subconductor radius; D_{eq} – equivalent spacing between conductors.

For present day overhead lines operating in Romania the surface using coefficient takes values from 0.45 (110 KV) to 0.7 (400 KV). Comparing these values with the maximum one ($k_{ut\max} = 0.90...0.95$ [1]), it results an important reserve from the viewpoint of the electrical component of the electromagnetic field not yet exploited.

The main method that can be used to increase k_{ut}, keeping at the same time reasonable values for the bundle radius, consists in adopting a compact design of the line, i.e. reducing spacing between phase-conductors (D_{eq}).

3. SCOL with Bundled Conductors

In the case of self-compensated overhead lines the equivalent spacing, D_{eq}, depends not only on distances between phase-conductors, but also on the phase shift between voltage phasors of the two circuits, θ. As a result, distance D_{eq} get a more emphasized conventional character and the geometry of the phase becomes much different in comparison with that of one-circuit overhead lines.

Among all possible conditions of operation for a SCOL (θ=0°...180°), afterwards we consider only the most favourable from the viewpoint of natural load [2], namely θ=180°.

In this conditions the equivalent spacing is:

$$D'_{\text{eq}} = D_{\text{eq}} \frac{D_{\text{eq}ii}}{D_{\text{eq}ij}}, \tag{2}$$

where: D_{eq} – equivalent spacing between conductors of the same circuit (equal in practice to that for one-circuit overhead line); $D_{\text{eq}ii}$ and $D_{\text{eq}ij}$ – equivalent spacing between homologous and nonhomologous phases of different circuits.

The principle of SCOL [2] necessarily implies the following relationship between these distances:

$$D_{\text{eq}} \approx D_{\text{eq}ij} > D_{\text{eq}ii},$$

so it might be considered:

$$D'_{\text{eq}} \approx D_{\text{eq}ii} < D_{\text{eq}}.$$

Therefore, for SCOL the distance D_{eq} from equation (1) considerably diminishes in comparison with that of one-circuit overhead line. This allows an efficient usage of subconductor's surface for reduced values of bundle radius.

At the same time it is to consider that putting in practice for SCOL the principle of "deep bundled conductors" will result in a more marked increase of the natural load. This is the reason why, using subconductors with standard cross section (240, 300, 450 mm^2), it can be possible to obtain high current densities.

If the natural load of the line is determined as:

$$P_N = \frac{1}{20} n r_0 E_{\text{adm}} k_{ut} U_{fn} \,, \tag{3}$$

the density of the current flowing through conductors, when the line operates at natural loading, may be determined as:

$$j_N = \frac{I_N}{S_{\text{tot}}} = \frac{P_N}{3U_{nf}} \cdot \frac{1}{\pi n r_0^2 \kappa_u} = \frac{100}{60\pi} \cdot \frac{E_{\text{adm}} k_{ut}}{r_0 \kappa_u} \,, \tag{4}$$

where κ_u – filling coefficient, equal to the ratio between the active and the whole sections of the conductor. Eq. (4) determines j_N, in A/mm^2, if E_{adm} and r_0 are given in KV/cm and mm, respectively.

It may be stated that an efficient usage of subconductor's surface implies an increase not only of the natural load, but also of the current density. The last one could exceed certain values considered as from economic point of view the most favourables.

On the other hand there is no dependence between the natural current density and the rated voltage of the line or the number of subconductors per phase.

Eq. (4) can be transformed so that it allows to determine the minimum radius of subconductors depending on k_{ut} and j_N, namely:

$$r_{0\,\min} = \frac{100}{60\pi} \cdot \frac{E_{\text{adm}} k_{ut}}{\kappa_u j_N}. \tag{5}$$

Considering k_{ut} as a parameter this equation leads to a hyperbolic dependence of $r_{0\,\min}$ versus j_N, as shown in Fig. 1. The curves in this figure demonstrate that, when using actual standard cross section of subconductors, a high value of k_{ut} could be ensured only at the cost of an important current density. Besides, this value grows as decreases the cross section of subconductor in bundle.

On the other hand higher cross sections (570 or 900 mm^2, used allready in Italy, Canada, USA, Australia), would permit to obtain the desired value of coefficient k_{ut} for a lower current density. This is the reason why in the following numerical analysis, some variants of bundled conductors that use subconductors with cross section out of the standard range will be considered.

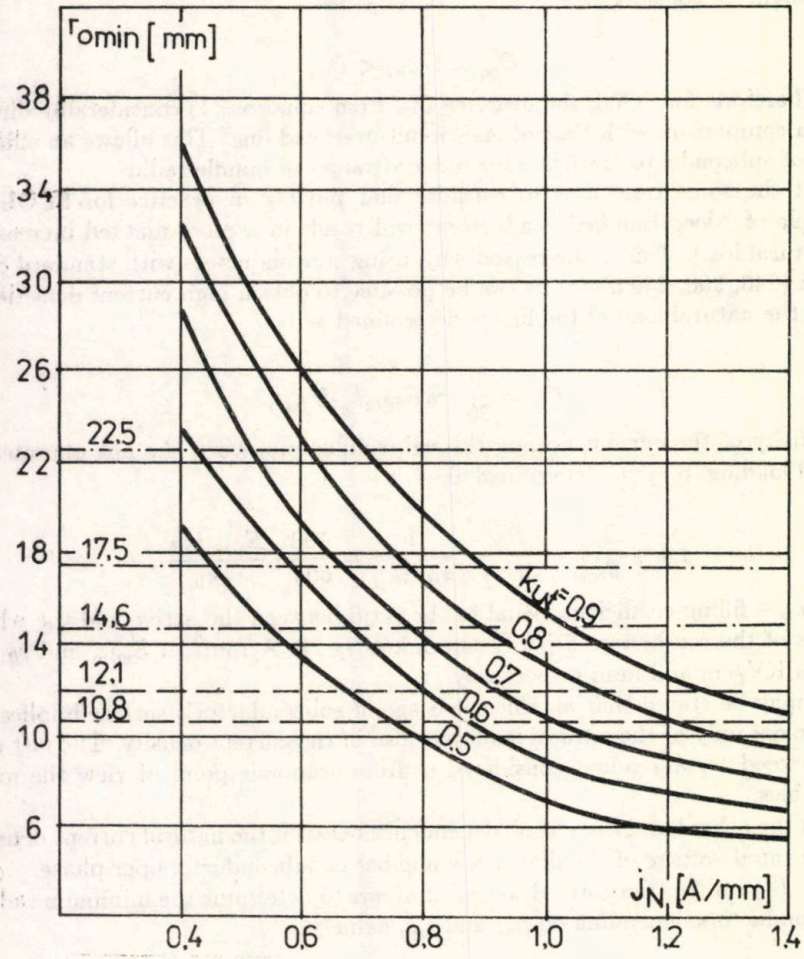

Fig. 1

4. Numerical Analysis

In this section we present some results calculated with help of the theoretical foundation above. The applications consider two SCOL with rated voltage 220 KV and 400 KV respectively, whose tower-top line configuration is shown in Fig. 2.

In both situations the phase was supposed to be composed from n=2...6 subconductors, with cross sections in the range 150...570 mm^2.

Also, for distances D and d from Fig. 2 were choosen the following values: a) SCOL 220 KV: D=6.2 m, d=1.7 m (determined in view to use existing poles); b) SCOL 400 KV: D=14 m, d=3 m.

Tables 1...4 present the numerical results determined in these conditions for two values of coefficient k_{ut}. Tables 1 (k_{ut}=0.85) and 2 (k_{ut}=0.75) correspond to the rated voltage 220 KV

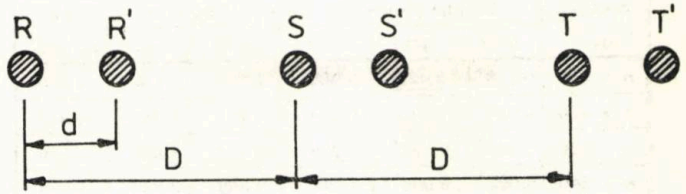

Fig. 2

Table 1

Section mm^2	Bundle radius, [m], for k_{ut}=0.85 and					j_N A/mm^2
	n=2	n=3	n=4	n=5	n=6	
n × 570	1.225	1.195	1.233	1.273	1.308	0.859
n × 450	0.632	0.859	0.989	1.079	1.125	0.949
n × 300	0.265	0.555	0.740	0.870	0.960	1.146
n × 240	0.144*)	0.410	0.604	0.746	0.853	1.279
n × 185	0.066*)	0.280	0.467	0.615	0.730	1.445
n × 150	0.031*)	0.191	0.363	0.510	0.628	1.604
R_{min}, [m]	0.150	0.173	0.212	0.255	0.300	—

*) In order to ensure a spacing of 0.3 m between subconductors, the minimum value of bundle radius, determined as $R_{min}=300/(2\sin(\pi/n))$, [mm], will be adopted.

Table 2

Section mm^2	Bundle radius, [m], for k_{ut}=0.75 and					j_N A/mm^2
	n=2	n=3	n=4	n=5	n=6	
n × 570	0.693	0.900	1.020	1.104	1.167	0.758
n × 450	0.320	0.611	0.788	0.910	1.000	0.837
n × 300	0.116*)	0.367	0.561	0.706	0.816	1.012
n × 240	0.058*)	0.259	0.445	0.593	0.710	1.128
n × 185	0.024*)	0.166*)	0.330	0.474	0.593	1.275
n × 150	0.010*)	0.108*)	0.248	0.382	0.500	1.415
R_{min}, [m]	0.150	0.173	0.212	0.255	0.300	—

*) In order to ensure a spacing of 0.3 m between subconductors, the minimum value of bundle radius, determined as $R_{min}=300/(2\sin(\pi/n))$, [mm], will be adopted.

and Tables 3 (k_{ut}=0.85) and 4 (k_{ut}=0.75), to 400 KV.

The analysis of these data allows to state that the principal restrictions which can influence the choise of one or another variant of bundled conductors are as follows:

a) An efficient usage of conductor's surface can lead to bundle radius inferior to the value

Table 3

Section mm^2	Bundle radius, [m], for k_{ut}=0.85 and					j_N
	n=2	n=3	n=4	n=5	n=6	A/mm^2
n × 570	0.113*)	0.479	0.969	1.264	1.494	0.859
n × 450	0.030*)	0.245	0.516	0.761	0.969	0.949
n × 300	0.005*)	0.102*)	0.288	0.492	0.683	1.146
n × 240	0.002*)	0.056*)	0.194*)	0.366	0.539	1.279
n × 185	0.001*)	0.026*)	0.117*)	0.250 *)	0.400	1.445
n × 150	0.000*)	0.013*)	0.072 *)	0.174*)	0.300	1.604
R_{min}, [m]	0.150	0.173	0.212	0.255	0.300	—

*) In order to ensure a spacing of 0.3 m between subconductors, the minimum value of bundle radius, determined as $R_{min}=300/(2\sin(\pi/n))$, [mm], will be adopted.

Table 4

Section mm^2	Bundle radius, [m], for k_{ut}=0.75 and					j_N
	n=2	n=3	n=4	n=5	n=6	A/mm^2
n × 570	0.040*)	0.286	0.678	0.976	1.215	0.758
n × 450	0.008*)	0.132*)	0.342	0.558	0.755	0.837
n × 300	0.000*)	0.048*)	0.175*)	0.338	0.506	1.012
n × 240	0.000*)	0.025*)	0.111*)	0.240 *)	0.385	1.128
n × 185	0.000*)	0.010*)	0.062*)	0.156 *)	0.273*)	1.275
n × 150	0.000*)	0.004*)	0.036*)	0.103 *)	0.196*)	1.415
R_{min}, [m]	0.150	0.173	0.212	0.255	0.300	—

*) In order to ensure a spacing of 0.3 m between subconductors, the minimum value of bundle radius, determined as $R_{min}=300/(2\sin(\pi/n))$, [mm], will be adopted.

determined by mechanical requirements (marked with an asterisk in Tables 1...4). In such cases the bundle radius will be choosen in order to ensure a minimum value for the spacing between subconductors, equal to 0.3 m. Of course, consequently, the surface using coefficient will decrease.

b) Too high values of the bundle radius will determine dimensions of the phase comparable to distances between phases. As a result the screening effect will strongly manifest itself, so that equations written above loose their validity. To avoid this disadvantage we retain only those values from Tables 1...4 that do not outrun certain values determined in connection with distances between phases (Fig. 2): R_{max}=0.7 m (U_n=220 KV) and R_{max}=0.9 m (U_n=400 KV).

c) Maintaining a high surface using coefficient when using subconductors of small cross section, can determine an important current density, with poor effects on power and energy losses. From this viewpoint this paper consider a high limit for current density equal to 1.3 A/mm^2.

All this restrictions practically eliminate a great part from the analysed variants. So, for a subsequent study can be kept on the following variants, corresponding to underlined values in Tables 1...4:

a) SCOL 220 KV: 2 × 450; 2,3 × 300; 3,4 × 240 mm^2, (k_{ut}=0.85);
2 × 570; 2,3 × 450; 3,4 × 300; 3,4,5 × 240; 4,5,6 × 185 mm^2, (k_{ut}=0.75).

b) ŞCOL 400 KV: 3×570; $3{,}4{,}5 \times 450$; $4{,}5{,}6 \times 300$; $5{,}6 \times 240$ mm^2, (k_{ut}=0.85);
$3{,}4 \times 570$; $4{,}5{,}6 \times 450$; $5{,}6 \times 300$; 6×240 mm^2, (k_{ut}=0.75).

5. Conclusions

The principle of "deep bundled conductors" applied with self-compensated lines allows an efficient usage of subconductors' surface. A certain value of the surface using coefficient can be obtained by arranging subconductors on a circle whose radius is inferior to that corresponding to one-circuit overhead lines.

Among the most important restrictions which strongly limit the structure of the phase can be mentioned the minimum and maximum dimensions of the phase and the natural current density.

The bundle radius necessary to guarantee a certain value of the surface using coefficient decreases when the rated voltage increases, thus amplifying the compaction degree of the line.

Although a final decision about the best bundled conductor solution implies a deeper analysis of self-compensated overhead lines' characteristics (parameters, performances, operation conditions, etc.) it could be considered that this paper represents a real foundation for future investigations.

Received, November 18, 1991

Polytechnic Institute, Jassy,
Department of Energetics

REFERENCES

1. Alexandrov G.N., *Peredača električeskoi energyi peremennym tokom.* Energoatomizdat, Leningrad, 1990.

2. Poeată Al., Asaftei C., Gavrilaş M., *Contribuţii la studiul compactizării liniilor aeriene de transport a energiei electrice.* Symp. "Optimization of Development a. Exploitation of Electrical Installations", Jassy, 1987.

CONTRIBUŢII LA STUDIUL LINIILOR ELECTRICE AUTOCOMPENSATE CU FAZE SCINDATE

(Rezumat)

Se prezintă unele consideraţii referitoare la utilizarea principiului scindării accentuate a fazei în cazul liniilor electrice autocompensate, subliniind avantajul obţinerii unor dimensiuni mai reduse ale fazei în comparaţie cu liniile tradiţionale, în condiţiile asigurării unui acelaşi coeficient de utilizare a suprafeţei conductoarelor.

BULETINUL INSTITUTULUI POLITEHNIC DIN IAŞI
Tomul XXXIX (XLIII), Fasc. 1–4, 1993
Secţia III
ELECTROTEHNICĂ. ENERGETICĂ. ELECTRONICĂ

C.D. 621.317.736

SUR L'APPLICATION DE LA MÉTHODE D'IDENTIFICATION ET LOCALISATION D'UNE MISE À TERRE À L'AIDE DU CONTRÔLE DES DÉPHASAGES DANS LES RÉSEAUX ÉLECTRIQUES DE MOYENNE TENSION AYANT LE POINT NEUTRE MIS À TERRE

PAR
JAN IGNAT

1. Introduction

Dans une Note précédente [1] on a proposé et étudié une méthode qui permet à identifier et localiser une simple mise à terre dans un réseau de distribution de moyeune tension (RED-MT) ayant le neutre isolé, basée sur le contrôle des déphasages entre les courants de deséquilibre dans ce régime et les tensions de phase $\underline{U}_a$, $\underline{U}_b$, $\underline{U}_c$ du secondaire de chaque poste de transformation (PT) muni avec des transformateurs de puissance ayant la groupe de connexions ΔY_0-5 ou ΔY_0-11. Cette méthode tient compte, toutefois, du fait que le système triphasé de tensions du RED-MT reste inchangé [2].

D'autre part, dans les RED-MT ayant le neutre mis à terre par la résistance de limitation R_L (Fig. 1), un problème qui s'avère intéressant est celui de l'identification et de la localisation des *courtcircuits* monophasés par une résistance de passage de valeur élevée ($R_D > R_{D\,\mathrm{lim}}$), qui constituent au fond une mise à terre monophasée [3]. La valeur $R_{D\,\mathrm{lim}}$ résulte de celle du courant d'amorçage de la protection maximale homopolaire de courant [3].

Les solution utilisées jusqu'à présent [3] pour le contrôle de ce type de défaut permettent à identifier l'existence de celui-ci et la localisation du distributeur (D_i) où s'est produit le défaut, jusqu'à $R_D \leq 23$ kΩ dans les réseaux de 20 kV, respectivement 11 kΩ dans celles de 10 kV.

Dans ce qui suit on propose l'application de la méthode étudiée en [1], basée sur le contrôle des déphasages, même dans le cas des RED-MT ayant le neutre mis à terre, compte tenu que lorsque $R_D > R_{D\,\mathrm{lim}}$ le système triphasé des tensions du réseau de moyenne tension ($\underline{U}_R$, $\underline{U}_S$, $\underline{U}_T$) reste pratiquement symétrique au long du distributeur à défaut (D_2 – Fig. 1) ainsi que dans le reste du réseau. Par suite, le système triphasé des tensions de phase $\underline{U}_a$, $\underline{U}_b$, $\underline{U}_c$, du secondaire du poste de transformation (PT), alimenté par le réseau de moyenne tension (Fig. 1), peut constituer un système de référence commun pour le RED-MT étudié.

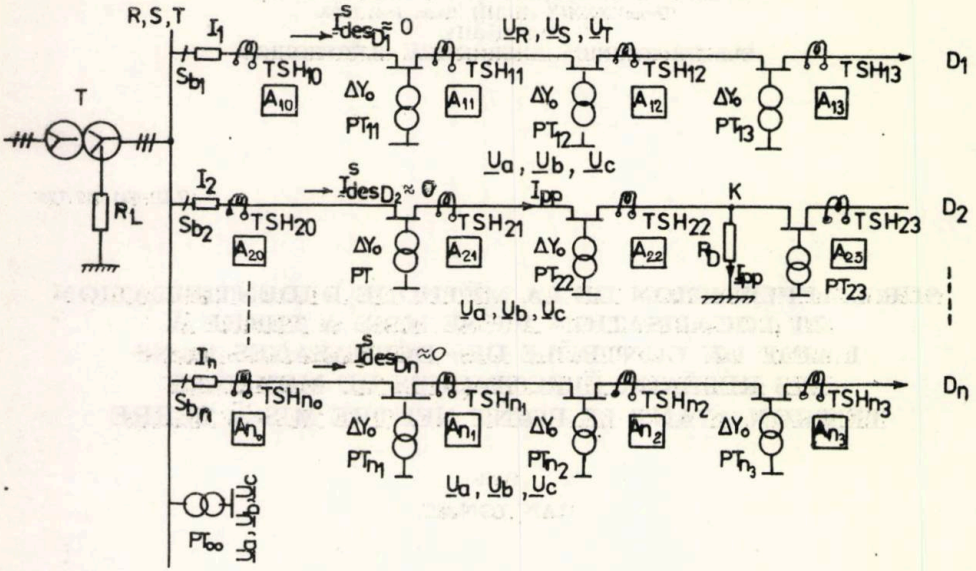

Fig. 1

2. Application de la méthode proposée

Compte tenu de l'expression du courant de court-circuit monophasé [2], écrite à l'aide des composants symétriques (par exemple sur la phase R):

$$\underline{I}_{k_{1R}}^{(1)} = \frac{\underline{E}_R}{\underline{Z}_1 + \underline{Z}_2 - \underline{Z}_0 + 3R_D}, \tag{1}$$

dans les conditions où $R_D \gg Z_1, Z_2, Z_0$, on obtient:

$$\underline{I}_{k_R}^{(1)} = 3\underline{I}_{k_{1R}}^{(1)} = \frac{\underline{E}_R}{R_D} \approx \frac{\underline{U}_R}{R_D}. \tag{2}$$

Par conséquent le courant de court-circuit monophasé dans un réseau ayant le neutre mis à terre, lorsque celui-ci se produit par une résistance de passage (R_D) de grande valeur, est pratiquement symphasique avec la tension de la phase à défaut (Fig. 2 *a*). Les hypothèses simplificatrices introduites déterminent une erreur de l'ordre de 2...5 degrés électriques, qui s'avèrent absolument acceptables.

Les courants capacitifs qui chargent les phases ($\underline{I}_{R_0}$, $\underline{I}_{S_0}$, $\underline{I}_{T_0}$), ont, dans l'hypothèse ci-dessus, des valeurs proches de celles en régime normal et par conséquent:

(3) $$\underline{I}^{S}_{\text{des}_R} = \underline{I}_{R_0} + \underline{I}_{S_0} + \underline{I}_{T_0} = 0.$$

Le courant de deséquilibre qui circule par le distributeur à défaut, mesuré à l'aide d'un filtre de courant de séquence homopolaire (TSH), aura, sur le tronçon délimité par les barres de la station et le lieu où se produit le défaut, la valeur:

(4) $$\underline{I}^{d}_{\text{des}_R} = \underline{I}^{(1)}_{k_R} + (\underline{I}_{R_0} + \underline{I}_{S_0} + \underline{I}_{T_0}) = \underline{I}^{(1)}_{k_R} \triangleq \underline{I}_{ppR},$$

tandis que sur le reste des distributeurs et en aval du distributeur à défaut, conformément à la relation (3), le courant mesuré à l'aide du TSH sera pratiquement nul.

Les déphasages entre le courant $\underline{I}_{pp}$, lorsqu'on considère que le défaut se produit succesivement sur chaque phase et le système triphasé des tensions de phase $\underline{U}_a$, $\underline{U}_b$, $\underline{U}_c$ du secondaire du PT, directement accessibles, aux bornes du distributeur à défaut (ayant la groupe de connexions ΔY_0-5 ou ΔY_0-11, Fig. 1), ont été synthétisés conformément à la Fig. 2 dans le Tableau 1, en négligeant les erreurs mentionées ci-dessus.

Tableau 1*a*

	$\underline{U}_R$	ΔY_0-5			ΔY_0-11		
		$\underline{U}_a$	$\underline{U}_b$	$\underline{U}_c$	$\underline{U}_a$	$\underline{U}_b$	$\underline{U}_c$
$\underline{U}'_r = K_{TPP_R}\underline{I}_{ppR}$	0	$-\frac{5\pi}{6}$	$\frac{\pi}{2}$	$-\frac{\pi}{6}$	$\frac{\pi}{6}$	$-\frac{\pi}{2}$	$\frac{5\pi}{6}$
$\underline{U}_r = \underline{U}_T e^{j\frac{2\pi}{3}}$	$-\frac{\pi}{2}$	$\frac{2\pi}{3}$	0	$-\frac{2\pi}{3}$	$-\frac{\pi}{3}$	π	$\frac{\pi}{3}$
$-\underline{U}_r$	$\frac{\pi}{2}$	$-\frac{\pi}{3}$	π	$\frac{\pi}{3}$	$\frac{2\pi}{3}$	0	$-\frac{2\pi}{3}$

Tableau 1*b*

	$\underline{U}_S$	ΔY_0-5			ΔY_0-11		
		$\underline{U}_a$	$\underline{U}_b$	$\underline{U}_c$	$\underline{U}_a$	$\underline{U}_b$	$\underline{U}_c$
$\underline{U}'_s = K_{TPP_S}\underline{I}_{ppS}$	0	$-\frac{\pi}{6}$	$-\frac{5\pi}{6}$	$\frac{\pi}{2}$	$\frac{5\pi}{6}$	$\frac{\pi}{6}$	$-\frac{\pi}{2}$
$\underline{U}_s$	$-\frac{\pi}{2}$	$-\frac{2\pi}{3}$	$\frac{2\pi}{3}$	0	$\frac{\pi}{3}$	$-\frac{\pi}{3}$	π
$-\underline{U}_s$	$\frac{\pi}{2}$	$\frac{\pi}{3}$	$-\frac{\pi}{3}$	π	$-\frac{2\pi}{3}$	$\frac{2\pi}{3}$	0

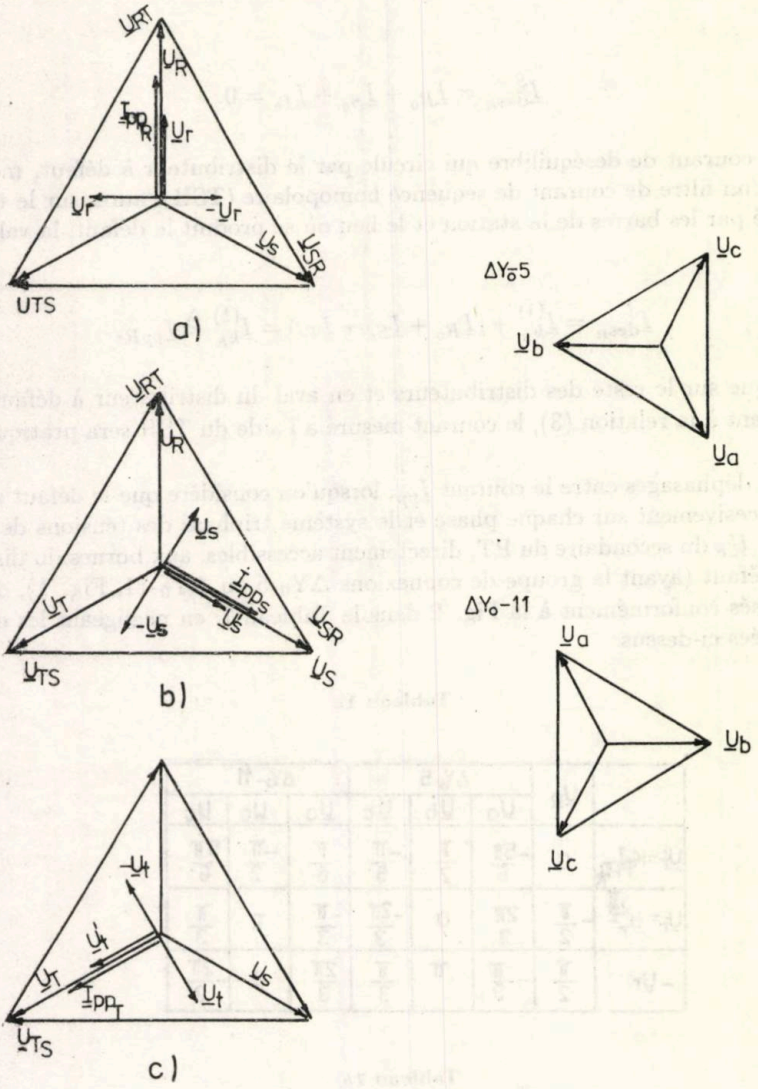

Fig. 2

Les données de ce Tableau prouvent que ces déphasages ont des valeurs différentes, fonction de la phase où s'est produit la mise à terre, ce qui permet l'identification sélective du défaut, à savoir l'identification du distributeur, de la phase et du tronçon délimité par deux PT, qui correspondent au défaut.

Tableau 1c

	U_T	$\Delta Y_0 - 5$			$\Delta Y_0 - 11$		
		U_a	U_b	U_c	U_a	U_b	U_c
$U'=k_T I_{pp_T}$	0	$\frac{\pi}{2}$	$-\frac{\pi}{6}$	$-\frac{5\pi}{6}$	$-\frac{\pi}{2}$	$\frac{5\pi}{6}$	$\frac{\pi}{6}$
U_t	$-\frac{\pi}{2}$	0	$-\frac{2\pi}{3}$	$\frac{2\pi}{3}$	π	$\frac{\pi}{3}$	$-\frac{\pi}{3}$
$-U_t$	$\frac{\pi}{2}$	π	$\frac{\pi}{3}$	$-\frac{\pi}{3}$	0	$-\frac{2\pi}{3}$	$\frac{2\pi}{3}$

On constate que les déphasages entre $\underline{I}_{pp}$, respectivement $\underline{U}' = k_T \underline{I}_{pp}$ (Fig. 3), et les tensions $\underline{U}_a$, $\underline{U}_b$, $\underline{U}_c$ ne sont jamais nulles. Si l'on modifie l'argument de la tension $\underline{U}'$ avec $\pm\pi/2$ rad., alors les déphasages de la tension

$$\underline{U} = \underline{U}' e^{\pm j\pi/2}, \tag{5}$$

par rapport aux mêmes tensions de référence ($\underline{U}_a$, $\underline{U}_b$, $\underline{U}_c$), se modifient d'une façon correspondante; ces nouvelles valeurs des déphasages sont indiquées, de même, dans le Tableau 1.

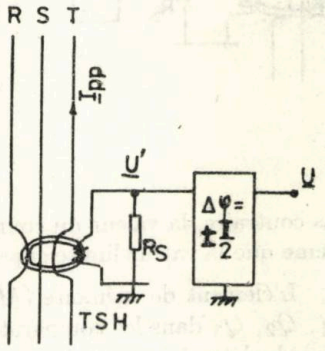

Fig. 3

Selon ce qu'on connaît il est assez facile à obtenir un signal retardé par rapport à un autre. Par conséquent en utilisant ce procédé on présente, dans la Fig. 4, le schéma de principe du dispositif (A_{ij} – Fig. 1) à l'aide duquel on peut localiser, conformément à la méthode mentionée ci-dessous, un court-circuit monophasé par une résistance de passage de grande valeur ($R_D > R_{D\,\mathrm{lim}}$) dans un RED-MT ayant le neutre mis à terre par l'intermédiare de R_L. Si l'on considère que les transformateurs de force ont la groupe de connexions ΔY_0-11 il s'ensuit que les comparateurs de phase φ_R, φ_S, φ_T doivent être réalisés d'une telle manière de sorte que les grandeurs de sortie Q_1, Q_2, Q_3 aient la valeur logique „0" lorsque les grandeurs d'entrée sont symphasiques ou dephasées avec $\delta \leq 2°...5°$él., respectivement „1" dans le cas contraire ou si l'une des grandeurs d'entrée est nulle.

Les cinq états du dispositif ont les significations ci-dessous: I, II, III – défaut sur la phase R, S, respectivement T, en aval; IV – inexistence d'une mise à terre en aval; c'est l'état des dispositifs qui ne sont pas parcourus par le courant $\underline{I}_{pp}$, à savoir ceux situés sur les distributeurs qui fonctionnent normalement et, en aval du défaut, sur le distributeur avarié.

S'il y a une nonsymétrie prononcée du réseau, qui détermine, en régime normal, un courant $\underline{I}^S_{\mathrm{des}}$ de grande valeur, alors il est possible l'apparition de l'état V. Il ne faut pas que le dispositif soit désensibilisé par rapport à un tel courant car, au

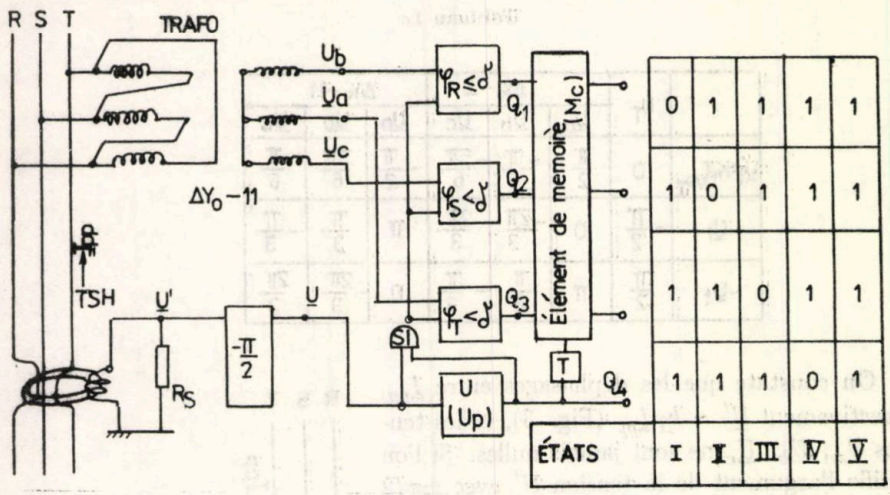

Fig. 4

cas contraire, la valeur du courant I_{pp}, qui pourrait être sésisée, serait limitée, de même que la valeur limite supérieure de la résistance R_D.

L'élément de mémoire (M_c) assûre la mémorisation des grandeurs de sortie Q_1, Q_2, Q_3 dans les comparateurs de phase, afin de permettre leur lecture même après le débranchement du distributeur en défaut; évidemment il s'avère nécessaire que Q_4 soit mémorisé, par la même raison. L'élément de temps (T) réalise la commande de la transcription des grandeurs d'entrée à la sortie du M_c après un intervalle de temps $\Delta t > \Delta t_{\text{trans.}}$, de telle manière que le contrôle des déphasages en régime de défaut stabilisé soit assûré.

L'opération de localisation du défaut commence par la lecture des indications des dispositifs (A_{i0}) situés dans la station et continue dans le distributeur D_2 (Fig. 1), dont le dispositif A_{20} se trouve dans l'un des états I, II, III, jusqu'on peut dépister le premier dispositif se trouvant dans l'état IV. Le défaut est situé, en ce cas, dans le premier tronçon situé en amonte de PT_{23}.

3. Essai expérimentaux

En utilisant un modèle physique de RED-MT on a réussi à confirmer les résultats des considérations ci-dessus. On a constaté toutefois, par voie expérimentale, que les courants I^S_{des} de nonsymétrie du réseau sont de cca. 20 fois moindres que la valeur du courant I_{pp}, les hypothèses ci-dessus en étant acceptées.

Le dispositif réalisé, dont le schéma de principe est donné dans la Fig. 4, fait l'objet d'une sollicitation de brevet d'invention [5].

4. Conclusions

On peut appliquer la méthode basée sur le contrôle des déphasages même dans la cas des RED-MT ayant le neutre mis à terre, en vue d'identifier et localiser un court-circuit monophasé qui se produit par l'intermédiaire d'une résistance de grande valeur.

Reçue le 15 décembre 1991

Institut Polytechnique, Jassy,
Chaire d'Energétique

BIBLIOGRAPHIE

1. I g n a t J., *Méthode d'identification et localisation d'une mise à terre dans un réseau électrique ayant le neutre isolé.* Bul. Inst. polit., Iaşi, **XXXVII (XLI)**, *1-4*, s. III, 71-76 (**1991**).
2. U l i a n o v S.A., *Regimurile tranzitorii ale sistemelor electrice* (trad. du russe). Ed. Tehnică, Bucureşti, 1967.
3. G o i a I.M. et al., *Tratarea neutrului reţelelor de medie tensiune.* Ed. Tehnică, Bucureşti, 1985.
4. A r d e l e a n I. et al., *Circuite integrate CMOS.* Ed. Tehnică, Bucureşti, 1986.
5. I g n a t J., *Dispozitiv pentru identificarea punerilor la pământ.* Sollicitation pour un brevet d'invention, OSIM, *145 373*, 1990.

CU PRIVIRE LA APLICAREA METODEI BAZATE PE CONTROLUL DEFAZAJELOR ÎN REŢELE CU NEUTRUL IZOLAT

(Rezumat)

Se pune în evidenţă faptul că există posibilitatea de a identifica şi localiza un scurtcircuit monofazat printr-o rezistenţă de trecere de valoare ridicată, într-o reţea de distribuţie de medie tensiune cu neutrul legat la pământ, prin controlul defazajelor dintre curentul de defect şi sistemul trifazat al tensiunilor de fază ($\underline{U}_a$, $\underline{U}_b$, $\underline{U}_c$) din secundarele posturilor de transformare recordate la această reţea.

BULETINUL INSTITUTULUI POLITEHNIC DIN IAŞI
Tomul XXXIX (XLIII), Fasc. 1–4, 1993
Secţia III
ELECTROTEHNICĂ. ENERGETICĂ. ELECTRONICĂ

RECENZII BOOK REVIEWS

VAN ROOSMALEN, A.J., BAGGERMAN, J.A.G., *Dry Etching for VLSI.* Plenum Publishing Corporation, New York, 1991, 237 pp., ISBN 0-306-43835-6.

This book has been written as part of a series of scientific books being published by Plenum Press.

This volume is dedicated to the field of dry (plasma) etching, as applied in silicon semiconductor processing. Although a number of books have appeared dealing with this area of physics and chemistry, these all deal with parts of the field. This book is unique in that it gives a compact, yet complete, in-depth overview of fundamentals, systems, processes, tools, and applications of etching with gas plasmas for VLSI. Examples are given throughout the fundamental sections, in order to give the reader a better insight in the meaning and magnitude of the many parameters relevant to dry etching. Electrical engineering concepts are emphasized to explain the pros and cons of reactor concepts and excitation frequency ranges. In the description of practical applications, extensive use is made of cross-referencing between processes and materials, as well as theory and practice. It is thus intended to provide a total model for understanding dry etching.

The book has been written such that no previous knowledge of the subject is required. It is intended as a review of all aspects of dry etching for silicon semiconductor processing. The level of the book is suitable to final year undergraduates and postgraduates. The book is well suited as an overview for new-comers to plasma etching, but may also serve as a source of review material for experienced workers in this extensive field. The text can be used as course, but is also suitable for individual reading.

TZAFESTAS, G., WATANABE, K. (Eds.), *Stochastic Large-Scale Engineering Systems.* Marcel Dekker, Inc., New York, 1992, 383 pp., ISBN 0-8247-8654-8654-8

Large-scale systems (LSS) analysis and control theory has attained considerable maturity and sophistication and is receiving increasing attention from theorists and practitioners, for both its methodological attraction and its important real-life applications.

This volume is devoted to the class of large-scale stochastic system, which has recently dominated the attention of many academic and research groups. Topics of great importance, such as distributed-sensor networks, decentralized detection theory, large sparse systems, large-scale stochastic control systems and econometric models with integrated and decentralized policymakers are included. The book contains fresh developments in the field and reflects the experience of many eminent specialists working indifferent environments. Unavoidably, the coverage of the subject in the book is not exhaustive, but the topics of the chapters are representative and well balanced and their contents were carefully reviewed.

Generously illustrated with more 1500 display equations, figures and tables, *Stochastic Large-Scale Engineering Systems* is a time-saving reference for electrical, electronics, systems, control, computer, communications and mechanical engineers, applied mathematicians and graduate-level students in these disciplines. The wide scope of the book means that it is also useful to

educational and research establishments as a reference work in a topic that is expected to be "hot" for a long time in the future. The volume is not intended to cover elementary aspects of stochastic LSS analysis and design, but each chapter is self-contained and readers can, without difficulty, restrict their study to chapters of special interest.

LILD, R., NIEDERREITER, H., *Introduction to Finite Fields and Their Applications.* Cambridge University Press, Cambridge, 1986, 407 pp., ISBN 0-521-30706-6

The theory of finite fields is a branch of modern algebra that has come to the fore in recent years because of its diverse applications in such areas as combinatorics, coding theory, cryptology and the mathematical study of switching circuits.

The first part of this book presents an introduction to this theory, emphasising these aspects that are relevant for application. The second part is devoted to a discussion of the most important applications of finite fields, especially to information theory, algebraic coding theory and cryptology (including here some very recent material that has never before appeared in book form). There is also a chapter on applications within mathematics, such as finite geometrics, combinatorics and pseudo-random sequences.

The book is meant to be used as a textbook: worked examples and copious exercises that range from the routine, to those giving alternative proofs of key theorems, to extensions of material covered in the text, are provided throughout. It will appeal to advanced undergraduates and graduate students taking courses on topics in applied algebra, whether they have backgrounds in mathematics, electrical engineering or computer science. Non-specialists will also find this a readily accesible introduction to an active and increasingly important subject.

ORSZÁGOS MŰSZAKI INFORMÁCIÓS KÖZPONT ÉS KÖNYVTÁR 1883

1994 JUL 28

ISSN 0258-9109